Progress in Additive Manufacturing (2025) 10:1003–1061
https://doi.org/10.1007/s40964-024-00703-z

REVIEW ARTICLE

Additive manufacturing of geopolymer composites for sustainable construction: critical factors, advancements, challenges, and future directions

R. S. Krishna[1,2] · Asif Ur Rehman[3,4] · Jyotirmoy Mishra[5] · Suman Saha[6] · Kinga Korniejenko[7] · Rashid Ur Rehman[8] · Metin Uymaz Salamci[4] · Vincenzo M. Sglavo[9] · Faiz Uddin Ahmed Shaikh[10] · Tanvir S. Qureshi[11,12]

Received: 30 October 2023 / Accepted: 19 June 2024 / Published online: 16 August 2024

Abstract

Increasing pollution poses enormous pressure on the global ecosystem, with a need to limit the carbon emissions from the construction materials industry. Mitigation of this carbon is possible by converting industrial wastes into alternative cement and optimisation in the building process. Taking this into account, advancement is taking place in sustainable geopolymer composites-based additive manufacturing (AM) technology. Typical precursors for geopolymer binder are industrial waste by-products (such as slag, fly ash, and metakaolin). In another aspect, AM entails several benefits such as easy fabrication, freedom of design, the ability to generate sophisticated structural elements and reduce: expenses, time, waste generation, and labor demands. This review journal paper on geopolymer AM presents a bibliometric study followed by an overview of AM methods and influencing parameters, techniques in geopolymer AM (such as extrusion and powder bed), materials, improvements in AM process, and fresh-state and hardened-state properties. Recent developments in AM processes within

✉ Tanvir S. Qureshi
tanvir.qureshi@uwe.ac.uk; tanvir.qureshi@cnl.ca

R. S. Krishna
22085198@student.westernsydney.edu.au

Asif Ur Rehman
Asif.rehman@ucl.ac.uk

Jyotirmoy Mishra
jmishra_phdce@vssut.ac.in

Suman Saha
sumansaha.ce@nitdgp.ac.in

Kinga Korniejenko
kinga.korniejenko@pk.edu.pk

Rashid Ur Rehman
rashid.urrehman@ntu.edu.sg

Metin Uymaz Salamci
msalamci@gazi.edu.tr

Vincenzo M. Sglavo
vincenzo.sglavo@unitn.it

Faiz Uddin Ahmed Shaikh
S.Ahmed@curtin.edu.au

[1] Centre for Infrastructure Engineering, Western Sydney University, Penrith, NSW 2751, Australia

[2] Department of Mechanical Engineering, Veer Surendra Sai University of Technology, Burla 768018, India

[3] Bartlett School of Sustainable Construction, University College London, WC1E 6BT London, UK

[4] Department of Mechanical Engineering, Gazi University, 06570 Ankara, Turkey

[5] Department of Civil Engineering, Veer Surendra Sai University of Technology, Burla 768018, India

[6] Department of Civil Engineering, National Institute of Technology, Durgapur 713209, India

[7] Faculty of Materials Engineering and Physics, Cracow University of Technology, Jana Pawła II 37, 31-864 Cracow, Poland

[8] Singapore Membrane Technology Centre, Nanyang Environment and Water Research Institute, Nanyang Technological University, Singapore 637141, Singapore

[9] Department of Industrial Engineering, University of Trento, 38123 Trento, Italy

[10] School of Civil and Mechanical Engineering, Curtin University, Perth, WA 6102, Australia

[11] Department of Geography and Environmental Management, The University of the West of England, Bristol BS16 1QY, UK

[12] Inspection and Monitoring Technologies Branch, Canadian Nuclear Laboratories Ltd, Chalk River, ON K0J 1J0, Canada

the geopolymer are critically discussed while investigating the properties and applications of the same. The discussion includes an analysis pinpointing research gaps essential in developing geopolymer AM.

Graphical abstract

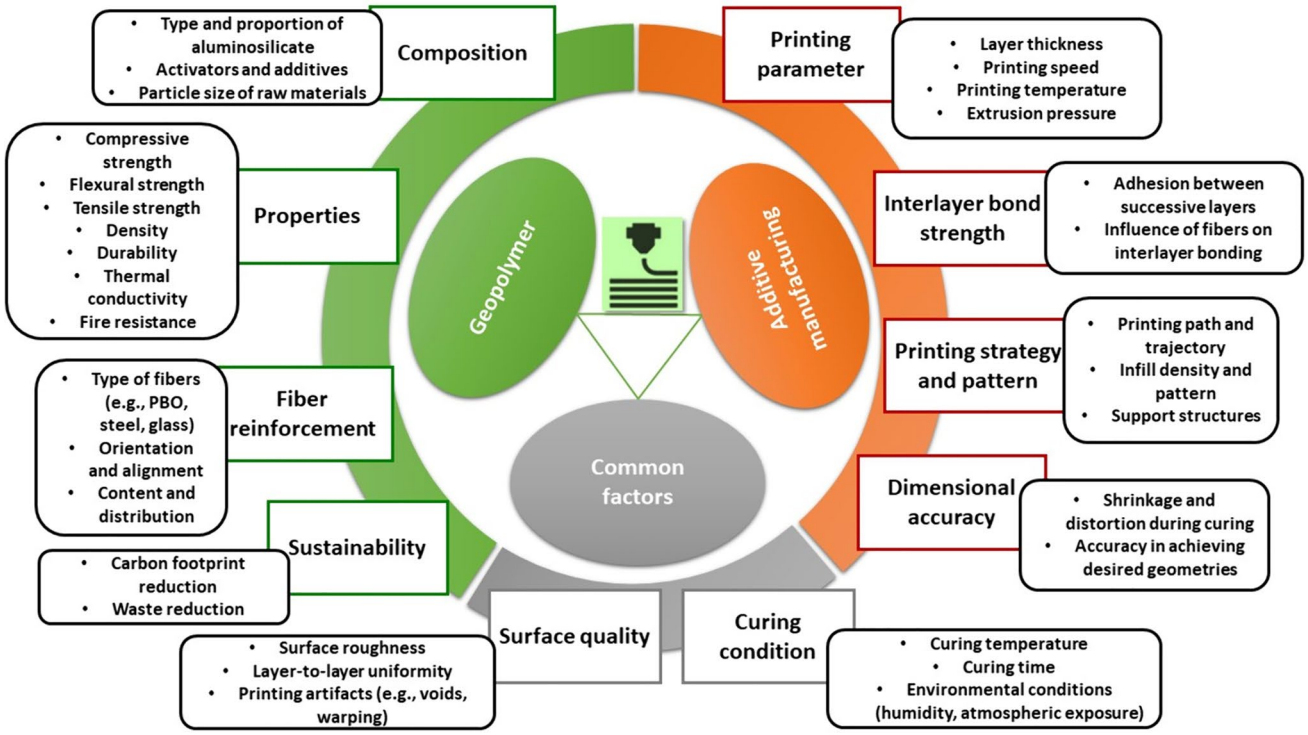

Keywords Geopolymer · Additive manufacturing · 3D printing · Composites · Sustainability

Abbreviations

3DP	3D printing
AAC	Alkali activated concrete
AD	Apparent density
ALSP	Alkaline source particles
AM	Additive manufacturing
ANC	Attapulgite nano-clay
AP	Apparent porosity
ASOP	Aluminosilicates source particles
ASTM	American Society for Testing and Materials
AV	Apparent viscosity
BD	Bulk density
BFS	Blast furnace slag
BJP	Binder jet printing
BW	Brick waste
CAD	Computer-aided design
CDW	Construction and demolition waste
CO_2	Carbon dioxide
CS	Compressive strength
EBM	Electron beam melting
EC	Electrical conductivity
ESA	European Space Agency
EU	European Union
FA	Fly ash
FDM	Fused deposition melting
FS	Flexural strength
GGBFS	Ground granulated blast furnace slag
GO	Graphene oxide
GS	Ground silica
GTF	Green tow flax
HA	Halloysite nanotube
HGPP	Hydrated geopolymer particles
HPMC	Hydroxy propyl methyl cellulose
HRWRA	High-range water-reducing agent
ILBS	Inter-layer bond strength
K_2SiO_3	Potassium silicate
KF	Kenaf fiber
KOH	Potassium hydroxide
KSC	Kenaf straw core
LRS	Lunar regolith simulant
M3D	Micro-3D printer
MAS	Magnesium alumino-silicate
MK	Metakaolin
MOR	Modulus of rupture

MS	Micro-silica
Na_2SiO_3	Sodium silicate
NaOH	Sodium hydroxide
NGP	Nano-graphene platelets
NGPs	Nano-graphite platelets
OPC	Ordinary Portland cement
PBO	Polyphenylene benzobisoxazole
PCM	Phase change material
PP	Polypropylene
PV	Plastic viscosity
PVA	Polyvinyl alcohol
RCA	Recycled coarse aggregate
RM	Red mud
SCSM	Sodium carboxy methyl starch
SD	Strut density
SEM	Scanning electron microscope
SF	Silica fume
SiC	Silicon carbide
SLA	Stereo-lithography apparatus
SLM	Selective laser melting
SLS	Selective laser sintering
SoD	Solid density
SRF	Shape retention factor
SRR	Shape retention ratio
TD	True density
TOT	Thixotropic open time
TP	Total porosity
UV	Ultraviolet
VMA	Viscosity-modifying admixture
XRD	X-ray diffraction
YM	Young's modulus
YSZ	Yttria-stabilized zirconia

1 Introduction

Pollution degrades the natural terrain around which we live, the waters we drink, and the atmosphere we breathe. Rapid technological advancements are intended to make our lives easier. Consequently, rapid industrialization severely impacted our global ecosystem by depleting the earth's natural resources, increasing pollution and producing a more significant amount of waste. According to data from Eurostat 2021 of the European Union (EU) as demonstrated in Fig. 1a [1], the average waste produced in Europe is majorly from construction and demolition waste (35.9%), followed by mining and quarrying waste (26.6%) and manufacturing waste (10.6%) [1]. Similarly, the World Bank in Fig. 1b has released the global trends in solid waste management and projected significant growth in waste generation until 2050 [2]. This has raised a significant concern worldwide about minimizing this major waste generation and then utilizing it efficiently for a sustainable future and circular economy.

The transformation of waste materials into a resource is not only critical to the economy but also for the environment. Waste materials could be reduced, reused, recycled, and remanufactured, removing the need to consume natural resources for modern purposes [3]. Fly-Ash (FA) [4], Blast Furnace Slag (BFS) [5], mine tailing [6], silica fume [7], rice husk [8], and red mud [9] are the primary industrial wastes that are generated in high quantities [10–12]. All the generation of waste in the construction industry is considerably influenced by the complexity of scaffolding, production time, and costs. Long series scaffolding is necessary to turn these molds cost-effective [13]. Another concern is the scaffold life cycle, especially for the greenhouse gas emissions, considering the environmental damage of scaffolding. Digital fabrication, or, more specifically, AM, can modernize and revolutionize several production processes used in the construction industry [14]. First, digital fabrication techniques can generate the article directly from the Computer-Aided Design (CAD) file, which is a substantial advantage [15]. Second, AM can reduce 30–65% of the cost and time [16] leading to the reduction of waste incurred in the construction industry by clearly eliminating the need for conventional formwork, which is a time-consuming process particularly for intricate shapes or designs. Further advantages of time reduction include on-demand construction which prevents the need for transportation of precast elements, and reduced manpower requirements, acting as a bottleneck in terms of time and efficiency. Finally, digital fabrication has increasing utility as more 3D technologies are being used, such as 3D scanning and generating files for CAD models [10]. However, achieving precise quality in freeform 3D printed components casted on-site still remains challenging [18].

Extra emission of CO_2 during in situ concrete castings is tied up to formwork [19] and over-ordering of concrete [20]. This is also generating vast amounts of waste that are difficult to handle. Eco-friendliness, construction utility, readiness, and economic benefits are the main driving factors in the development of digital fabrication. Introducing energy-efficient materials like geopolymer concrete (e.g., OPC and FA) AM is a promising step toward limiting typical Portland cement use [13, 21] and associated CO_2 emissions.

There are several advantages to 3D-printing concrete, but the most important one is that it can swiftly produce complicated and non-standard shapes with fine details. This manufacturing process does not need formwork and uses a specified printing method dependent on the mixture properties and article design. Cement-based concrete AM is still in its early phases of development [22], and much attention is being paid to the development of AM geopolymer concrete, considering sustainability factors in construction.

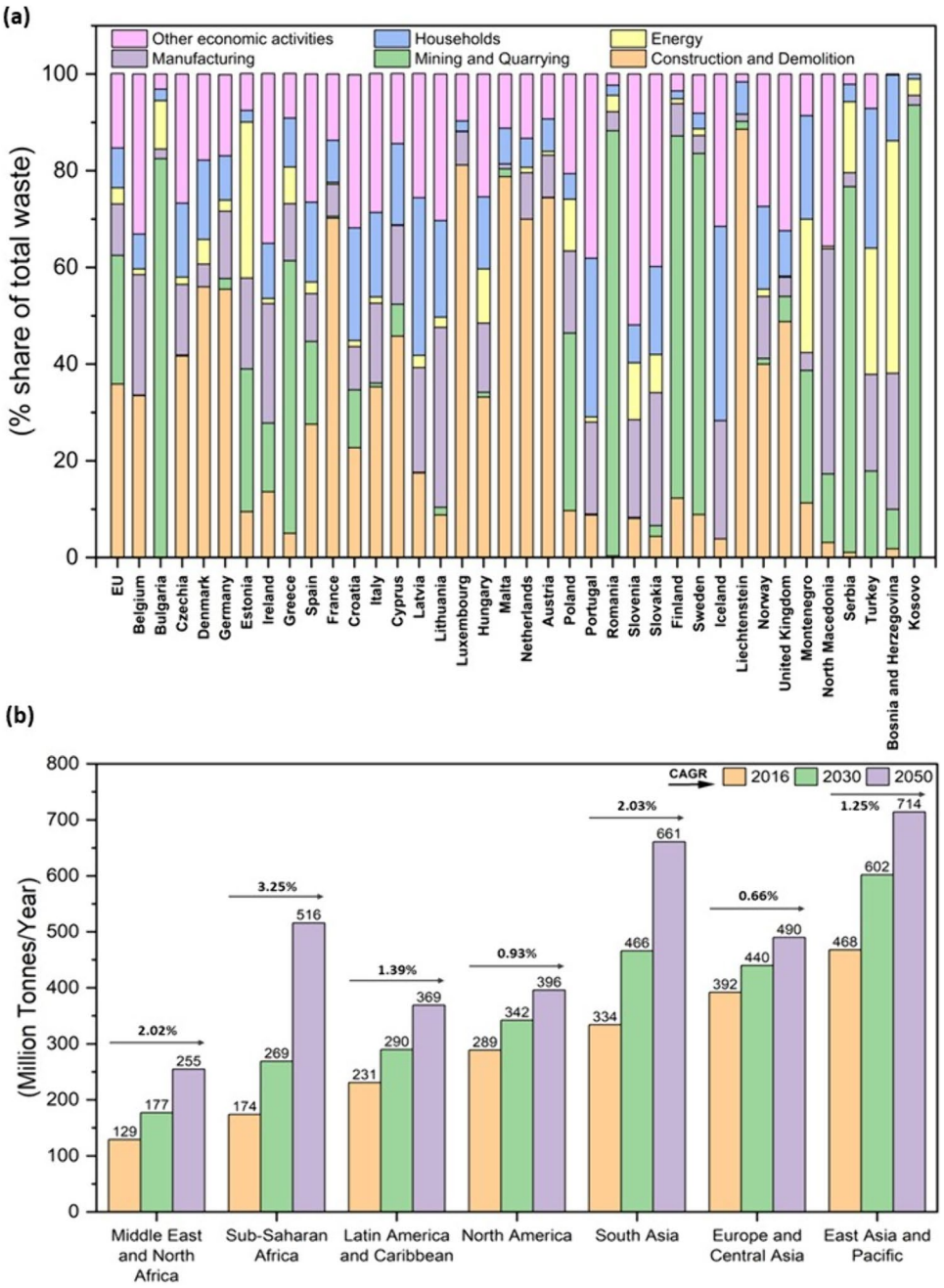

Fig. 1 Waste production **a** Europe split down into industrial sectors, including households, Data source: Eurostat (online data code:env_wasgen), **b** Trends in solid waste management, Data source: The World Bank [1, 2]

This review journal paper investigates critical factors, advancements, and challenges relating to geopolymer composite mixes and their utilization for AM. A bibliometric analysis was carried out first to configure the present stage of knowledge on geopolymer and AM. The next section discussed materials used for geopolymer composites and AM methods. Figure 2 presents several interdepending factors that need consideration to understand and optimize geopolymer-based AM. In order to work with AM processes, an ideal activator-to-alkaline solution ratio (FA: BFS) is explored explicitly from the literature. Optimization for technical specifications of the geopolymer AM machine performance, open time, spreadability, and workability are being discussed. Then, the geopolymer AM system is critically reviewed for the virgin mixture parameters' effects on fresh-state and hardened properties, such as mechanical properties (yielding flexural stresses and tensile bonding strength). Discussion includes potential geopolymer mix designs tailored to the specific 3D printing process considering varying speeds, pressures, printing nozzle types, and methodology. The study finally presents the existing research gap and the prospects for future progress in the geopolymer composite AM field.

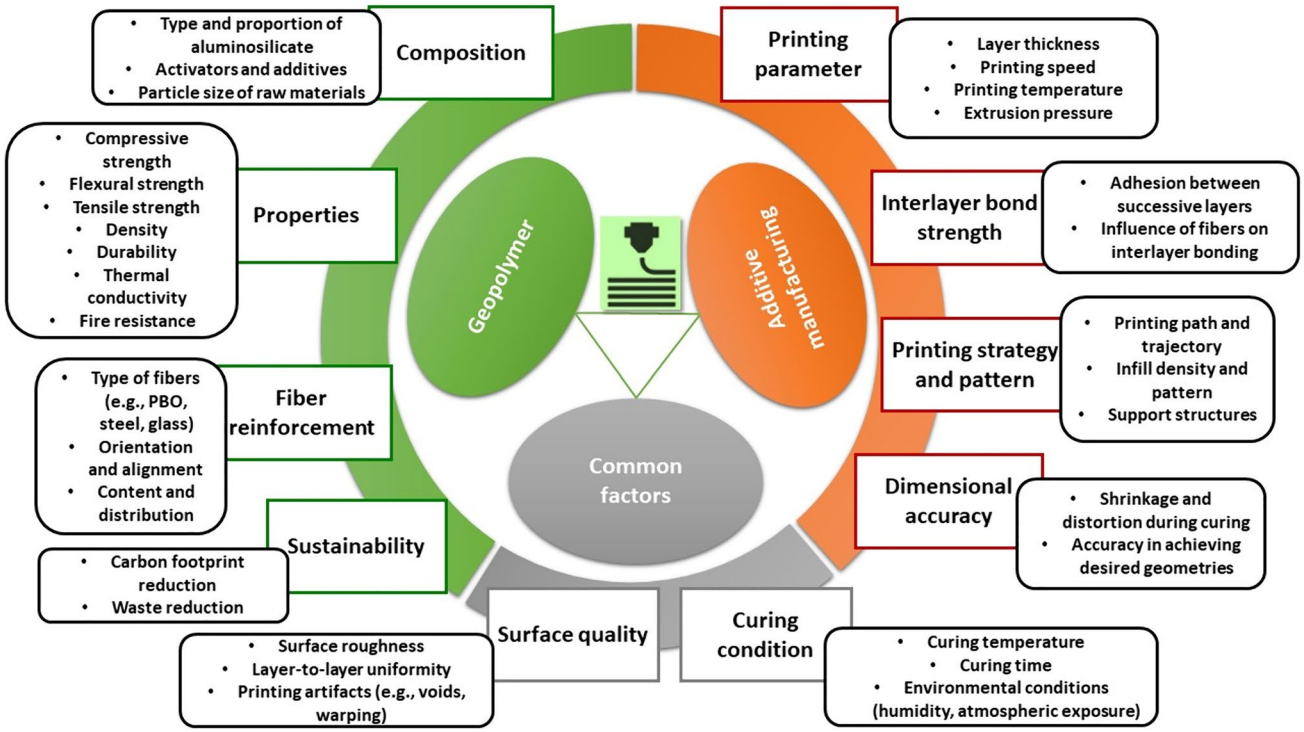

Fig. 2 Factors affecting the AM process of silicate-based geopolymer composites

2 Bibliometric study

This section provides a comprehensive and systematic bibliometric overview of the published research data associated with AM of geopolymer composites (i.e., in the paste, mortar, concrete configuration). It includes an extensive table of the research constituents from the concurrent literature along with a network visualization of the associated keywords. The rationale behind the adoption of this strategy is directed at a clear and concise comparison and interpretation of the research insights. Table 6 ("Appendix") comprises publications from various databases, with the Boolean search strategy of keywords including ["Additive Manufacturing" AND "3D Printing" AND Geopolymer]. Crucial particulars like the author's name, year and type of publication, 3D printing principle, raw materials, and applications are analyzed in Table 6 ("Appendix") comprised 156 reference work, which provides in-depth information on the research progress and developments of geopolymer AM over the years. The articles ranged from 2015 to 2024 (Cont.) and included journals, conference proceedings, reviews, and reports.

Both extrusion and powder bed-based 3D printing techniques have been utilized for geopolymer AM. However, the former found is most common and has been profoundly accepted by industry and the research community. Binder materials were commonly sourced from silicate-based waste and abound minerals, such as different types of slag, FA, MK, and mine tailings. Reinforcements in binders included nanomaterials, glass waste, SF, and different types of fibers (carbon, glass, steel, plastic). Different forms of geopolymer (paste, mater, concrete) were used for AM, targeting conventional applications, such as construction, insulation, and backfill, while exploring multifunctional applications, such as thermal energy storage and adsorption. Further research works are essential to explore novel application scenarios associated with geopolymer AM. The number of publications has been considerably increasing compared to that of a few papers back in 2015. Bibliometric data analysis is presented in Fig. 3, which presents a network of visualization data analysis using the VOS viewer software based on the keywords of publications from Table 6 ("Appendix"). Figure 3 depicts the network visualization of the extensive keyword occurrence (i.e., each keyword is repeated at least five times in different publications) with variable link strength parameters. This network visualization plays a crucial role in identifying research trends and understanding research focus through clustering and categorization. The analysis provides an array of keywords which can be specifically divided under different heads as follows:

(i) Process (3D Printing, Concrete Printing, Additive manufacturing, 3D Concrete Printing, Mixture, Reinforcement, Extrusion, Digital Construction, Curing, Blast Furnaces, Construction, 3D Printing

Selected	Keyword	Occurrences	Total link strength
☑	inorganic polymers	95	919
☑	geopolymers	95	914
☑	3d printers	86	844
☑	geopolymer	89	774
☑	3-d printing	51	554
☑	compressive strength	45	472
☑	3d-printing	35	388
☑	3d printing	41	387
☑	fly ash	29	327
☑	concretes	32	322
☑	concrete printings	27	308
☑	rheology	23	261
☑	additive manufacturing	33	257
☑	3d concrete printing	29	247
☑	slags	18	227
☑	mechanical properties	20	208
☑	sustainable development	15	180
☑	portland cement	16	163
☑	geopolymer concrete	18	159

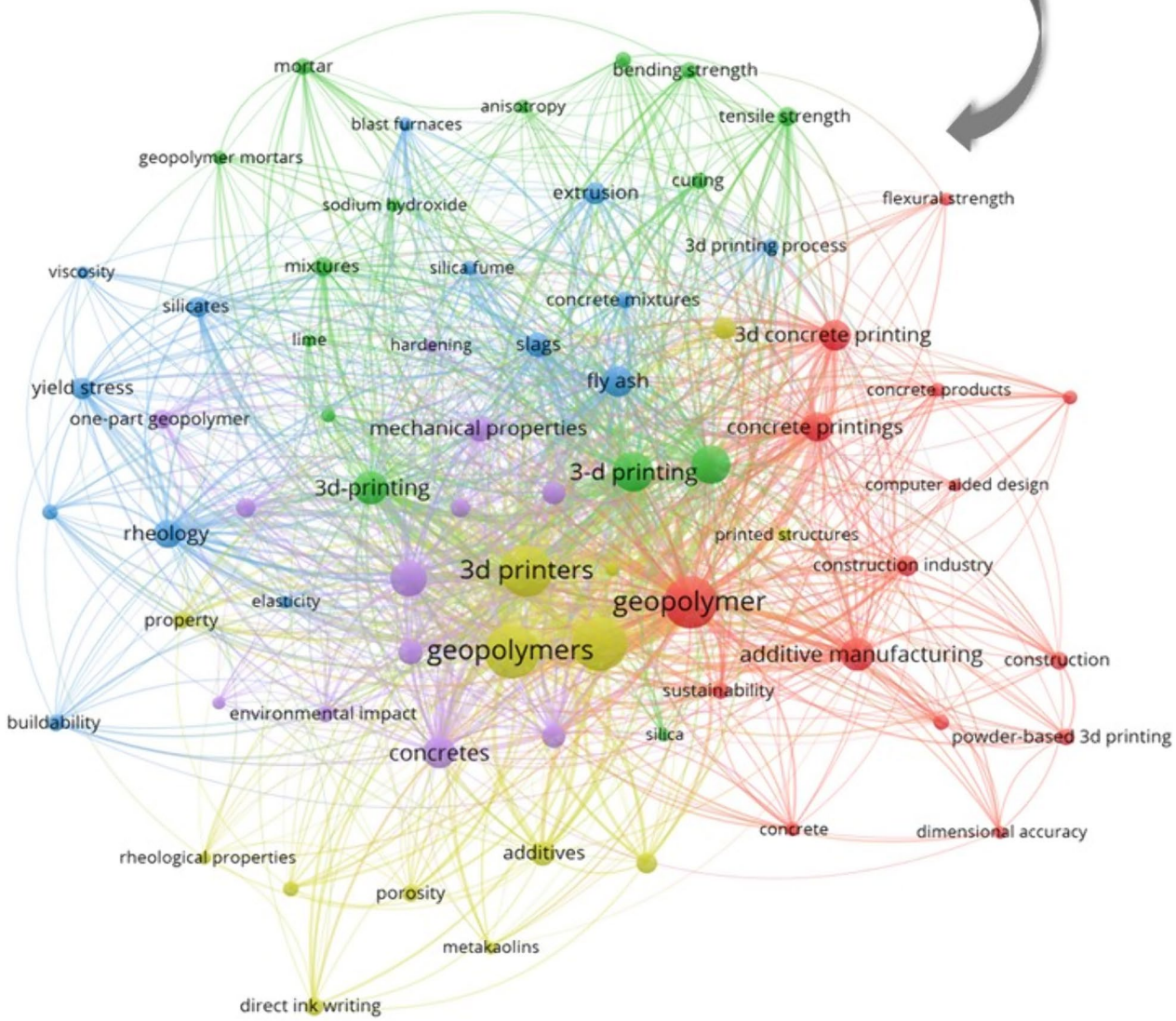

Fig. 3 Bibliometric analysis through the co-occurrence and network of the keywords

Process, Printing Presses, Direct Ink Writing, Printed Structures, Powder-Based 3D Printing, Dimensional Accuracy, Computer-Aided Design)

(ii) Material (Inorganic polymers, Geopolymers, Fly-ash, Concrete, Slag, Portland Cement, Geopolymer Concrete, Additives, Silicates, Binders, Geopolymer Composites, Concrete Mixtures, One-Part Geopolymer, Mortar, Silica Fume, Concrete Products, Sodium Hydroxide, Lime, Geopolymer Mortars, Geopolymer Materials, Silica, Metakaolins)

(iii) Property (Compressive strength, Rheology, Mechanical Properties, Yield Stress, Tensile Strength, Property, Bending Strength, Bond Strength, Rheological Property, Performance, Porosity, Anisotropy, Hardening, Buildability, Mechanical Performance, Elasticity, Thermal Conductivity, Viscosity, Fresh Properties, Flexural Strength)

(iv) Environment (Sustainable Development, Construction Industry, Sustainability, Environmental Impact)

The above keywords allow deeper insights into the key areas of geopolymer 3D printing, and it can be inferred that the focus of the research community is most likely centered on optimizing construction processes, developing environmentally friendly materials, ensuring mechanical integrity, and promoting sustainable practices within the construction industry. These research efforts have the potential to revolutionize the construction sector, offering more efficient, cost-effective, and sustainable solutions for building infrastructure.

3 Geopolymer materials and AM methods

Several rapid prototyping AM techniques are currently used in the construction industry. Cementitious materials are fundamentally utilized to produce concrete-like structures. Such technologies are differentiated by feedstock, the capability of producing dense structure, particle size, surface quality, precision, and cost, among many other parameters. The parameters mostly depend upon the AM process and the resulting product (ceramics, plastics, and metals). The big-scale AM techniques for ceramics are 3D Printing (3DP) and Fused Deposition Modeling (FDM). The challenges in most of the techniques are associated with the appropriate mix design and supporting structures used until the concrete and geopolymer-based composite gains the required strength. FDM is typically suitable for 3D printing with thermoplastic polymer where heat needs to be applied to molten and extrude the polymer through the nozzle.

3.1 Materials in geopolymer for AM

3.1.1 Geopolymer precursors

Commonly used precursors for geopolymer composite are FA, slag, and both of their compositions. Multi-component compositions, such as FA and SF, are also often used in AM technologies. Additionally, trials for incorporating sustainable waste materials, such as construction and demolition waste (CDW), mining tailings, bauxite residue (red mud), rice husk ash, and waste glass, have been successfully used along with a few other potential precursors [86, 111]. Continuous efforts are undertaken by researchers to identify and utilize potential waste materials as precursors in geopolymer AM and could be further broadened in future studies. The distribution of the available studies for major raw materials used for AM geopolymers and their composition can be identified from Table 6 ("Appendix"), which includes FA, MK, Slag, and SF. In comparison with a similar analysis made in [180], it is possible to notice that:

- Slag is less prevalent in AM applications than in traditional technologies such as casting.
- The OPC is only incidentally used as a composition component dedicated to AM applications. It has often been used as an admixture for geopolymer composites manufactured by traditional casting technology.
- The geopolymer composites based on mine tailings were not analyzed in [180], except for the red mud. The red mud has not been applied to the AM of geopolymers yet.
- The SF is a quite popular component for composition, but it has not yet been studied as the only ingredient.

3.1.2 Alkali activators

The alkali activators used in AM are mainly sodium-based chemicals. The activators based on potassium have been tested, but usually, the properties of the final products using this activator are not as satisfactory as in sodium-based [80, 108]. Solid activators are preferable to liquids because of their safety and convenience during their use in the AM process. However, the interlinked studies connected with the final products' mechanical properties have not yet been carried out for AM. Nevertheless, the liquid activator performs better than the solid activators for geopolymer [115, 180]. It is also worth noting that alkali activators have been used in conventional (extrusion) as well as powder bed AM technologies as compounds for post-processing.

3.1.3 Admixtures

The used admixtures are essential elements connected with increasing AM effectiveness. Admixtures have different

functions in the AM process and are added at different stages. Typically, the admixtures are applied in first stages of the process: (i) pumping and deposition in the case of extrusion-based technology [62], and (ii) the first stage of powder preparation and mixing in the case of powder bed technologies. In the analyzed articles, the most common admixtures were rheological agents, especially polyethene glycol, and reinforcements included fiber or mineral admixtures [62]. The other popular admixtures were retarders, sucrose [116], and viscosity-modifying agents, including anhydrous borax, sodium carboxymethyl cellulose, sodium carboxymethyl starch, and commercial compounds marked as Zb® 63 and AE agent [51, 55, 80, 89]. The thixotropy was modified by adding magnesium aluminosilicate, attapulgite nano-clay, or commercial compounds marked as ATTAGEL-50 [54, 83, 116]. Some admixtures were also dedicated to the properties required for a specific final product, for example, the porous structure (achieved through the addition of Lightcrete 02™ foaming agent and foam stabilizer) [61] or ion-exchanging properties given by such admixtures as Ba $(NO_3)_2$ and Sr $(NO_3)_2$ [57]. The other group of admixtures is connected with material formability which could work against crack propagation. Examples of those admixtures are PVA or polypropylene fibers [56, 76] or improve the mechanical properties, such as steel micro-cable and glass fibers [56, 90, 124]. Recently nanomaterials, such as graphene derivatives, carbon nanotubes (CNT), nano-silica are also used as admixtures to develop advanced geopolymer-based composite and AM applications [181–186].

Different admixtures are used to uniquely modify properties of geopolymers such as foamed materials [75, 187]. Their use gives new perspectives for applying geopolymers in AM. Modifying geopolymer mixes may open new perspectives for advanced AM applications, such as in water treatment, enzyme immobilization, catalyst process, an artificial reef, high-performance radiation shielding, electromagnetic interference shielding, and multifunctional advanced composites [87, 104, 184, 188, 189]. A promising option is the development of functional geopolymer-based applications in the building industry [121, 187]. AM geopolymer is also the better replacement option for ordinary Portland cement as a building material in future [190]. Although high processing and components are required for geopolymer composition [187], advanced and sustainable geopolymer composites progressing fast for exceptional applications made in AM industry.

3.2 AM methods

The AM currently used in building & construction applications can be classified into two fundamental groups: materials extrusion (extrusion-based) and binder jetting (powder-based). Different types of printing configurations currently being utilized by researchers and industries are shown in Table 1. Most of them refer to material extrusion technology, where fresh concrete is extruded through a nozzle moved by a robot-like apparatus to realize the final component layer by layer. This technology is often referred to as robocasting. Notably, when confronting intricate architectural configurations, the robocasting process encounters certain constraints, most conspicuously the absence of a support mechanism to buttress individual layers. This makes it challenging to obtain precise dimensions on the final printed part.

Table 1 AM configurations used in the construction and composite industry

Company	Printing System	Printer	Build size (m)	Country	References
BetAbram	Gantry^{E}	P1	16×8.2×2.5	Slovenia	[194]
COBOD	Gantry^{E}	BOD2	14.62×50.52×8.14	Denmark	[195]
Constructions-3D	Robotic Arm^{E}	MAXI PRINTER	12.25×12.25×7	France	[196]
CyBe	Robotic Arm^{E}	RC 3Dp	2.75×2.75×2.75	The Netherlands	[197]
ICON	Gantry^{E}	Vulcan II	2.6×8.5×∞	The USA	[198]
MudBots	Gantry^{E}	Concrete 3D Printer	1.83×1.83×1.22	The USA	[199]
Total Kustom	Gantry^{E}	StroyBot 6.2	10×20×6	The USA	[200]
WASP	Dela^{E}	Infinity 3D Printer	Ø 6.3×3	Italy	[201]
Apis Cor	Robotic Arm^{E}	3D printer	8.5×1.6×1.5	The USA	[202]
Batiprint3D	Robotic Arm^{E}	3D printer	7 (Height)	Italy	[203]
SQ4D	Gantry^{E}	ARCS	9.1×4.4×∞	The USA	[204]
XtreeE	Robotic Arm^{E}	3D printer	–	France	[205]
CONCR3DE	Gantry^{P}	Large-Scale Printer	0.6×1.2×0.3	The Netherlands	[206]
ExOne	Robotic^{P}	S-Max® Flex	1.9 1 1	USA	[207]
Voxeljet	Gantry^{P}	VX4000	4 2 1	Germany	[208]

E, extrusion; P, PowderBed

In additive manufacturing (AM), geopolymers are a promising way to develop materials for practical application in manufacturing on a larger scale. Still, it requires the development and optimization of geopolymer composites. The full exploitation of AM in the construction industry is currently limited due to the in-process and in-service performance of the available materials [82]. The materials requirements are strictly in line with the technology used. In the case of geopolymers, both materials extrusion and powder bed-based AM technologies have been tested [37, 191–193]. The design of the proper materials for these technologies is slightly different. A gantry-based printing setup is commonly used for powder bed-based AM, where both gantry and robot arm are found common in the extrusion AM. The extrusion-based AM are progressing fast, considering its versatility and large scale of printing objects, particularly in the civil infrastructure construction field. A key parameter in the extrusion-based AM process is to have a consistent flow of extruded geopolymer materials with desirable printed layer retention capacity.

3.2.1 Extrusion-based AM

Figure 4 presents several extrusion-based AM using geopolymer composites. Based on the extrusion process, the AM requires materials in the form of a paste that is injected into the extruder, usually through systems of nozzles. The end composites should have a good combination of essential material properties, such as pumpability, extrudability, buildability, thixotropic properties, short time of curing and the possibility of curing in low temperature, interlayer bonding, and segregation prevention, durability, ductility, high tensile and compressive strength (CS), low coefficient of thermal expansion, resistance to UV light, etc. [37, 191–193]. Further, the most important, according to the final price and properties of the geopolymer products made in AM, are also post-processing procedures. The appropriate methods could considerably increase the geopolymer properties but are hard for practical application. For example, curing in high temperatures, such as 50–80 °C, significantly increases the mechanical properties of the geopolymers. Still, it is tough to apply in AM, requiring technical solutions [25].

Nowadays, from the material point of view, one of the most critical issues is the possibility of modifying geopolymer mixes to gain particular properties and enhance the eco-efficiency of AM [121]. It could be achieved using eco-friendly components, such as industrial waste, mine tiling, etc. However, the most often used raw materials for extrusion-based AM are FA, slag, and MK; the other raw materials are also becoming increasingly popular. Table 7 ("Appendix") presents the precursors and the critical findings of

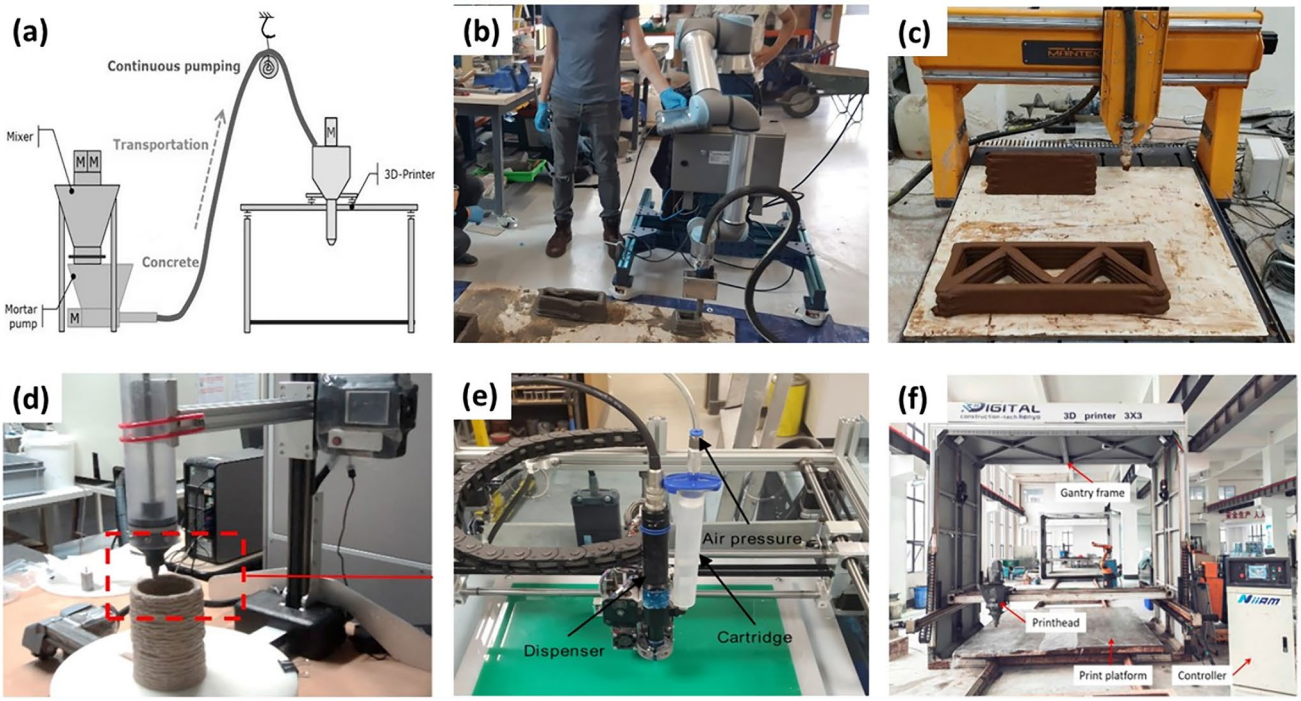

Fig. 4 Extrusion-based AM using geopolymer composites: **a** Schematic of geopolymer extrusion, **b** extrusion-based geopolymer extrusion-based 3D printing using a robot arm at UWE Bristol laboratory, **c–f** Extrusion AM using a gantry-based system Reproduced with permission from Refs. [70, 124, 146, 151, 209]

studies focused on extrusion-based AM geopolymer technologies. It is based mainly on recent research, especially in the last 6 years. This Table 7 especially shows the variety of used materials and their obtained compositions, as well as additives that can improve the material properties, such as extrudability.

Table 7 ("Appendix") also provides a few notable advantages and disadvantages of extrusion-based geopolymer AM. Indeed, the merits include the cost-effectiveness of the 3D printer, ease of customization according to the requirements, and the unconstrained scale of printing, while some of the shortcomings consisted of low printing accuracy, low interlayer bonding strength, high rheology precision control, difficulty in printing sharp corners and anisotropic nature of the printed object. Therefore, future works could focus on the issues/constraints of extrusion-based geopolymer AM, which include the workability of the fresh mix, deformation of the placed material, conformity to the desired geometry, and geometrical freedom in design afforded through the process [215].

3.2.2 Powder bed-based AM

Contemporary AM technology based on powder bed is less common compared to the extrusion process applied to geopolymers. This is because of their main advantage—cost-effectiveness. However, the extrusion process of 3D printing has some disadvantages. The most important ones are limitations in shape—overhangs can only be printed with the help of support structures, and the accuracy is low [36].

Figure 5 presents several powder bed-based AM technologies. The powder bed technology, such as binder jetting, requires material from very fine particles (powder). The elements are created by depositing the activator liquid (or "ink") selectively onto the powder bed to bind powder where it impacts the bed [35]. In this case, the powder geometries have a significant meaning, including the specific area of the grains [35]. The other important factor is wettability, which allows the joining of the grains and strongly influences the powder's activation time with the activator. Because of that, powder bed technology requires knowledge in the area of powder mechanics as well. This technology allows for more esthetic elements than extrusion-based technology but requires a longer time for element production [216]. The powder bed technology is also more environmentally friendly, but it significantly limits the size of the elements [25]. This has a significant meaning in the case of the building industry.

Chen et al., in their investigation, identified an optimal value of inorganic activator (activator) in MK-based geopolymer to obtain the highest mechanical properties [219]. The MK–sand (1:8) mixture powder bed was a printer with the same inorganic solution as activator liquid, and the effects on the geometry of the printed article were studied. The varying amount of activator has been printed to achieve the optimum value of the activator amount in the powder bed. The

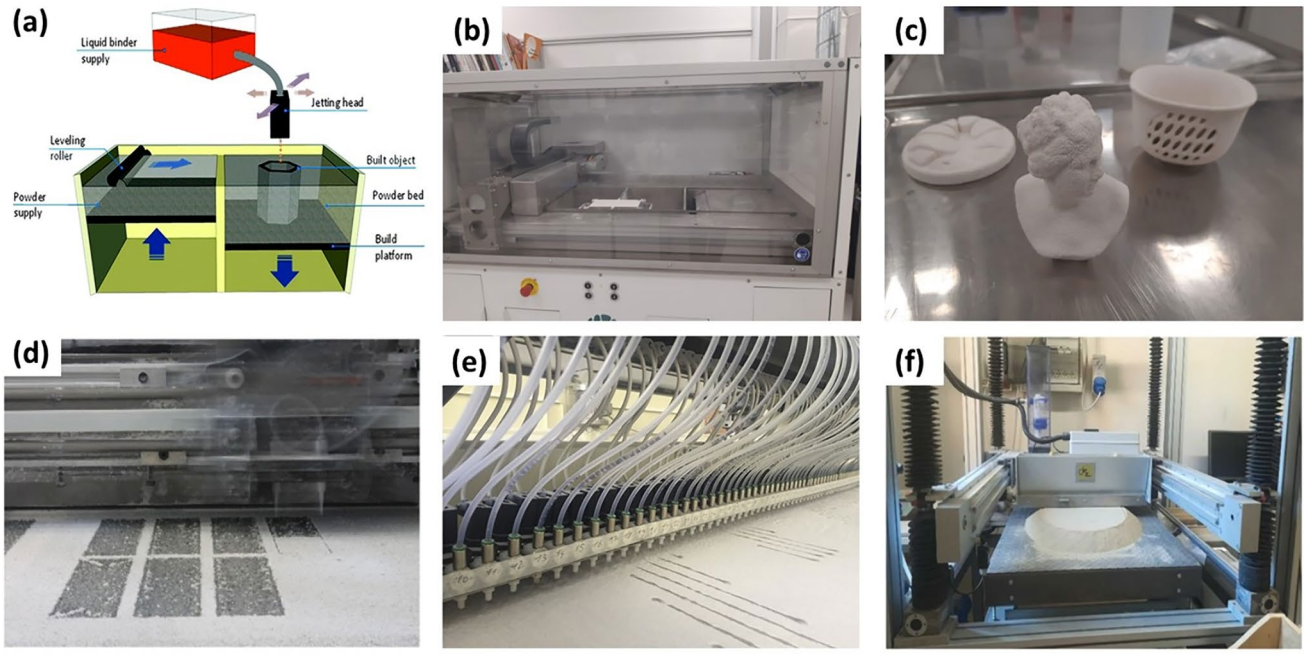

Fig. 5 Powder bed-based AM technology: **a** Schematic of powder bed-based AM process, **b**, **c** AM system and few high precision printed objects at the UWE Bristol laboratory, **d**–**f** Other geopolymer powder bed-based AM. Reproduced with permission from Refs. [117, 142, 217, 218]

absorption of the silicate-based activator into the MK-based powder bed was studied [219]. Then, a geometric model in all three dimensions for absorption was presented.

Interestingly, due to the deficient secondary absorption of Alkali-Activated Concrete (AAC) [220]-based powder bed, only the printed specimen's depth changes dimension when the amount of activator increases. That is contrary to the OPC concrete or organic activator printing [147]. The best ratio of the activator (Na_2SiO_3, NaOH, and water) in terms of geometric accuracy and mechanical properties were achieved at ~ 7.5 min.

Another research study [72] demonstrated the binder jetting of alkali-activated geopolymer precursor for the environmentally friendly use of this technology. The geopolymer cement was used in a custom-built 3D printer based on binder jetting technology. An innovative construction printer was built to increase the ease of powder deposition and its utility by shifting the powder deposition platform above the printing platform. The printer could change the layer thickness, activator jet spacing, speed, activator flow rate, and several other parameters. The powder bed has been prepared by mixing the commercially available silica sand and MK (8:1) [72]. The inorganic liquid activator was prepared by mixing Na_2SiO_3, NaOH, and water. Each constituent of the activator mixture has been added to achieve the desired properties during geopolymerization [72]. The printed specimen showed a modulus of rupture (MOR) and compressive strength (CS) of 5.15 MPa and 4.3 MPa, respectively, which is significantly higher than the ordinary Portland concrete (OPC) printed sample as an organic activator printed sample. The analysis of the geopolymerization/activation using SEM and XRD shows the increase in geopolymer phases with the amount of activator. These AM structures (MK-based geopolymer) can be used in various structural applications, from construction elements to thermal insulations.

Moreover, powder bed technologies are tested for extreme applications, such as space one. The D-shape large-scale 3D printer was tested by the European Space Agency (ESA) for the printing process in the simulation of the lunar environment, where lunar regolith was used to create stone-like objects [221]. AM has been positively validated also for planetary regolith-based concrete and geopolymers, such as sorel-type cement (MgO-based), sulfur cement, polymers/trash composites, and Portland cement [30]. Despite testing the space applications, there are still a lot of challenges connected with the materials used for powder bed technologies, as included in Table 8 ("Appendix"), which shows the geopolymers and their composites tested for powder bed technologies from the same period. It is visible that this technology is less popular than extrusion-based; however, this could have a significant influence on the development of these materials for further applications such as space habitants [222, 223].

Like Table 7 ("Appendix"), powder-based geopolymer AM, as in Table 8 ("Appendix"), also faces challenges, including uneven surface texture, complex and costly 3D printers, slow print rate, limitation in print size, and post-processing requirements. While printing parameters can influence macro-porosity to some extent, achieving consistent control remains a limitation in the fabrication process [81, 224]. Additionally, achieving comparable strength between heat-cured and ambient temperature-cured samples poses challenges, despite advancements in post-processing methods [59]. These issues have restrained the utilization of powder-based geopolymer AM in the commercial and industrial market by reducing the application base and could be followed in future studies. However, the method allows for the printing of geopolymer products with high accuracy and resolution without the requirement of support, which provides an edge over the extrusion-based geopolymer AM.

4 Properties of AM geopolymer composites

AM of geopolymer composites is governed by diverse components, which determine the end print of the composites. The variable features include the type of printing method, geopolymer precursor materials, activators, additives, curing conditions, etc. These bring about the end property transitions in the end print while providing room for further enhancement and modifications along with the required characteristic properties. Factual evidence from Table 9 ("Appendix") can be assimilated to highlight the growth and development of AM geopolymer composites in different applications with adequate properties. CS and FS were one of the most investigated properties by the investigators. Table 7 ("Appendix") also showcases other crucial properties and parameters of past literature studies in the development of the printing of geopolymer composites.

Figure 6 presents the collective depiction of all the significant parameters of geopolymer AM and its properties. The important factors for fresh state properties of geopolymer AM are extrudability, shape retention, thixotropic open time, buildability, and reaction kinetics. The hardened state properties are shrinkage, bulk density, mechanical properties and layer adhesion. The following section describes the requirement and fresh and hardened properties of geopolymer composites in the application of AM. The section describes the necessity of recent AM in geopolymer concrete construction and follows up to present a brief idea about the different suitable materials used by past studies. The development of the materials in geopolymer AM has been discussed in detail, starting from the material selection to end engineering properties.

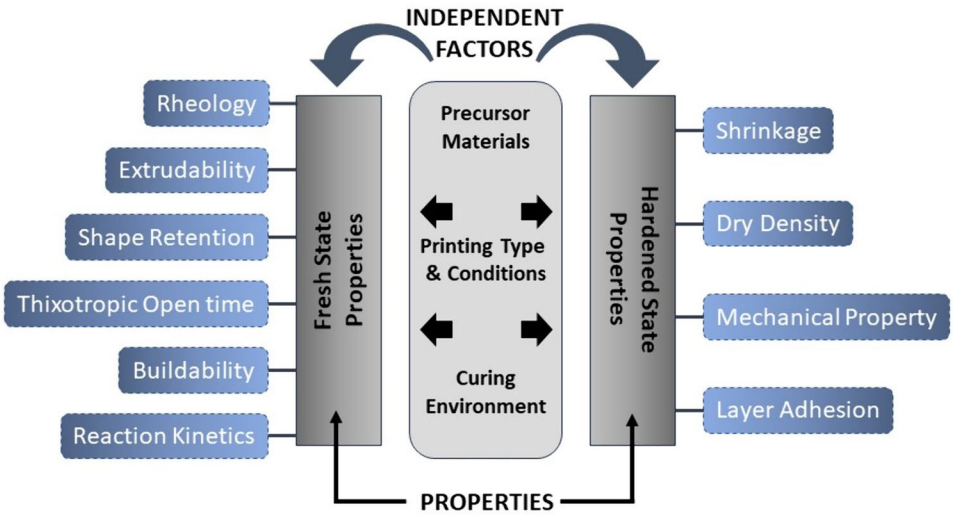

Fig. 6 Parameters and properties of geopolymer AM

4.1 Fresh-state properties

4.1.1 Rheology

The rheological properties of geopolymer materials are considered decisive for 3D printing for several reasons. An optimal mix of geopolymer should possess: (i) high-yield stress for favorable extrusion without collapsing, (ii) low viscosity for smooth flowability, and (iii) good thixotropic properties for higher shape retention ability. The scope of the geopolymer rheological properties includes the buildability of 3D-printed parts, apart from the yield stress, viscosity and thixotropy. Any imbalance in the rheological properties can induce defects in the end products. Zhao et al. analyzed the geopolymer printing materials parameters for rheological and mechanical properties improvement [115]. Rheological agents could modify specific parameters of geopolymer fresh properties. The authors identified four key geopolymer parameters for rheological property improvements in AM [115]:

- Particle spacing increases (reduction in particle concentration) with the increase in w/s ratio, increasing the amount of suspending fluid, or the increase of activator solution-to-activator ratio.
- Particle size decreases (by adding finer particles or getting a higher particle surface).
- Particle interaction force increases (by adding thixotropic agents and reinforcing agents, including microfibers and nanomaterials) by altering Van Der Waals forces.
- Modification of alkali activator viscosity by increasing the molar ratio or the concentration of alkali activator as well as admixture (decreasing the migration rate of water and active particles).

Few of the adopted thixotropic agents include hexagonal boron nitride [91], urea, naphthalene, polycarboxylate [100], MAS [116], Sodium carboxymethyl starch [68], Sucrose [116], polyethylene glycol [104], Sodium polyacrylate [226], Lateritic clay [54], Acti gel [227], Borax [171] etc. Similarly, the familiar fiber reinforcements include carbon fiber [106], wollastonite [78], glass fiber [28], PP fiber [33] and nanomaterials GO [71], Nanographite [210], Nanoclay [54], micro-crystalline cellulose [228], Attapulgite nano-clay [229].

Table 2 provides information on the range of rheological parameters and measuring instruments for AM geopolymer. The table summarizes the rheological parameters of various construction materials and mixtures. Notable findings include a paste composition of FA (Class F) + GGBS + SF + NaOH + Na_2SiO_3 with a slump range of 330–496 Pa [37] and various mortar mixtures exhibiting distinct rheological behaviors, with yield stress and viscosity values ranging from 6.74–106.97 Pa and 5.50–8.80 Pa s (PV) measured using the RVDV-2 instrument [35, 54, 62, 78, 83, 171, 210, 229, 230]. Additionally, diverse rheological properties were observed in paste compositions, such as high viscosity ranging from 4950 to 30,000 Pa s (AV) for MK + Na_2SiO_3 + Hexaboron Nitride + Water [91] and lower viscosity ranging from 20,000 to 200,000 Pa s (PV) for DNA 1 LRS + NaOH + Urea + Water [127]. The influence of fibers on rheological parameters was noted in mixes containing materials like Wollastonite Fiber and PVA [78, 229, 230]. These findings offer insights into the rheological behaviors of construction materials, which are crucial for optimizing formulations for various construction applications.

Table 2 Review of rheological properties and instruments used

Matrix	Precursor materials	Rheological parameter			Rheological instrument	References
		Slump	Yield stress	Viscosity		
Paste	FA (Class F) + GGBS + SF + NaOH + Na_2SiO_3		330–496 Pa		Anton Par (MCR102)	[37]
Mortar	FA + Slag + SF + Na_2SiO_3 + Sand + MAS + Water		6.74–106.97 Pa	5.50–8.80 Pa s (PV)	RVDV-2	[83]
Mortar	FA (Class F) + GGBS + SF + NaOH + K_2SiO_3 + Sand + Water		0.39–1.63 kPa		Anton Par (MCR102)	[35]
Mortar	FA + GGBS + SF + NGP + NaOH (10 M) + Na_2SiO_3 + Sand + Water	23–57.5%	11.95–36.5 Pa	6.61–17.27 Pa s	Kinexus Prime lab +	[210]
Mortar	FA (Class F) + GGBS + Nano-clay + KOH + K_2SiO_3 + Sand + Water		1.42–7.71 kPa	15.4–18.83 Pa s (AV)		[54]
Paste	MK + Na_2SiO_3 + Hexaboron Nitride + Water			4950–30,000 Pa s (AV)	TA Instruments (AR2000 EX)	[91]
Paste	DNA 1 LRS + NaOH + Urea + Water		2.61–43 Pa	20,000–200,000 Pa s (PV)	Anton Par (MCR302)	[127]
Paste	GGBS + Steel Slag + NaOH + Na_2SiO_3 + Defoamer + Superplasti-cizer + Latex		0.34–3.44 Pa	0.42–0.78 Pa s		[49]
Paste	MK + NaOH (10 M) + Na_2SiO_3 + Water		0.52–0.60 kPa		RheoWin (HAAKE Viscotester iQ)	[123]
Mortar	FA (Class F) + GGBS + KOH + K_2SiO_3 + Sand + Water		2648–4828 Pa	6.4–8 Pa s (AV)		[62]
Concrete	FA (Class F) + GGBS + Na_2SiO_3 + Sand + MAS + Su crose + Water		0.06–1.71 kPa	210–1000 Pa s (AV)	Viskomat XL	[116]
				30,000–100,000 Pa s (PV)		
Mortar	FA (Class F) + GGBS + Na_2SiO_3 + Sand + Wollastonite Fiber + Water + Sucrose		1–2.50 kPa			[78]
Mortar	FA + GGBS + SF + PVA + NaOH + Na_2SiO_3 + Sand	22.5–34.5%	1.21–1.36 kPa			[229]
	FA + GGBS + SF + Attapulgite Nano-Clay + NaOH + Na_2SiO_3 + Sand	18.5–34.5%	1.21–1.7 kPa			
Paste	MK + K_2SiO_3 + Wollastonite Fiber			23- > 6000 Pa s (AV)	Brookfield DV-II	[230]
Mortar	FA (Class F) + GGBS + Na_2SiO_3 + Sand + Borax + Water	1.95–46.1 mm				[171]
Mortar	FA (Class F) + GGBS + Ground BW + Na_2SiO_3 + Sand + Water + Nanoclay + Sucrose	135–152.5 mm	536–2748 Pa	8253–237,692 Pa s (AV)	Viskomat XL	

PV, plastic viscosity; AV apparent viscosity

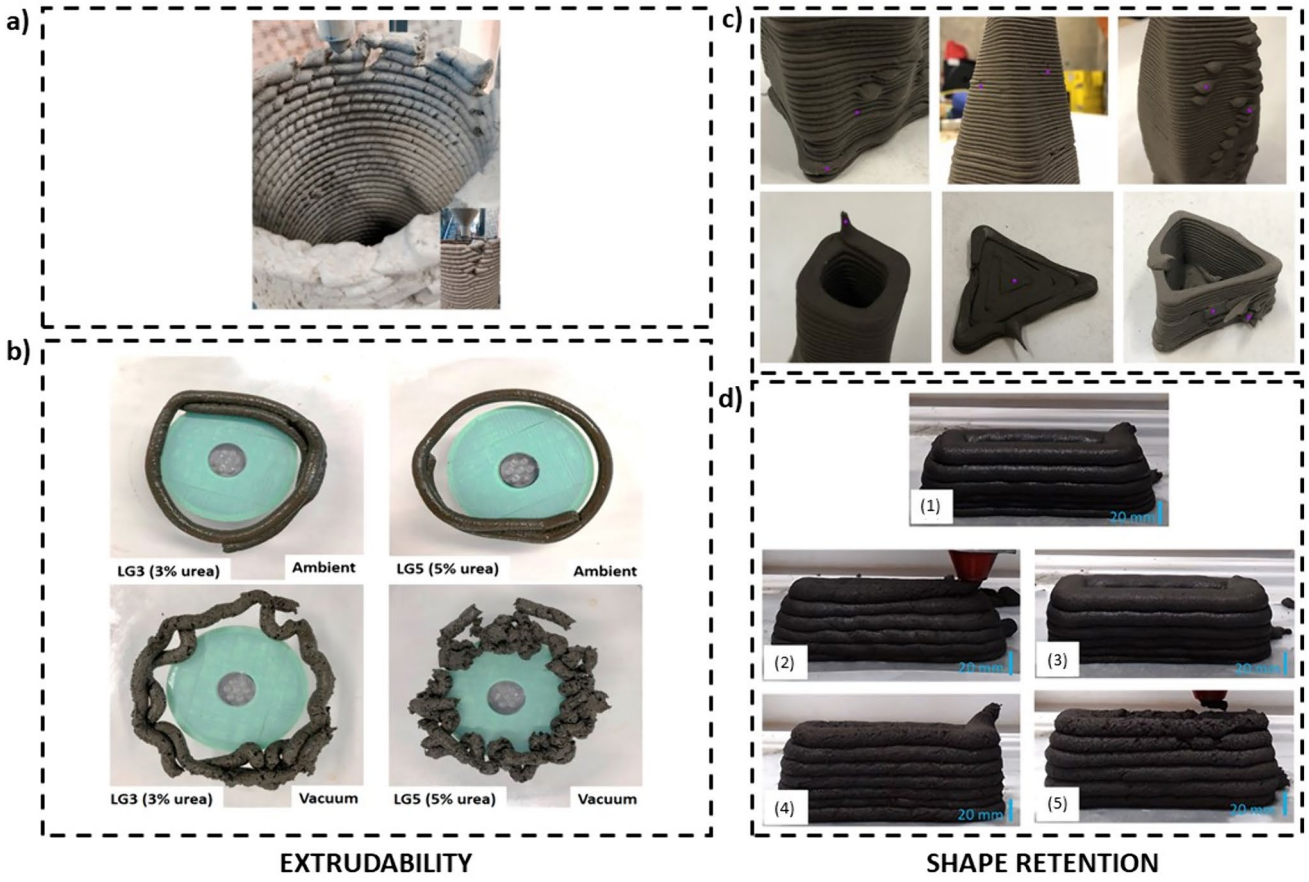

Fig. 7 Literature analysis of Geopolymer 3D printing Extrudability, **a** Discontinuous Extrusion, **b** Different Environments, Shape Retention **c** Robotic Arm printing, **d** Gantry printing. Reproduced with permission from Refs. [116, 127, 230, 234]

4.1.2 Extrudability

Extrudability of an AM material is vital for smooth pumping ability without any disruption or clogging in the extrusion pipe. Inappropriate geopolymer mixtures or mixing procedures can cause a decrease in extrudability, including segregation of the particles, nozzle lodging or filament tearing [127]. Extrudability can be directly correlated with the build speed and structural integrity to increase consistency and reduce waste generation. Rheological properties, including plastic viscosity and yield stress, play a major role in determining extrudability. Higher rheological values mostly contribute to enhancing the buildability but decrease the extrudability and vice versa [131]. Different internal factors, such as the physical and chemical properties of the precursor source materials, activator and aggregate content and quality, generate a significant impact on the viscosity of the geopolymer mixtures [110]. Figure 7a depicts the typical representation of a discontinuous type of extrusion of geopolymer material, whereas Fig. 7b demonstrates the same in different printing environments, such as ambient and vacuum conditions.

Extrudability is influenced by different alkali activators, blending of precursors and their proportions in geopolymer composites. The effect of sand on the extrudability of FA-slag-SF-based geopolymer activated by NaOH and K_2SiO_3 was investigated by measuring torque and yield stress [35]. Results exhibit poor extrudability of geopolymer with higher sand/activator ratios of 1.7 and 1.9 due to high static yield stress. Another study investigated the effect of time interval on the extrudability of FA-slag-SF-based geopolymer activated by K_2SiO_3 [39]. The observation suggests that the geopolymer was extrudable up to 20 min, which was reflected in higher yield stress and viscosity beyond 20 min. The investigation into sodium-based activator-activated FA geopolymer revealed that the presence of 10% SF, 10% slag, and a combined slag-SF ratio of 10% led to significantly higher yield stress compared to the control FA geopolymer [37]. The yield stress of these geopolymers also increases with an increase in resting time. A similar study suggests that FA-slag-SF geopolymer activated by K_2SiO_3 is reasonably extrudable even after 25 min of mixing [27]. Static yield stress and viscosity of FA-based one-part geopolymer increase with the increase in slag and activator contents,

where the low viscosity and high-yield stress of the FA-slag blended geopolymer exhibit buildability property [62]. Yin et al. [69] studied the effect of slag contents on the setting time of FA geopolymer and reported slag contents of 20–30%, and the final setting time is just below 35 min. This indicates that the FA geopolymer containing 20–30% slag should be extruded before this time to prevent clogging in the pipe. Zhang et al. [49] studied the effect of Si/Na ratios on the yield stress of GGBFS and steel slag blended geopolymer. By increasing the sodium activators ratio, the yield stress of printable geopolymer paste is increased by 10 folds. They also observed that yield stress increases with time in a non-linear manner, which is favorable for holding the upper layer by the bottom layer in AM. Likewise, another study by [231] also reported a similar increase in yield stress with an increase in activator content and time, irrespective of water/activator ratios. They reported that yield stress above 2 kPa is not possible to measure.

Admixtures and viscosity modifiers can predominantly affect the extrudability factor of the geopolymer mix. Sun et al. [68] studied the effect of sodium carboxymethyl starch (SCSM) on shear stress and viscosity of slag-calcium carbonate blended geopolymer and observed an increase in shear stress with an increase in shear rate irrespective of SCSM content and at any shear rate the shear stress increase with the increase in SCSM content. They also observed the shear-thinning phenomenon with an increase in SCSM content, which is beneficial for the easy movement of geopolymer slurry through the nozzle due to the breaking of the molecular chain of the SCSM. The introduction of fiber reinforcement can significantly increase the viscosity of the geopolymer mix. Nevertheless, the influence of the fibers can be reduced if the shear rate of the printing process is kept high. Appropriate optimization measures are essential to control the influence of the reinforcing materials on the extrudability factor since the utilization of reinforcing fibers is inevitable in the development of geopolymer AM. The effect of different commonly adopted fiber reinforcements on the geopolymer extrudability can be estimated through the slump flow and rheology test of the geopolymer mix. Higher viscosity values of the geopolymer slurry tend to obtain higher values of hardened properties. Maximum compressive and flexural strength was achieved with a viscosity of 2.5–10 Pa s [232]. Nevertheless, there is a lack of generalization in the data for optimizing the extrudability parameters of AM geopolymers due to limited studies on geopolymer AM. Possible research gaps include appropriate standardization methods for evaluating the geopolymer extrudability and optimization of geopolymer formulations for 3D printing.

4.1.3 Shape retention

Shape retention is an essential factor for geopolymer AM. The printed geopolymer is expected to retain its shape as per the extruder dimension after extruding. The material should possess low slump characteristics to achieve good shape retention, i.e., high-yield stress, so it will be stable under its weight. The shape retention of the AM geopolymer has been evaluated through different approaches by different authors and has been summarized in Table 3. The geopolymerization reaction rate impacts the shape retention capability of the AM geopolymer (Rheological properties and compressive strength of construction and demolition waste-based geopolymer mortars for 3D printing). The shape retention of FA-slag-SF geopolymer reported an increase in shape retention factor with the increase in sand content [35]. A correlation between geopolymers' yield stress and shape retention factor was also reported [35]. The authors have also explored the viscosity recovery potential of the AM geopolymer, which is beneficial for higher shape retention characteristics [35]. Bong et al. [55] studied the effect of different types of sodium and K_2SiO_3s and the silicate-to-hydroxide ratios on the shape retention of FA-slag geopolymer. They observed that the shape retention of geopolymer made by N-grade Na_2SiO_3 is much higher than that of D-grade

Table 3 Summary of evaluation criteria for shape retention by various authors

Sl. no.	Evaluation criteria	References
1.	$\text{SRF} = \frac{\text{Cross Sectional area of 3D sample before demoulding}}{\text{Cross Sectional area of 3D sample after demoulding}}$	[35]
2.	$\text{SRF} = \frac{\text{Cross Section area of extrudates after printing}}{\text{Cross Section area of the orifice}}$	[54]
3.	$\text{SRF} = \frac{\text{Designed layer width of Filament}}{\text{Actual printed layer width of Filament}}$	[61]
4.	$\text{Shape Deformation} = \frac{\text{After Demolding}-\text{Before Demolding}}{\text{Before Demolding}} \times 100$	[100]
5.	$\text{SRR} = \frac{\text{Width of Nozzle}}{\text{Width of Filament}}$	[55]
6.	$\text{DDR} = \frac{\text{Measured Length}-\text{Length of CAD designed model}}{\text{Length of CAD designed model}} \times 100$	[74]
7.	$\text{SRR} = \frac{\text{Top widths of the printed prismatic specimen}}{\text{Bottom widths of the printed prismatic specimen}}$	[65]
8.	$\text{SRR (Thickness)} = \frac{\text{Thickness of specimen at measuring time}}{\text{Thickness of specimen when it was just extruded}}$	[157]

SRF, shape retention factor; SRR, shape retention ratio

Na_2SiO_3. No correlation between shape retention factors and ratios of Na_2SiO_3 to NaOH is observed in this study. The same is also true for K_2SiO_3s. Additionally, the authors evaluated the shape stability of one-part (FA/GGBS) AM geopolymer by forced physical deformation and observed that the mixture was able to sustain a load of around nine times its self-weight [110]. Increasing the activator quantity improves the shape retention factor due to mixture re-flocculation. The re-flocculation rate can assist in estimating the plastic collapse of the extruded material [116]. Ilcan et al. advocated the employment of CDW for geopolymer AM, as no admixtures or rheology modifying agents were needed to obtain the required shape retention during his experiments [151]. Consequently, the shape retention of geopolymers with different printing systems has been shown in Fig. 7c, d. Further research should explore the relation of geopolymer layer shape stability through different mixing protocols and in different printing environments.

4.1.4 Thixotropic open time

The thixotropic open time (TOT) for geopolymer AM could be easily explained as the time period, starting from the addition of alkaline activators to the precursor materials until the mixture shows poor extrudability and cannot further be deposited without collapsing or slumping [65]. The TOT is generally shorter than the initial setting time, which is considered for conventionally casted geopolymers and is often confused to be the same [79, 110]. Experimental investigations by Le et al. [234] found that the open time of 3D-printed cementitious material significantly depends on the same setting time. As time passes, difficulties in printing the concrete arise as the workability of the concrete gets reduced with time. TOT of the geopolymers must be considered necessarily during the mix design inception phase to avoid hardening of the mixture in the nozzle or the container [210]. Similarly, Le et al. [234] found the change in shear strength with time to indicate the end of open time at which printing of the materials is complex. Their study stated a 0.3 kPa increase in the shear strength of the printed layer at the end of open time.

On the other hand, a different study by [231] defined open time as a time span to print a subsequent layer of material directly affected by the initial setting time. This, in other words, influences the bond between the layers. They reported that the initial setting time of AM geopolymer is significantly reduced if alkali activator content is increased, presumably due to faster geopolymer reaction owing to a higher rate of dissolution of particles and higher pH. On the other hand, the initial setting time is increased with an increase in water/solid ratios due to lower pH and a slower rate of dissolution of particles. Likewise, Panda et al. [39] reported that tensile bond strength between printed geopolymer layers decreased with an increase in the time gap between layers. The reduction in bond strength with increased time gap is fomented due to drying the outer layer surface; hence, the bond between the layers is hampered. A recent work by Tran et al. explored the potential of higher open time potential for a one-part geopolymer AM mix containing FA/Slag = 1, with the incorporation of borax. An appropriate printable open time of about 20 min was obtained with borax (2–4%) and w/b (> 0.34) [171]. Similarly, Table 4 provides a detailed overview of the TOT of geopolymer AM. Apparently, the TOT can be correlated with the repolymerization reaction, which allows generalized customization by utilizing appropriate aluminosilicate precursors and activators for specific applications and printing environments. The availability of higher calcium content has been observed to increase the

Table 4 Summary of thixotropic open time of 3D printed geopolymer

Matrix	Precursor	Open time range	Highlight	References
Mortar	FA + GGBS + Steel Slag + Gypsum + Na_2SiO_3 + Water + Sand	35–95 min	Steel Slag is observed to be decisive in controlling the TOT of the one-part AM geopolymer mix	[156]
Mortar	FA (Class F) + GGBS + SF + K_2SiO_3 + Water + Sand	20 min	The TOT was targeted for a 350 mm tool path, which can be modified with the mix composition	[39]
Paste	FA (Class F) + GGBS + SF + Na_2SiO_3	35–230 min	Activator quantity and W/S ratio have a significant impact on regulating the TOT of geopolymers	[44]
Mortar	FA (Class F) + GGBS + Sand + Na/K_2SiO_3 + Na/KOH (8 M) + Sodium carboxymethyl cellulose + Borax	15–29 min	The lower SiO_2/Na_2O ratio of the activator results in higher geopolymer TOT	[65]
Mortar	FA + GGBS + SF + NaOH (10 M) + Na_2SiO_3 + NGP + Sand	10–35 min	Higher CaO content in GGBS accelerates the hardening process and lowers the TOT	[210]
Mortar	FA (Class F) + GGBS + Sand + Na_2SiO_3 + Sucrose	10–75 min	Optimization of the mixture parameters is essential in obtaining the required TOT	[110]
Mortar	CWD + Bark ash + FA + MK + Glass Wool + Sand + Na_2SiO_3	8–10 min	–	[120]

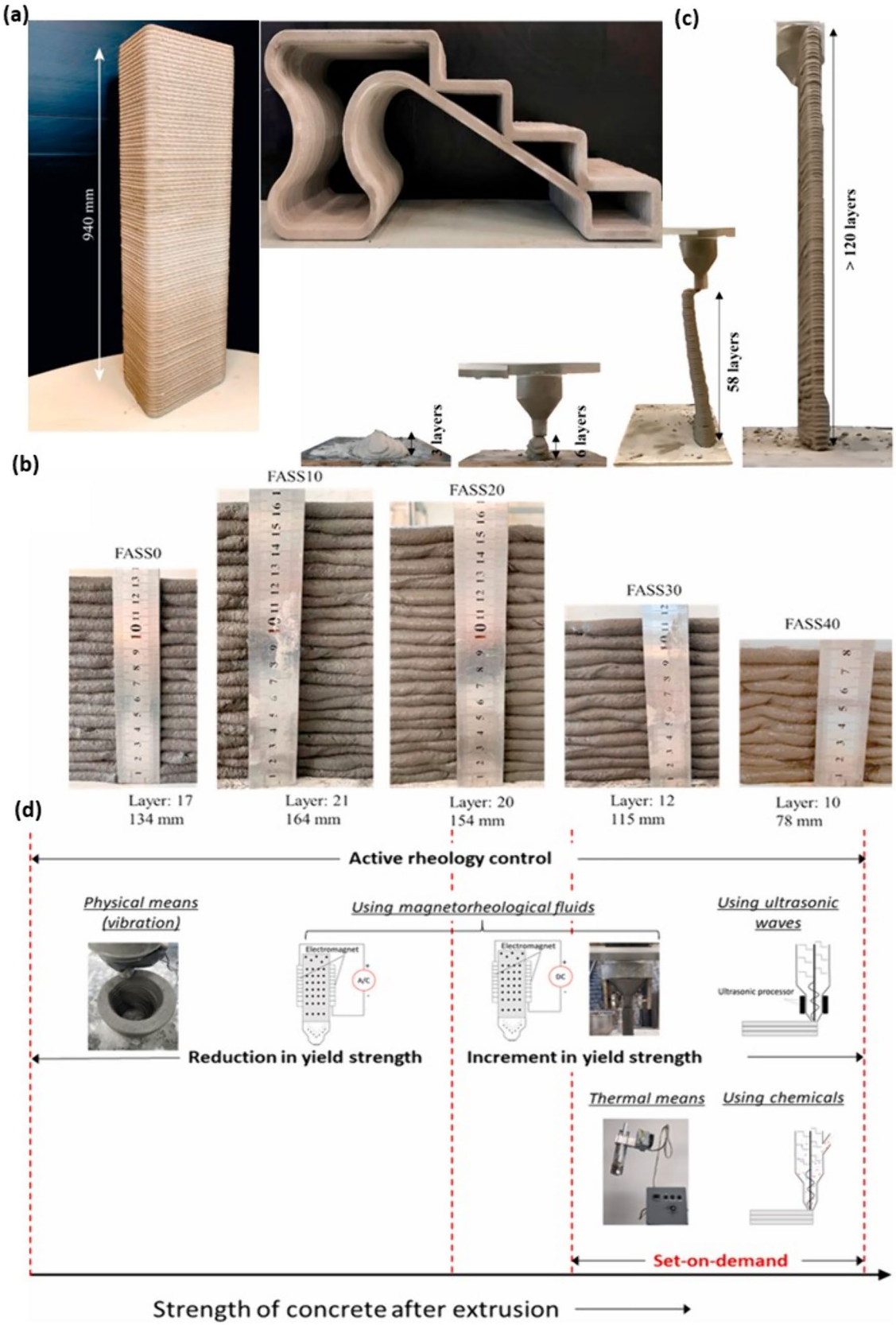

Fig. 8 Literature analysis of Geopolymer 3D printing buildability, **a** Conventional geopolymer, **b** Influence of steel slag, **c** One-part geopolymer, **d** Active rheology control. Reproduced with permission from Refs. [110, 116, 134, 156]

rate of hardening due to the early C–A–S–H reactions and decrease the TOT printability window.

The thixotropy of geopolymer can be modified through various means such as adjusting the composition of aluminosilicate precursors and activators, incorporating rheological additives, optimizing printing conditions, and exploring different mixing procedures. These modifications influence the repolymerization reaction, which in turn affects TOT of the material and its printability. Additionally, the presence of higher calcium content has been observed to impact the rate of hardening and decrease the TOT printability window. The current understanding of the TOT of geopolymer AM is limited, which can be expanded through further research on the end effect of different rheological additives, printing conditions, and mixing procedures.

4.1.5 Buildability

In geopolymer AM, printing buildability refers to the recovery of original viscosity and yield stress of freshly deposited material and stiffening of the layer before the deposition of the second layer. It is considered to be one of the crucial fresh properties as it is related to the extrudability, shape retention capacity, and TOT parameters, resulting in the ability to print and sustain the subsequent layers [235]. Therefore, the research carried out by [35] studied the buildability of FA-Slag-SF-based geopolymer in terms of viscosity and reported that adding 1.2% nanoclay could significantly recover the viscosity and yield stress. It was also noted that the yield stress exceeded the extrusion-limiting yield stress of 1.0 kPa and did not cause clogging and discontinuity problems. However, the authors anticipated that the under-pump pressure should break down, and the small addition of fiber (0.25%) helped recover this yield stress. Bong et al. developed an optimum conventional geopolymer mix with FA and GGBS, obtaining superior buildability, as displayed in Fig. 8a [110]. The effect of steel slag on the buildability of quaternary binder-based geopolymer was evaluated by Ma et al. and is shown in Fig. 8b [156]. The buildability of the 10% steel slag mixture was seen to be higher, but the actual layer height was lower than the estimated layer height due to the conflicting influence of steel slag on the geopolymerization. Likewise, Qaidi et al. discussed the conflicting relationship between extrudability, which requires low dynamic yield stress to increase flow and buildability, which demands high static yield stress to resist flow [227]. Moreover, Muthukrishnan et al. investigated the buildability of one-part geopolymer mortar, as displayed in Fig. 8c [116]. The positive influence of thixotropic additives (MAS) and retarders (Sucrose) aided in reaching beyond 120 layers. Additionally, the authors endorsed the application of microwave heating to enhance geopolymer buildability as 10 s exposure resulted in 70% viscosity recovery, with increased mechanical properties [211]. The authors also elaborated that in order to enhance the buildability, printed layers must demonstrate a high stiffening rate and greater malleability to increase the interlayer contact. In another work, the same authors also discussed the buildability enhancement options, including introducing additives during the initial mixing of the geopolymer and intervention at the print head (set-on-demand) [134]. The former has been practiced for a long time. Still, it has limitations on the extrudability, which can be resolved by the latter, which comprises the application of active rheology control, as illustrated in Fig. 8d.

Similarly, the buildability of an MK and Slag-based geopolymer was evaluated and validated by Jaji et al. through a buildability prediction model. The model incorporated input parameters, such as printing speed, path length, layer dimensions, density, and a strength correction factor, and resulted in a partial overestimation of 10% along with an underestimation of 26%, focusing on the need for a proper understanding of slag-based geopolymer mixes. The authors were able to print columns of 27 and 42 layers consecutively [236]. Nevertheless, the essential factors influencing the buildability parameters of geopolymers are still ambiguous and, therefore, require comprehensive experimental investigations.

4.1.6 Reaction kinetics

The effects of SF and slag-SF blends on the heat flow of FA geopolymer were evaluated by Panda et al. [37]. The heat of the reaction obtained by isothermal calorimetry was considered an indicator of the overall geopolymer reaction of geopolymer paste. It was shown that the addition of slag increased the heat flow and cumulative heat of geopolymer paste. Slag contributed to higher intensity of heat and cumulative heat due to polycondensation reaction during the first 48 h of the reaction. This higher heat flow indicated a geopolymer reaction in the presence of an amorphous phase, which dissolved in an alkaline reagent and released more heat than the FA geopolymer.

4.2 Hardened-state properties

4.2.1 Shrinkage

Shrinkage is a complex and inevitable phenomenon pertaining to the geopolymer as well as other cementitious materials. Due to the unavailability of formwork in 3d printing, the printed specimens are subjected to plastic and drying shrinkage owing to the loss of water from evaporation leading to volume change. Careful consideration and mitigation

Table 5 Summary of the density of 3D printed geopolymer element

Matrix	Precursor	Density range	Highlight	References
Paste	FA + GGBS + KSC + KF + Na2SiO3 + NaOH + Sodium gluconate	1560–1749 kg/m^3 (BD)	KSC significantly reduced the dry density of the extrusion-based printed geopolymers, whereas KF had a negligible effect	[157]
Mortar	Slag Powder + Plaster Powder + Sand + Na_2SiO_3	0.99–1.20 g/cm^3	Slag powder-based powder bed printing gained higher density than plaster powder due to better geopolymerization reaction	[25]
Paste	MK + Na_2SiO_3 + NaOH + Water + Polyethylene Glycol	0.924 g/cm^3 (BD), 2.121 g/cm^3 (AD), 2.157 g/cm^3 (TD)	–	[104]
Mortar	FA + Slag + Na_2SiO_3 + Sand	0.69–0.78 g/cm^3 (BD), 2.51–2.81 g/cm^3 (TD)	–	[60]
Mortar	CWD + FA + MK + Glass Wool + Sand + Na_2SiO_3 + Water	2050–2250 kg/m^3 (BD)	The printed specimens had 5–8% higher density than the casted specimens, owing to the pumping pressure in the extrusion phase	[120]
Mortar	FA + GGBS + SF + NGP + Sand + Na_2SiO_3 + NaOH (10 M)	2–2.3 g/cm^3 (BD)	The density of the printed specimens was associated with the flowability and the setting time of the mixtures	[210]
Mortar	FA + GGBS + SF + Sand + K_2SiO_3 + Additives + Water	1920 kg/m^3 (BD)	Lower densities were observed with the printed geopolymers due to the inclusion of voids during the printing process	[242]
Mortar	FA + GGBS + Ground Brick Waste + Na_2SiO_3 + Sand + Sucrose + Nano-Clay	2038–2097 kg/m^3 (BD)	Low amounts of ground brick waste induce a micro-filling effect and increase the density	[167]
Mortar	FA + GGBS + Sand + Na_2SiO_3 + PVA Fibers + Water + Sucrose + Sodium carboxymethyl cellulose	1513–1526 kg/m^3 (BD)	Short polymeric fibers resulted in increased entrapped air and reduced density	[93]
Paste	FA + SF + OPC + Limestone + Na_2SiO_3 + NaOH + Na_2SO_4 + Surfactant (Lightcrete 02™)	0.63–1.15 g/cm^3 (BD)	The surfactant dosage is crucial in determining the density of printed geopolymer foams, as the density decreases with increased surfactant	[61]
Paste	MK + Na_2SiO_3 + NaOH + Water + Polyethylene Glycol +	895 kg/m^3 (BD), 2007 kg/m^3 (SD), 2055 kg/m^3 (SoD)	–	[243]
Mortar	Lunar Regolith + NaOH + Sol-Silica + Sand + Carbon fibers	3.04 g/cm^3 (TD)	–	[244]
Paste	MK + Na_2SiO_3 + NaOH + YSZ + Alumina + Polyethylene Glycol	0.78–1.94 g/cm^3 (BD)	The density of the geopolymer ink decreases with pre-aging time	[245]

BD, bulk density; AD, apparent density; TD, true density; SD, strut density; SoD, solid density

of shrinkage are essential in avoiding crack deformation and layer separation due to shrinkage and obtaining long-term dimensional stability. Shrinkage characteristics of conventional cast geopolymers have been studied comprehensively during the last decade [237–241]. However, limited investigations are available on the shrinkage behavior of geopolymer AM. Among them, Sun et al. [68] studied the drying shrinkage of AM geopolymer made of slag and calcium carbonate and the effect of SCMS contents on the shrinkage. The geopolymer specimens were exposed to constant temperature and humidity of 23 ± 2 °C and 90 ± 2% RH for 28 days after printing. Their results show a gradual decrease in drying shrinkage of printed geopolymer with an increase in SCMS contents from 2 to 8%. The incorporation of SCMS slowed the depolymerization and polycondensation of slag, resulting in increased free and absorbed water in the paste while decreasing the gel and other forms of water in the geopolymer. The loss of gel and interlayer water in the geopolymer played an essential role in the drying shrinkage [68]. Another study by Scanferla et al. highlighted the impact of high-temperature, and sand particle fillers on the drying volumetric shrinkage behavior of 3D-printed MK-based geopolymer lattices [126]. The printed specimens containing sand fillers at higher temperatures demonstrated lower shrinkage (~ 15%) but generated more cracks due to the uneven thermal expansion between the geopolymer matrix and the fillers. Although the effect of shrinkage reduction cannot be eliminated, it can be controlled through the careful consideration of incorporating fiber reinforcements and viscosity-modifying rheological additives, which provide a deterrent effect on shrinkage. Moreover, no investigations were found on the plastic shrinkage behavior of the geopolymer AM. Therefore, future research should be aimed at characterizing the plastic and drying shrinkage performance of the printed geopolymers.

4.2.2 Dry density

Dry density is considered to be a key parameter in apprehending the mechanical strength, the functional properties, the performance, the weight, and the application economics of the printed geopolymers, and it is significantly different to the cast geopolymers. Table 5 provides a brief overview and understanding of the density development of the printed geopolymers. The resulting density of freshly printed geopolymer may depend on a number of internal and external factors, including the precursor materials, reinforcements, printing process, curing regime, etc. The printing parameters should be carefully considered during the mixture preparation, and the process must be monitored to avoid the inception of any defects and heterogeneities which can form voids in the cured specimens. These voids can result in decreased density and mechanical properties and can be avoided with high-pressure extrusion (effective extrusion-based 3D printing system design for cementitious-based materials). The effect of FA, slag, and SF on the bulk density of AM geopolymer is evaluated by Chougan et al. [210] and compared with mold cast geopolymer. Four of the six combinations show a higher bulk density of AM geopolymer than cast geopolymer. This study also observed no particular trend in bulk density for printed and cast geopolymers. Chougan et al. also evaluated the effect of nano-graphene platelets (nGP) on the bulk density of printed geopolymer containing 60% FA, 25% slag, and 15% SF. They reported higher bulk density at all nGPs contents. Nano-graphene platelet contents of 0.1% and 0.3% show higher bulk density than higher nGPs contents of 0.5% and 1.0%. The density increase is attributed to the lubricating effect of the nGPs during extrusion by decreasing the friction between geopolymer components. Subsequently, a research investigation by [61] studied the effect of various foaming surfactant contents on the bulk density of printable FA-limestone, FA-limestone-SF, and FA-limestone-cement-based foam geopolymers with their counterpart cast geopolymers. They generally observed a lower bulk density of printable foam geopolymers than the cast foam geopolymers. However, they observed a decreasing trend in bulk density of both printable and cast foam geopolymers with increased surfactant contents.

Interestingly, after hardening of geopolymers, the authors observed a higher volume of pore sizes of all pore sizes at 2% and 3% surfactant contents in FA-limestone and FA-limestone-SF geopolymers than those for 1%. The difference in pore volumes among surfactant contents is insignificant in the FA-limestone-cement geopolymer. Their results also noted that the porosity of hardened cast geopolymers is lower than that of printed geopolymers, irrespective of surfactant contents and geopolymer type.

Similar to extrusion printing, the density of powder-based printing is determined by the degree of the pore saturation of the aluminosilicate powder precursor layer with alkaline solution (from casting to 3D printing geopolymers: a proof of concept). Voney et al. demonstrated that the density of powder bed-based printed geopolymers increased with the saturation degree of the powder bed to a specific point beyond which the shape stability decreases owing to the sufficient liquid content in the mixture (from casting to 3D printing geopolymers: a proof of concept). However, although few studies have highlighted the evolution of density in printed geopolymers, a complete understanding with respect to the geopolymerization reaction, external reinforcements, and curing environments is still undefined. Also, comparison is greatly affected due to the lack of standardized methods for measuring the density of geopolymer 3D printed objects.

4.2.3 Mechanical properties

The mechanical properties of printed geopolymers have been significantly investigated by different researchers. Table 9 ("Appendix") presents the mechanical properties of geopolymer-based AM elements. An FA-slag-SF blended geopolymer AM composite is compared with the same cast-in molds geopolymer by Panda et al. [37]. They reported slightly higher (approximately 1.14 times) compressive strength (CS) of AM geopolymer than mold-cased geopolymer. This observation was derived due to the efficient printing process, which didn't allow any formation of voids due to the extrusion process. The mechanical strength properties of the printed geopolymers generally demonstrate an anisotropic behavior owing to a number of factors. Major factors reported to have manipulated the mechanical properties of geopolymer AM composites are (i) Alkali activators, (ii) Orientation of AM composite layers, (iii) SCM in mix design, (iv) Reinforcements and fibers, and (v) Carbon-based nanomaterials.

(i) Alkali activators:

Alkali activators have a significant role in the mechanical properties of geopolymer composites. Tables 7 and 8 ("Appendix") provide brief information on different activators used by researchers. An investigation carried out by [231] reported a reduction in the CS of FA-slag-SF-based geopolymer with an increase in metasilicate powder activator and water/activator ratios. Lower alkalinity might have produced particular geopolymer gels, which had increased the CS, and an 8% activator was reported as optimum for the AM process. Sun et al. [68] reported a study on AM geopolymer where the activator consisted of slag and calcium carbonate powders and was activated by sodium-based alkali activators. They observed a reduction in compressive and FSs of printed geopolymer with an increase in SCMS content. The increase in porosity in printed geopolymer with an increase in SCMS is due to its aeration effect in geopolymer, resulting in loose integrity of the mortar and, hence, poor mechanical properties. They found that geopolymer with SCMS content in the 4–6% range can be extruded at 30 mm/s without any fracture/discontinuity in the printing layer. The effects of two types of Na_2SiO_3s and K_2SiO_3s and silicate-to-hydroxide ratios on the CS of AM one-layer FA-slag blended ambient cured geopolymer is evaluated by Bong et al. [55] and reported that the CS increased with an increase in silicate-to-hydroxide ratios of D-grade Na_2SiO_3 and 2010 grade K_2SiO_3. However, no such trend was observed in the case of N-grade Na_2SiO_3 and 2236 grade K_2SiO_3. The effect of different alkaline activators apart from Na/K and lower activator dosages on long-term strength can be studied further.

(ii) Orientation of printed layers:

The mechanical properties of geopolymer AM composite have been investigated in different orientations of printed layers. Figure 9 presents the mechanical properties testing arrangement scheme and sample loading arrangement. Panda et al. [62] evaluated the CS of the printed geopolymer layer where the load was applied in three different orthogonal directions, shown in Fig. 9a. Their results show that the CS of printed geopolymer loaded perpendicular to

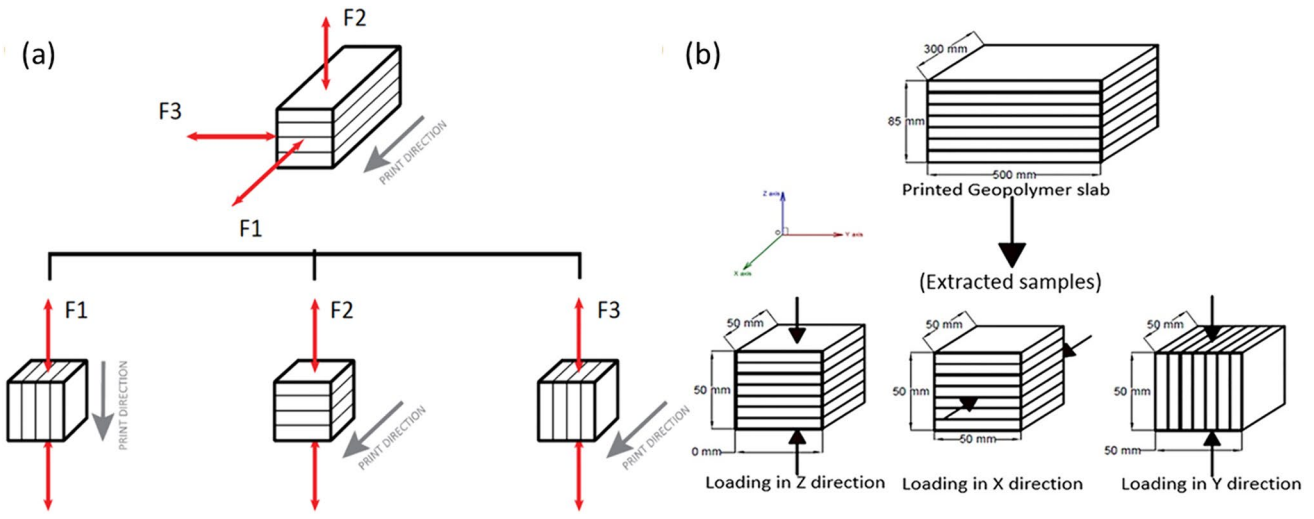

Fig. 9 Schematic diagram of mechanical properties testing arrangements in geopolymer AM samples, **a** Reproduced with permission from Ref. [62], and **b** Reproduced with permission from Ref. [27]

the printing direction (F2 and F3) is almost the same but slightly higher for parallel direction (F1). The CS of the printed geopolymer was measured parallel to the printed geopolymer. The CS of the printed geopolymer was higher than the conventionally cast geopolymer. However, the cast geopolymer showed slightly higher CS than that measured in the printed geopolymer, where the load was applied in F2 and F3 directions. As the printing direction was in F1, the dispersion of geopolymer material was much lower than in the F3 direction due to higher restraint provided to the layer in the longitudinal direction (F1) than in the transverse direction (F3), which is the reason for higher CS in F1 direction than in F3. Panda et al. [27] also evaluated the CS and FS of AM FA-slag-SF geopolymer activated by a potassium-based activator under three loading directions, as shown in Fig. 9b. The CS of printed geopolymer loaded in the *Y* direction was more substantial than the loaded directions of *X* and *Z*. The same trend is observed at all curing ages. The printed samples were around 5% weaker in the *X* and *Z* directions while 2% stronger in the *Y* direction when compared to conventional casting geopolymer. However, in the case of FS, an opposite trend was reported.

Another study by Bong et al. [55] suggests that the maximum CS tested in the longitudinal direction at both test ages of 7 and 28 days agrees well with the results reported by Panda et al. [62]. However, the FS was 1.32 and 1.13 times higher in the perpendicular direction than tested in the lateral direction at 7 and 28 days of curing, respectively. The higher FS in the perpendicular loading direction is due to the higher FS of the bottom layer owing to higher compaction due to the weight of the top geopolymer layer. It was also observed that both strengths are higher at 28 days due to more extended curing than those at 7 days.

It can generally be stated that the longitudinal direction of printing will preferably obtain higher strength than in the lateral or perpendicular directions due to the print material characteristics, i.e., greater alignment of the extruded particles, higher surface area for bonding, better compaction due to the extrusion pressure [160, 246]. Potential research gaps include investigations on the effect of printing orientation on impact resistance, density, failure behavior and long-term mechanical performance of geopolymers.

(iii) SCM in mix design:

Common SCMs used in geopolymer mix for AM are slag and SF. The use of SCM and different admixtures in geopolymer AM formulations are included in Tables 7 and 8 ("Appendix"). Albar et al. [79] studied the CS and FS of AM FA-slag-SF blended geopolymer with conventional cast geopolymer. It was observed that both CS and FS of AM geopolymers having different combinations of FA, slag, and SF are lower than those of conventional cast geopolymers. One interesting phenomenon observed in their results is that both strength properties of conventional cast geopolymers decreased with the decrease in slag contents from 35 to 15%. Conscious utilization of SCM in the mix design is, therefore, necessary to avoid the negative impact on the mechanical performance of the printed geopolymers. Improper mixture or incompatible SCMs can lead to the reduction of the dissolution rate of the mineral particles and can also affect the extrudability as well as the TOT of the geopolymer mix [247]. Moreover, the physiochemical characteristics of the SCMs preferably affect the early age properties of the geopolymers. It is conceived that new mix compositions with suitable SCMs will be devised for resolving issues, such as achieving rapid hardening, in the coming years. Calcined clay has been one of the least explored SCMs in the field of geopolymer AM.

(iv) Reinforcements and fibers:

Reinforcements and fibers are commonly used in geopolymer composite to compensate for ductility. Reinforcements restrict the propagation of cracks in brittle geopolymer matrix under tensile and flexural stress. Different types of reinforcements in the AM of geopolymer composites have been studied by researchers, including cables, fibers, nanomaterials, etc., as shown in Fig. 10. In the AM, reinforcement can play an additional role in regulating material viscosity and its formability. The most popular one is reinforcement, using different types of fibers. Traditionally, steel bars are used as a reinforcement for this composite – concrete and geopolymers [248, 249]. Nowadays, only a few studies have been provided to replace the conventional steel bars, well-known for traditional concrete technology, with short or long fibers possible to apply in AM [249]. The most popular method of reinforcement AM geopolymer composites is steel micro-cable [36, 56]. The experimental results show that the AM micro-cable reinforced geopolymer composites, as depicted in Fig. 10a, b, are promising materials for applications in the building industry. The effectiveness of the reinforcement depends on the way the reinforcement is deposited in an incline-crossed printing configuration. In a proper configuration, the FS can be seventy times higher than the corresponding value of the nonreinforced one [56, 84]. In addition, the behavior of the failure

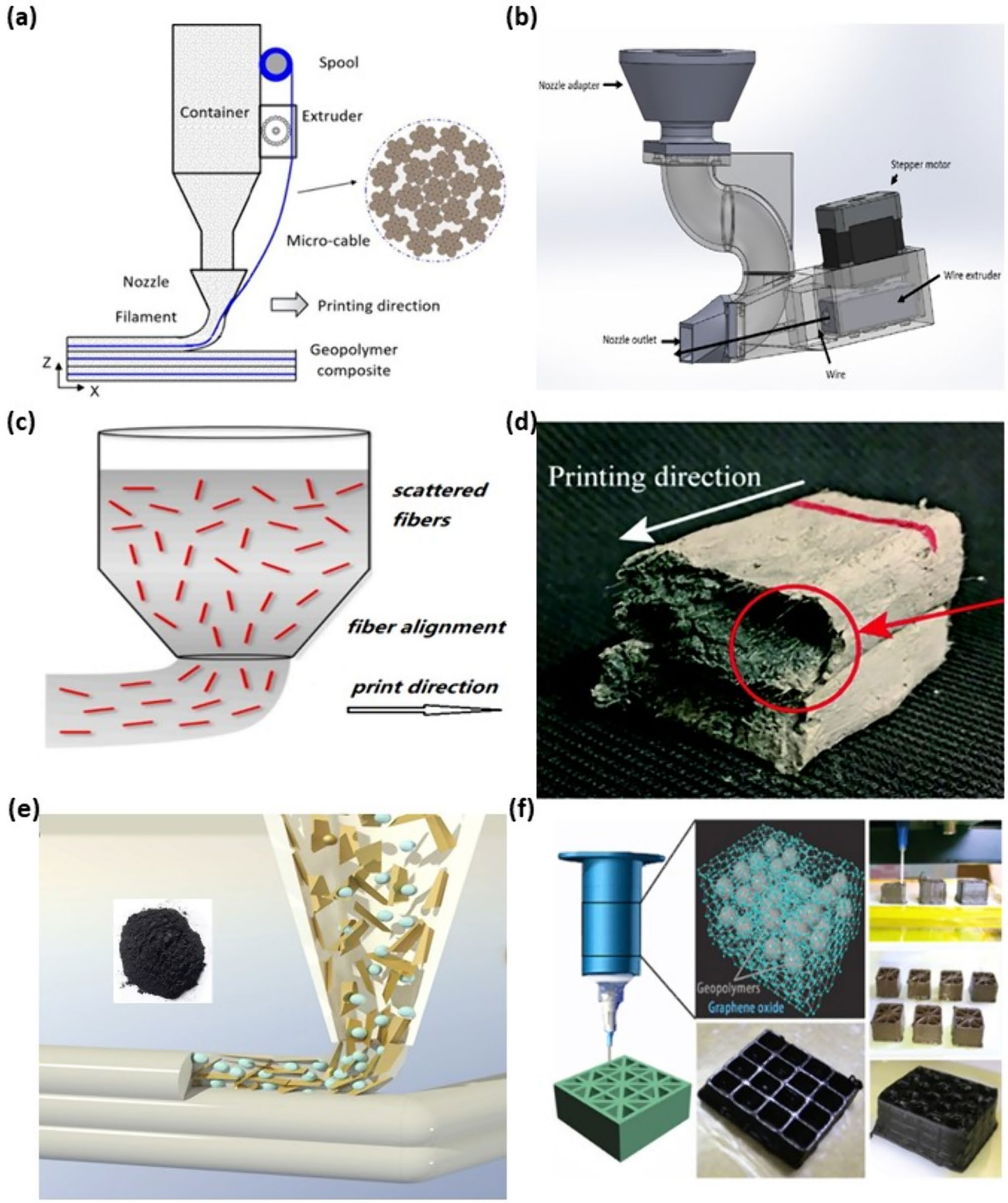

Fig. 10 Reinforcements in Geopolymer AM **a**, **b** Steel/Micro cable, **c**, **d** fibers, **e**, **f** nanomaterial. Reproduced with permission from Refs. [26, 36, 56, 71, 93, 148]

mode of the reinforced composites changed from brittle to ductile [90]. A slightly different matrix for testing the steel micro-cable was used by Lim et al. [36], where steel cable improved the FS of AM material by about 290% compared to the plain geopolymer [80].

The short steel fibers and the polypropylene fibers are used and compared AM geopolymers by different researchers. A geopolymer produced from class F FA mixed with sand and activated by Na_2SiO_3 and NaOH solution shows that fibers negatively affect the bond strength between layers, reduce time gaps between subsequent layers, and increase FS results [38]. The impact of three types of polymeric fibers: PVA, PP, and PBO fibers (all 6 mm in length) was investigated on a geopolymer mixture from class F FA and silica sands activated by sodium-based activators (Na_2SiO_3, NaOH) and used as a matrix [34]. The results show that the FS of AM geopolymer incorporating PVA, PP, and PBO fibers comparatively provide 13, 23, and 33% higher enhancement than that of the AM geopolymer with no fiber [34]. Several researches have been conducted on geopolymer AM using PVA, as shown in Fig. 10c, d [70, 76, 93]. Oil-coated PVA fibers (40 µm diameter, 8 mm length) result in increased mechanical properties and anisotropic behavior of geopolymer, with fibers mainly oriented parallel to the printing direction [93]. In related studies, PVA fibers were employed as anti-shrinkage agents to address micro-crack propagation limitations in the composite [70, 76]. Similar outcomes were observed with short glass fibers in a potassium-based matrix, using raw materials like MK with calcined argillite [124] and class F FA combined with slag, MS, and fine river sand [28]. This admixture resulted in heightened viscosity and reduced workability (castability) of the composite [28, 124]. Moreover, a parallel orientation of short polymeric fibers along the printing path was confirmed during the process [54].

The research was also done for natural fibers [85], based on a matrix composed of class F FA and sand, activated by solution Na_2SiO_3 and NaOH. The green tow flax fiber 30–50 mm was added in 1% by weight [85, 250]. Their behavior was compared with short carbon fibers (carbon fiber has a length of 5 mm and a diameter of 8 µm) [85]. The results indicate that including the fibers slightly enhanced the CS and improved the FS. Surprisingly, the mechanical properties of specimens with flax fibers were better than those containing carbon [85, 250]. Investigating replacement with traditional reinforcement is an important issue for AM development. The traditional reinforcement causes many problems, including the speed limit during the AM process and design limitations, such as curved shapes that are required from an architectural point of view [27]. The replacement could be made of steel fibers or an alternative one [82]. From the environmental point of view, the most beneficial is using natural or waste fibers, but its investigation is minimal [82]. It is important to stress that the research shows a lot of benefits connected with using fiber admixture in AM, such as increasing FS up to 600% compared to plain samples [56], improving interlayer bonding [34], limiting the cracking propagation, and shrinkage [84], reduction of brittle behavior of the geopolymers [85]. Similarly, the effects of adding wollastonite (a naturally occurring calcium silicate) micro-fiber show benefits in enhancing the buildability of the geopolymer AM layers [78]. It increases the shape retention ability and static yield stress and improves the FS. The fiber reinforcement of AM geopolymers is a promising way to develop materials for application in manufacturing on a large scale in the construction industry.

Other possibilities to improve geopolymer mechanical properties, which seem to be very promising, are nano-additives, which are represented in Fig. 10e, f. The nanoparticle reinforcement of geopolymers can be considered a novel development in advanced construction materials [210]. Some tested nano-additives are carbon-based materials, such as carbon nanotubes, graphene nanoplates, and GO [181]. They improve both mechanical and superior physical properties, including electrical and thermal conductivity [210]. The other tested admixture is nano-clay [54]. This admixture improves the rheological properties, which are crucial for the effectiveness of the AM process [54].

Among three loading directions, the load applied perpendicular to the printing direction (T1-direction) exhibited much higher FS of glass fiber geopolymer composites than that of load applied in longitudinal (T3-direction) and transverse (T2-direction) directions irrespective of fiber contents. FS also increased with an increase in glass fiber lengths. In the case of CS, a slightly decreasing trend in CS of AM glass fiber geopolymer composite was observed with increasing fiber contents. Interestingly, the maximum CS was observed in the longitudinal direction (T3-direction) of loading, and it decreases with an increase in glass fiber contents. The tensile strength of AM glass fiber geopolymer composite is also increased with an increase in fiber contents. In geopolymer AM, 6 mm PP fibers at varying volume percentages (0.25%, 0.50%, 0.75%, and 1%) in

an FA-based matrix exhibited anisotropic behavior [33]. PP fibers increase the CS of the material only in the perpendicular direction. Fiber reinforcement, at the same time, increases the ductility of the material, deflection capacity, and fracture energy. However, fiber reduces the interlayer bond strength [33]. This can be interpreted as the formation of increasing porosity due to higher PP fiber contents. Composite tested in the perpendicular direction of printing exhibited much higher CS than tested in longitudinal and lateral directions at all PP fiber contents. However, an opposite trend is observed in AM geopolymer without PP fiber, where CS was higher in the lateral direction than in other directions. Interestingly, the addition of PP fibers did not significantly improve the FS of AM FA geopolymer composites tested in both perpendicular and lateral directions, which is quite unusual compared to other researchers' results, e.g., in [33, 55].

A few research gaps need to be further investigated to amplify the significance of the fibers apart from the mechanical performance enhancements. The introduction mechanism and proper dispersion of the fibers into the geopolymer AM mix are the few major challenges that need to be investigated to decrease shrinkage and increase the structural integrity of the freeform printed geopolymer structures.

(v) Carbon-based nanomaterials:

Recently, carbon-based nanomaterials, particularly different allotropes of graphene, have been progressively used to improve the mechanical properties of geopolymer AM. Zhong et al. [26] reported improvement in the CS of geopolymer due to the addition of GO up to 12% by volume and an increase in its elastic modulus value at GO content of 6% by volume. However, an increase in GO content adversely affected these mechanical properties. On the other hand, Chougan et al. [210] reported that the CS of FA-slag-SF blended AM geopolymer is lower than that of conventional cast geopolymer. However, with the addition of 0.1% graphene nanoparticles, the CS of AM geopolymer increased significantly and exceeded the conventional cast geopolymer. With an increase in graphene nanoparticle contents, no such improvement was observed. They also compared the FS of printed geopolymers with those of cast geopolymers specimens. They found similar results for CS except for one mix, which consisted of 60% FA, 25% slag, and 15% SF. The reason is unclear, but according to the authors, the higher tensile strength of the bottom layer due to higher compaction is the reason for such higher FS in that particular mix, which is supposed to happen to other combinations in their study. However, when graphene nanoparticles were added to the printed geopolymer, the FS increased at all graphene nanoparticle contents from 0.1% to 1.0%, which is not consistent with the CS of respective mixes. Additionally, the utilization of carbon-based nanomaterials also provides functional properties, including thermal and electrical conductivity, adsorption, improved flame resistance, radiation shielding and electromagnetic interference, piezoresistivity for smart functionality, etc. [181, 189, 251, 252]. No studies have yet been reported with the introduction of biochar in geopolymer AM.

(vi) Overall comparison of geopolymer AM mechanical properties:

Mechanical properties (i.e., CS and FS) of geopolymer AM from previous literature are compared and presented in Fig. 11. Besides five major mechanical properties influencing factors as discussed (i.e., alkali activator, AM layer orientation, SCM, fibers, and nanomaterials), their combined impact, layering direction and the rate of layer building also may impact the mechanical properties of geopolymer AM.

The 7-day CS of powder bed AM FA-slag geopolymer subjected to three different curing regimes was evaluated by Xia et al. [60]. Their results show that the CS of geopolymers in the activator binder jetting direction (X-direction) is slightly higher than that of the layer stacking direction (Z-direction), irrespective of curing types applied and FA contents. The results also show a decreasing trend of CS with an increase in FA contents (hence, a decrease in slag contents) irrespective of testing directions and curing types. Alkali activator solution consisted of grade D Na_2SiO_3 and 8 M NaOH exhibited higher CS than those activated by anhydrous sodium meta-silicate solution and combined 8 M NaOH and anhydrous Na_2SiO_3 solution. In another study, Xia et al. [48] studied the effect of different curing temperatures ranging from 25 to 80 °C on the CS of powder bed AM slag geopolymer after post-processing. Their results displayed an increase in CS with an increase in temperature up to 60 °C with a significant drop in strength at 80 °C.

FS of geopolymer AM over different curing times is presented in Fig. 11b. Perrot et al. [253] proposed a theoretical framework to determine the highest building rate for layer-wise AM concrete using the extrusion technique. They found average yield stress of 3.95 kPa, 4.76 kPa, 4.86 kPa, and 5.20 kPa for the time gap between each layer deposit of 11, 17, 22, and 34 s, respectively when activator paste containing 50% cement, 25% kaolin, 25% limestone filler, water/cement ratio = 0.41 and 0.3%

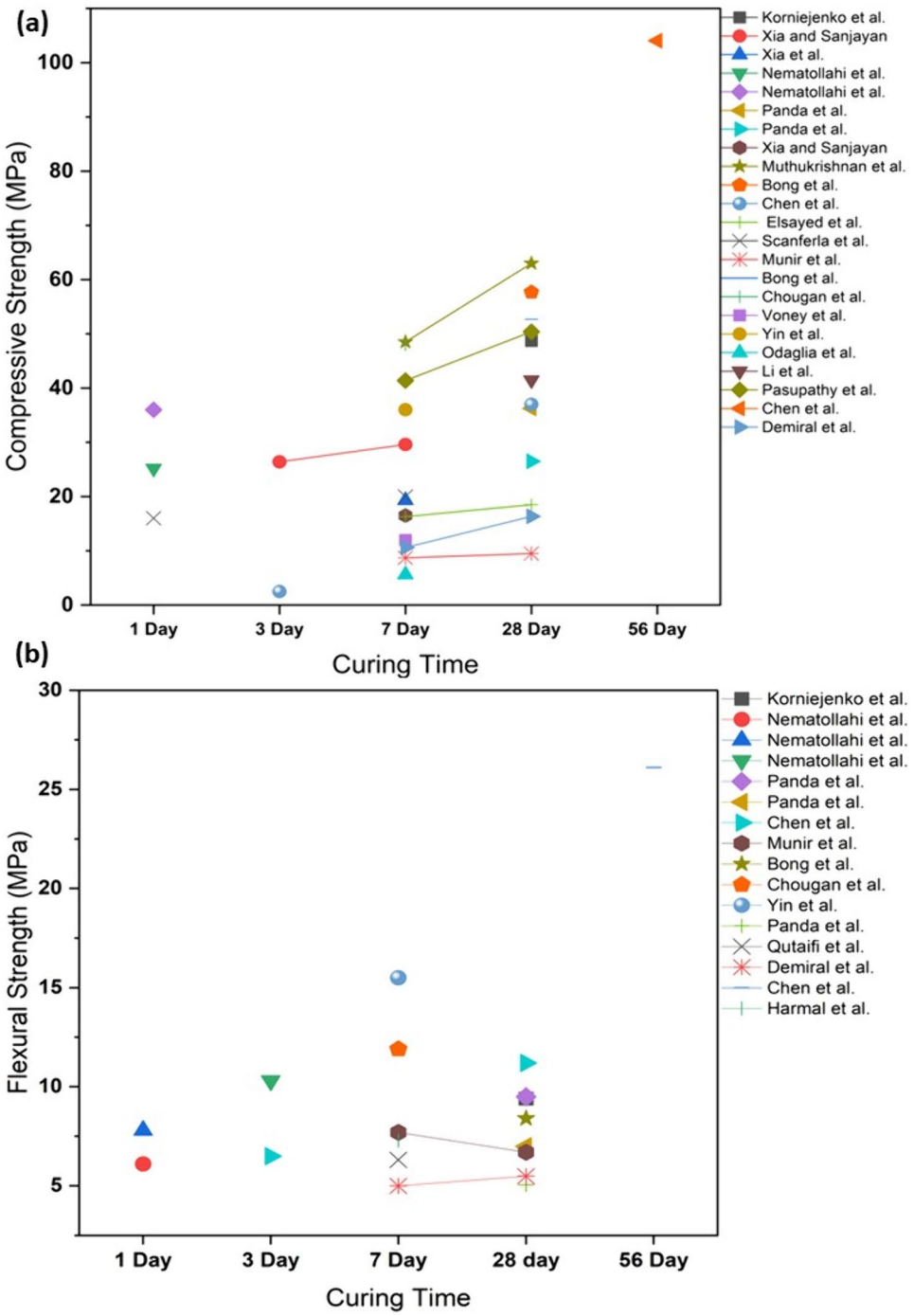

Fig. 11 Mechanical properties of geopolymer AM from previous literature, **a** Compressive strength, and **b** Flexural strength

Polycarboxylate-type polymer powder SP was added to the concrete mix. One of the research investigations by [254] found the highest FS of 30 MPa for a printable concrete with the composition of 61.5% type I 52.5 R Portland cement, 21% SF, 15% water, 2.5% water-reducing agent, 0.3% by weight of a hydration inhibitor, water/cement ratio = 0.3, an 1% carbon fiber. They also noticed no significant improvements in FS when glass and basalt fibers were added. Another study by [193] indicated the best suitable printable mix with the composition of 72% cement, 23% class F FA, 5% calcium aluminate cement, 45% silica sand, 10% micro-silica, 5% ground silica, 43% water 0.5% attapulgite nano-clay, 0.4% hydroxypropyl methylcellulose, 0.8% high range water-reducing agent and 2% PVA (by vol) and the same mix achieved CS at 6 days and tensile strength of approximately 30 MPA and 6 MPa respectively. Le et al. [234] developed the optimum mix, which can be printed through a 9 mm diameter nozzle to

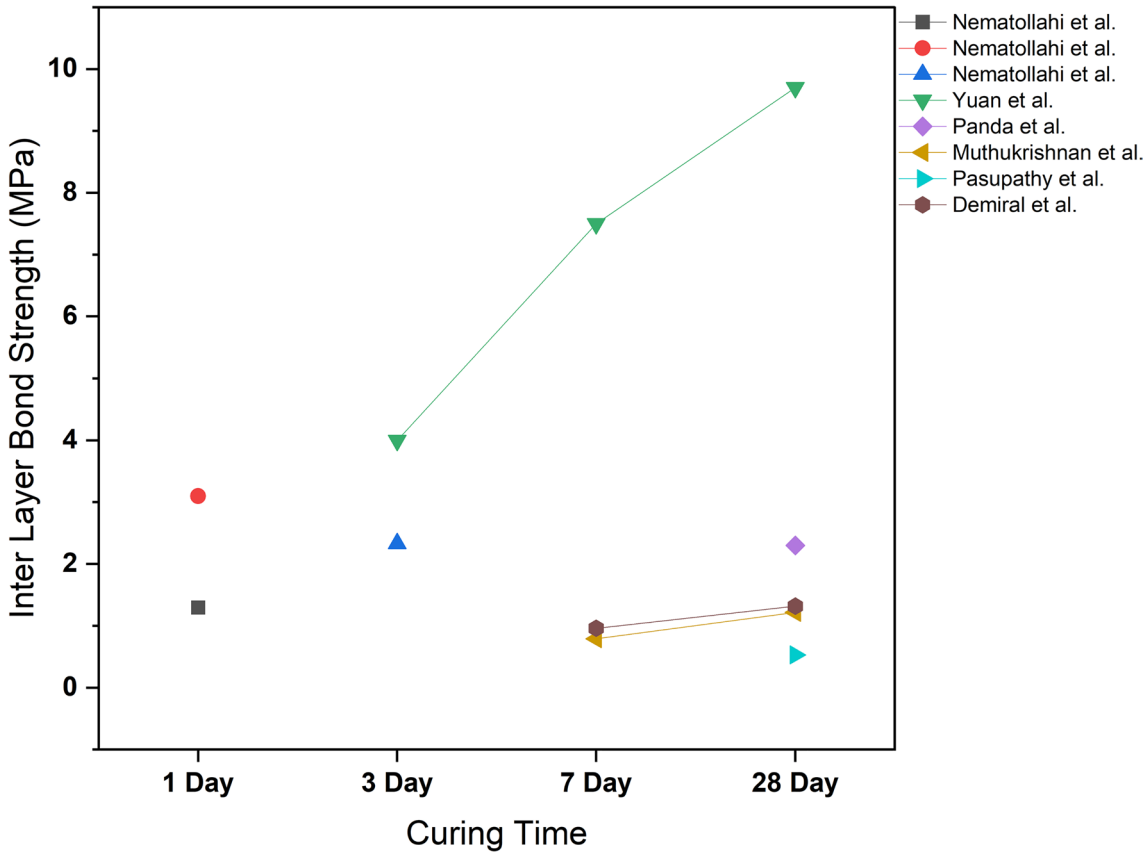

Fig. 12 Inter-Layer Bond strength of geopolymer AM from previous literature

build up to 61 layers in one go and more than 110 MPa CS at 28 days with the consideration of 70% cement, 20% FA, 10% SF, and 1.2 kg/m^3 fibers, Water/activator ratio = 0.26 1% superplasticizer, 0.5% retarder (by weight of the activator), and Sand/activator ratio = 1.5.

The literature analysis confirmed the application of all listed methods and developed them for AM. The methods of mechanical property improvement presented in the analyzed articles were similar to those described by Zhao et al. [115]**.** For the improvement of CS, it was found that the addition of GGBFS [60], application of steel micro-cables [90], using different curing methods [59], the addition of Nano-graphite platelets [51], or proper post-processing procedures [59]. The best methods of increasing the bond strength are adjusting printing methods: printing time gap, printing speed, and nozzle standoff distance, and adjusting the Si/Na ratio of the alkali activator [59, 115]. The most effective ways for FS enhancement are adding short steel or different fibers [124], the addition of nano-particles, such as graphite, platelets, or wollastonite [78, 124], and the application of micro-cables [90].

4.2.4 Layer adhesion

The Inter-Layer Bond Strength (ILBS) between layers of AM geopolymer is specific to extrusion-based printing and significant for the integrity of printed material. A higher ILBS is essential to prevent delamination and to improve the mechanical properties. Essentially, the printing speed and the time gap between the subsequent layers can directly impact the development of ILBS properties (Shaping of geopolymer composites by 3D printing). Shorter time gaps and higher print speed have been observed to facilitate improved interface layer bonding by the early geopolymerization reaction (Mechanical properties of layered geopolymer structures applicable in concrete 3D-printing). Apart from that, the geopolymer mixture composition, printing orientation, and printing environment are also likely to be imperative. Figure 12 presents analyzed data from the literature, which indicates that the interlayer bond strength between AM geopolymer layers is enhanced with increasing curing time, particularly in Yuan et al. study [143]. Panda et al. [64] studied the effect of modular ratios of sodium-based alkali activators on bond strength between AM geopolymer layers. They reported an increase in tensile bond strength with an increase in modular ratios. Their study also reported that

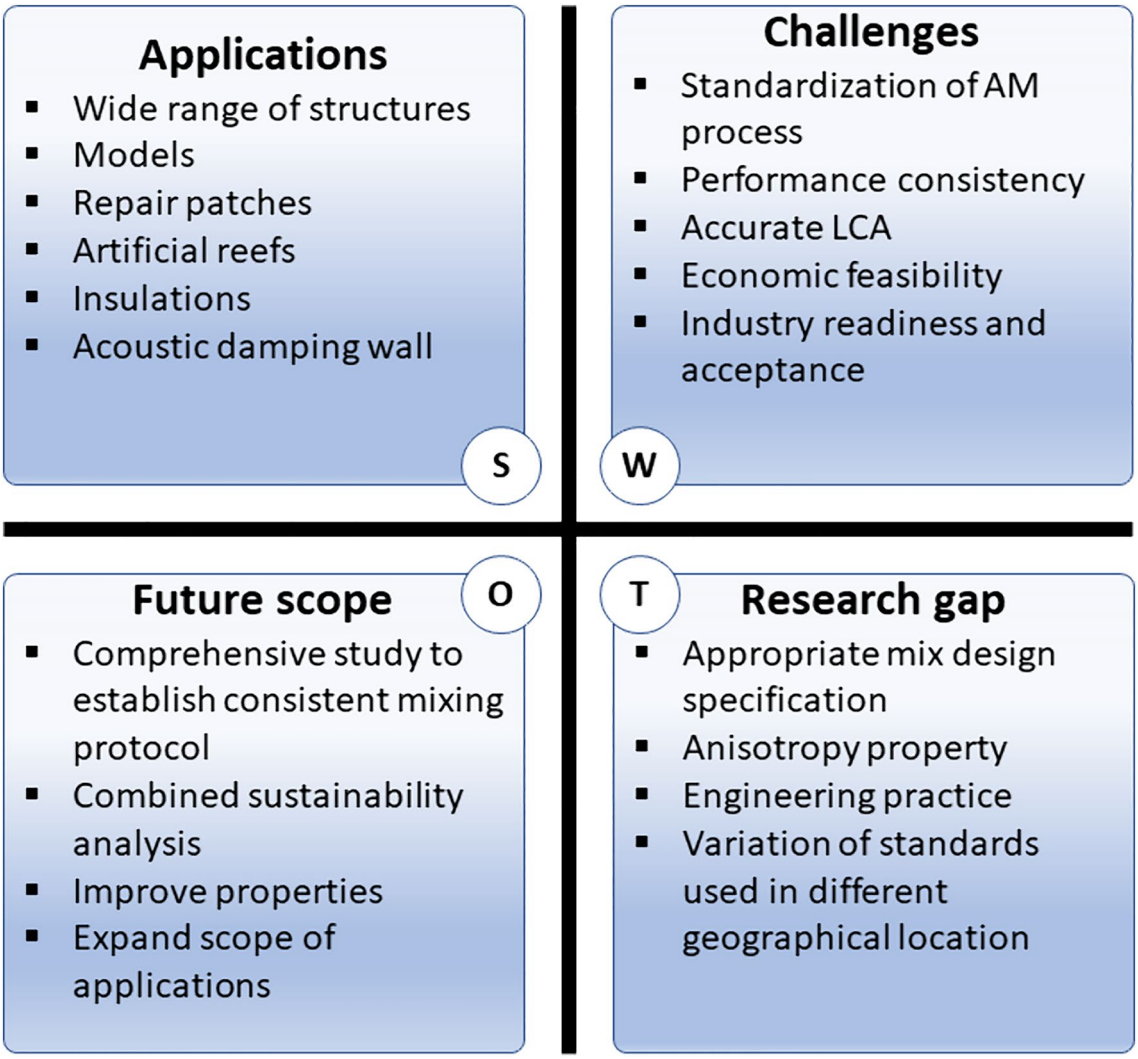

Fig. 13 SWOT analysis on geopolymer AM state-of-the-art

due to faster poly-condensation reaction, the surface moisture level becomes less in the geopolymer layer of modular ratio 1.6 compared to those of 1.85 and 1.60, which might cause poor interface bonding in the former than the latter. The same authors [39] also reported that the tensile bond strength of printed FA-slag-SF geopolymer decreases with an increase in the time gap between layers. This reduction in tensile bond strength with gap time was attributed to the loss of moisture from the outer surface of the geopolymer layer, which diminishes the interface layer.

Bong et al. [55] described that the interlayer tensile bond strength of FA-slag geopolymer increases with an increase in curing age of 7–18 days, and the 7 days bond strength of 0.9 MPa is adequate to avoid any interfacial shear failure. Nematollahi et al. [33] reported no increase in the interlayer bond strength of FA geopolymer due to the addition of PP fiber except at a PP fiber content of 0.25%, which showed a slight increase in bond strength. No improvement in the interlayer bond strength of their FA geopolymer was also observed due to the addition of 0.25% polyvinyl alcohol and polyphenylene benzobisoxazole fibers [34]. The current literature on the ILBS of geopolymer AM lacks the necessary comprehensive investigation of the effect of different geopolymer compositions, reinforcements and long-term durability of bond strength.

5 Applications, challenges, and research prospects

A SWOT analysis of the state-of-the-art of geopolymer AM is presented in Fig. 13 to highlight geopolymer AM applications, challenges, research gap and future scope. Specific aspects are elaborated on in the sub-section that follows.

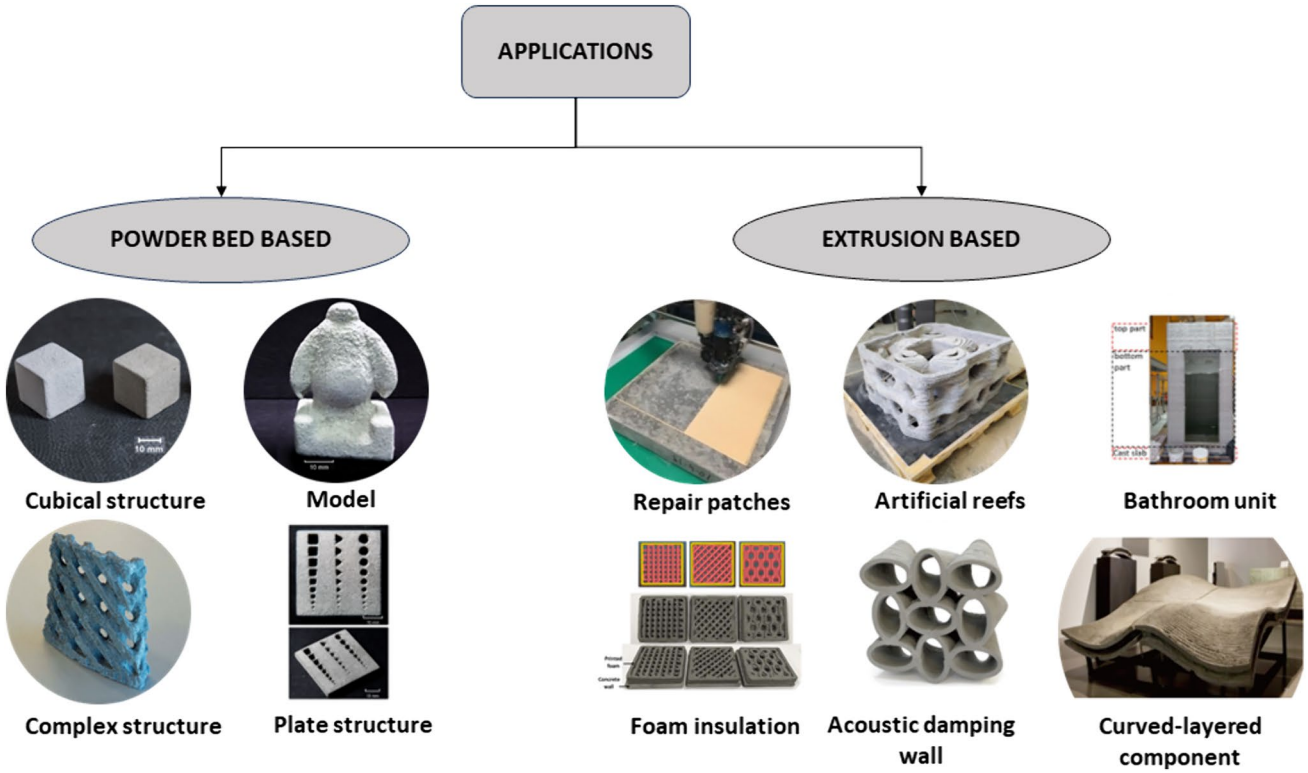

Fig. 14 Few applications of AM Geopolymer composites in construction. Reproduced with permission from Refs. [17, 25, 60, 61, 70, 86, 119, 257]

5.1 Applications

Geopolymers have gained immense attention recently due to their low carbon footprints and excellent properties. The geopolymer composites, made with aluminosilicate wastes, could be easily fabricated (onsite/offsite) and are therefore suitable for various structural and non-structural applications, as depicted in Fig. 14 and also mentioned in Table 6 ("Appendix"). On the other hand, challenges exist, such as production costs, a large amount of waste, huge human resources, and complex structural configurations, which stresses the need for modern construction procedures such as AM over traditional ones. This section presents a few potential applications of AM geopolymer composites relevant to the present scenario.

A study done by [158] showed an AM bar-shaped structure using MK (inorganic waste) in one of the investigations. The mechanical properties of the prototypes indicated that this powder bed AM technique of geopolymer concrete could be used in the construction of thermal insulation structures as well as other large-scale structural applications. The powder bed AM was reported to have an enormous possibility of pre-cast applications in the construction industry, and in a study by Xia et al. [60], the cubical specimens, as shown in Fig. 14a, made up of 50% slag and 50% FA (by wt.), resulted in a CS of 25 MPa at the age of 7 days, which expands the scope of AM geopolymer materials for residential construction applications.

Likewise, in another study by [255], the authors reported the suitability of extrusion-based AM geopolymer concrete using FA for digital construction applications while simultaneously investigating the role of short fibers on the properties of interlayer bond strength and FS. The PBO fibers were the most effective and significantly improved the interlayer bond strength and FS of AM geopolymer specimens. The authors stated that due to high interlayer bond strength, this AM technique and the mix design of the geopolymer base material could potentially tackle the limitations of the powder bed AM, providing a pathway for on-site construction applications. On the other hand, incorporating steel fibers for additive manufacturing of geopolymer concrete-based structures could impact the bond strength negatively; hence, it is

not recommended. This effect was observed by Al-Qutaifi et al. [38], who used Gladstone FA as a geopolymer precursor for building AM-layered geopolymer structures.

Another potential application of AM (additive manufacturing) geopolymer technology is in the repair and sensing applications domain. Vlachakis et al. [70] outlined the process developments of the AM MK-based geopolymer repair patches onto the concrete membranes. The adhesion strength of the repair patches to the concrete was 0.6 MPa, while the patches inherently held a CS of 24 MPa and temperature sensing accuracy of 0.1 °C. With the aid of robotics, this functionality of the AM geopolymer technology could enable the practitioners to closely monitor the existing structure under dangerous conditions like nuclear/oil/gas environments.

Therefore, the applications of this innovative AM geopolymer technology, particularly in the precast industries, have been eminent [112, 256]. The building elements like formworks, interior structures, and beams could be easily prefabricated under controlled conditions with less human resources and waste and later assembled on-site [42]. Furthermore, to increase the application prospects of 3D printed geopolymer composites in the precast industries, novel technologies such as extrusion-based AM "one-part" geopolymer composites are being developed [63]. As a result, the process developments would be more user-friendly as the practitioners only need to add water to the ready-made activator composition. This excludes the handling of the user-hostile alkaline liquids, contrary to the traditional geopolymer manufacturing methods. A few more applications of AM geopolymer composites can be perceived in Fig. 14. This includes the production of advanced structural components, such as block structures, model structures, repair patches, artificial reefs, and curved-layer components.

5.2 Cost of geopolymer AM

The economic viability of utilizing geopolymers in 3D printing, particularly concerning cost implications for large-scale construction projects, has been examined in this section. Analysis of cost factors reveals that in geopolymer concrete (GPC) production, pretreatments play a significant role, constituting approximately 87% of the final product cost, as evidenced by the cost estimation analysis provided by [112]. Specifically, it was found that the total estimated cost for one ton of geopolymer 3D printing, including pretreatments and production costs, amounts to €422 per ton [112]. However, it is important to note that this figure does not encompass the costs associated with 3D printing technology and labor. Comparative cost assessments between traditional construction methods utilizing ordinary Portland cement (OPC) and those incorporating GPC in 3D printing underscore the potential economic advantages of GPC-based construction. Despite marginally higher production costs for GPC compared to OPC, the overall construction expenses for 3D-printed houses using GPC remain competitive. In comparison, a 50 m^2 3D-printed house using GPC incurs an average cost of €192,327.232 [112], while a similar structure employing OPC costs €189,000 [257]. This cost-effectiveness is further reinforced by the inherent sustainability and energy efficiency of GPC, attributable to its utilization of waste materials and reduced energy consumption compared to OPC production. Thus, the findings highlight the economic feasibility and promising prospects of integrating geopolymers in 3D printing for large-scale construction projects.

5.3 Challenges and future prospects

Despite recent progress in geopolymer AM, several challenges exist toward the progress of geopolymer AM. Major challenges, research gap, and scope of future research are as follows:

Major challenges:

(i) Standardization of AM process: Specific standardization on extrusion and powder bed 3D printing is yet to be developed. Different research groups and companies have been developing unique AM configuration techniques, such as flow speed, materials mixing procedure, flow properties, pumping process, setting time, layer shapes, and aggregate distribution. All those parameters need to be standardized to produce geopolymer elements with uniform properties.

(ii) Geopolymer composite consistency in performance: The mix design of geopolymer is often sensitive to consistent performance. Workability, mechanical properties and durability performance considerably vary due to the wide variation of silicate-based mineral precursors, fineness, and reactivity. In some cases, waste minerals (such as FA and slag) from the same source may vary from batch-to-batch production. Another challenge lies in the variation in the variety of activators and their sustainability. Curing condition optimization, such as elevated temperature, often requires tuning to achieve desirable geopolymer AM element performance for specific applications.

Therefore, definite guidelines for selecting the mix parameters to the best level to achieve the desired geopolymer composite for AM are the need of the hour. On the other hand, the integration of geopolymer with desirable reinforcement in AM still poses several challenges.

(iii) Accurate life cycle assessment (LCA) and carbon footprint: LCA and the low carbon footprint of geopolymer AM are dependent on several key parameters. Out of those, transportation, service life performance, and activator sustainability strongly impact the overall LCA performance. This may considerably be based on different geographical locations.

(iv) Economic feasibility: Capital investment involved in AM of geopolymer is one of the crucial parameters in the advancement process. A few key parameters include materials cost, printing cost, manufacturing and management cost, assembly cost, postprocessing techniques, etc., which primarily determine the economic efficiency and essentially aid in the commercialization of the technology. Comprehensive future works in the field of cost analysis are essential in regulating the significance of each parameter with respect to the area of application because price factors are subject to change with location.

(v) Industry readiness and acceptance: There is a lack of industry policies that couple with standards and geopolymer AM specifications, causing challenges in wide-scale industrial acceptance. The cost is also high in the start-up phase, while AM technology is mostly developed in laboratories and by companies. Finally, the technical knowledge of construction field workers is limited, along with the overall complexity of the procedure, which, if not followed precisely, could result in highly undesirable AM products. Lack of knowledge about geopolymer and AM process becomes one of the biggest challenges for not having real-scale applications of geopolymer AM elements.

(vi) Size of the printed articles: A major constraint related to AM is the size of the printed article [13, 258]. Nevertheless, Bos et al. referred to printers able to print significant building components of dimensions $(36.5 \times 12.2 \times 6.1)$ m^3 produced by the WinSun company [13]. Similarly, Weger et al. reported a printer that can print construction parts [258]. The scale of AM capacity is increasing continuously with the advancement of relevant research.

Geopolymer is getting used hardly in the general practice of construction applications because of their complexity in terms of the use of chemical solutions, lack of awareness, etc. However, it is advantageous in terms of characteristics compared to conventional concrete. The development of a framework to use geopolymer with the adoption of additive manufacturing techniques will help implement general construction practices in future. In order to implement geopolymer AM elements successfully on a large-scale, rigorous research must be conducted to establish all its advantages in a definite way and find the solutions for all the existing difficulties.

Major research gap identified:

(i) Theoretical and experimental research on appropriate mix design and the interaction between different parent and reinforcement materials in 3D printed geopolymer matrix materials is insufficient, especially between the layers, and needs further research.

(ii) The anisotropy property phenomenon in the geopolymer AM is a common obstacle, which exhibits different mechanical behavior depending on the direction of load due to a laminated approach to structure manufacturing.

(iii) There is a lack of persistent engineering practice and application cases of geopolymer AM, which would provide results relevant to the progress and acceptance of the technology.

(iv) Different researchers adopted distinct ways to measure the properties of the geopolymers for AM. Due to the various standards followed, it is difficult to define the optimum range based on the recommended values of the papers. Therefore, these recommended values must be validated within different geographical locations to achieve acceptable uniform properties.

Future scope of research and progression:

(i) Comprehensive studies are essential to develop consistent mixing protocols and investigate the effect of different mixing parameters on the geopolymer AM for both extrusion and powder-based technologies.

(ii) Studies on the compatibility between different raw materials, activators, and admixtures are essential to prevent unexpected reactions that may affect product quality.

(iii) A combined sustainability analysis of geopolymer 3D printing can be critical in providing a greener direction to the construction sector. Therefore, a cradle-

to-grave assessment of 3DPG is required, with more relevant functional indicators included in the analysis.

(iv) Research has focused on various combinations of raw materials, but there is a need for further exploration to identify novel raw material combinations that offer improved properties for geopolymer AM.

(v) More research is needed to optimize curing conditions for geopolymer AM. This includes investigating the effects of curing temperature, duration, and post-curing methods on mechanical properties.

(vi) The influence of printing path configurations on the mechanical properties of printed geopolymer products, including the direction of printing and layering, requires further study.

(vii) Exploring the incorporation of nanomaterials and hybrid reinforcement materials into geopolymer AM to further improve mechanical properties and functionality.

(viii) Studies on the long-term durability and aging behavior of geopolymer AM products under different environmental conditions are needed to assess their suitability for real-world applications.

(ix) Actively explore ways to expand the applications. The development of standardized procedures and guidelines for geopolymer AM, including material characterization, testing, and quality control, would be beneficial for industry adoption.

6 Conclusions

This comprehensive review sheds light on the critical parameters, current advancements, challenges, and research gaps in Additive Manufacturing (AM) using geopolymer composites. The synthesis of information from critical literature analysis leads to the following key findings:

- The AM technique does not require any framework or mold, bringing significant benefits to the construction industry. The advanced AM technology enhances the environmental benefits of geopolymer materials by reducing waste during construction.
- Materials extrusion-based AM method through layer-by-layer deposition is most commonly used in AM geopolymer. Binder jetting AM is also developing, considering its advantage in high utility while the powder flowability, particle size, and wettability match the printer. Geopolymer mix in binder jetting depends on the printing requirement. Layer size and the printed article's resolution (for printing time) have inverse relations that need to be critically adjusted based on the printing element complexity and requirement.
- AM geopolymer activator system produced by alkali-activation of waste and alternative source materials. Commonly MK, FA, kaolin, and slag are used as a geopolymer precursor. Typical admixtures for AM of geopolymer are superplasticizers, thixotropy additives, viscosity-modifying agents, retarders or accelerators, and reinforcement (fiber or mineral admixtures). Admixtures are applied during the pumping and deposition stage of the extrusion-based AM, while those are mixed during powder mixing in the case of powder bed AM.
- The desirable geopolymer composite for AM must have several essential material properties, such as pumpability, extrudability, buildability, thixotropic properties, short time of curing and possibility of curing in low temperature, interlayer bonding, and segregation prevention, durability, ductility, high tensile and CS, low coefficient of thermal expansion, resistance to UV light and others. A combination of different types of admixtures in geopolymer can provide those desirable material properties.
- Reinforcements are used in AM geopolymer to minimize the brittleness of the composite. Different types of steel, glass, carbon, and polymeric fibers, as well as steel micro-cable, are used in AM geopolymer, which is vital for controlling printed layers' fresh and mechanical properties. Natural fibers such as green tow flax fiber of 30–50 mm long also show promising mechanical performance in AM geopolymer.
- There are several challenges in the development of AM geopolymer composite technology. These are associated with the cost of printing setup, size limitation, the in-process and in-service performance of the available materials, post-processing procedures, the mix design, and supporting structure until gaining its desirable strength.

- Robocasting-based materials extrusion AM is most used for geopolymer printing. However, this process has significant shortcomings, such as the complex structure not being able to be printed due to the lack of support, the limitation of smaller particle size in the mix to allow passing through the nozzle head, and the consistent quality of printed geopolymer and standardization. On the other hand, the binder jetting AM process is advantageous as the critical parameters, such as the layer thickness, activator jet spacing, speed, and activator flow rate, could be adjusted desirably. However, powder compatibility with the printer is a major challenge in the binder jetting AM technique, which needs further research and up-gradation.
- Typically, sodium-based powder alkali activators are used in the AM geopolymer extrusion process. Alkali activators are also used in powder bed printing as a compound for post-processing. However, several studies suggest that liquid-based alkali activators are more efficient for geopolymers than the solid powder form. Hence, comprehensive research is required on the mechanical and durability properties of the final AM geopolymer products and the effect of different alkali activators.
- Typical steel rebar reinforcement in geopolymer is a complex setup that also results in several technical problems, such as controlling the speed limit during the AM process and design limitations, such as curved shapes that are required from an architectural point of view. The replacement of steel rebar could be made with steel and polymer fibers or other alternatives. Different reinforcing nano-additives carbon-based materials, such as carbon nanotubes, graphene nanoplates, and GO, have recently been getting much attention in the geopolymer composite field. This is another broad and promising sector in the development of AM geopolymer technology. Besides, natural or waste-based fibers could be beneficial from a sustainability point of view, which should be broadly investigated.
- Quality and performance of AM geopolymer composite depend on several interdepending components. Major components are the type of printing, software used for generating the 3D model, geopolymer precursors, activators, additives, and curing conditions. Alternation and optimization of those components are vital fields of research to modify the end property of printed geopolymer elements.
- An eco-friendly AM for the future construction industry can be developed by modifying geopolymer mixes to achieve particular properties. More research is required to establish the use of eco-friendly geopolymer precursors, such as industrial waste, CDW, waste glass, and mine tailing. Modification of geopolymer could also be explored using different types of nanomaterials, such as graphene and carbon nanotubes.

Geopolymers, as low carbon footprint materials, are increasingly getting attention for the application of typical structural elements. The application of AM geopolymer is making much progress in precast industries, such as formworks, interior structures, beams, etc. The typical extrusion-based AM geopolymer could be adopted in on-site construction applications. Powder bed AM geopolymer, for example, could be used in the construction of thermal insulation structures and other large-scale structural applications. The AM geopolymer could also be helpful in repairing existing structures and sensing applications.

Appendix

See Tables 6, 7, 8, and 9.

Table 6 Summary of research in geopolymer AM

Authors	Year	Document type	Publication type	3D printing type	Binder materials	Composite matrix	Applications	References
Franchin and Colombo	2015	Experimental	Journal	Extrusion	MK	NA	Filtering/Catalyst Support	[23]
Montes et al.	2015	Experimental	Journal	NA	Lunar regolith simulant (JSC-1A)	Concrete	Radioactive Shielding	[24]
Xia and Sanjayan et al.	2016	Experimental	Journal	Powder Bed	Slag powder, Zp® 150 powder	Concrete	Construction	[25]
Zhong et al.	2017	Experimental	Journal	Extrusion	Na powder, GO	Paste	Smart material, Structural	[26]
Panda et al.	2017	Experimental	Journal	Extrusion	FA (Class F)	Mortar, Concrete	Concrete	[27]
Panda et al.	2017	Experimental	Journal	Extrusion	FA (Class F), GGBFS, Short Glass Fiber	Mortar, Concrete	Concrete	[28]
Nematollahi et al.	2017	Review	Conference Proceedings	Extrusion & Powder Bed	NA	NA	Concrete	[29]
Davis et al.	2017	Experimental	Journal	NA	Lunar regolith simulant (JSC-1A)	NA	Construction, Radioactive Shielding	[30]
Dechang et al.	2017	Review	Journal	NA	NA	NA	NA	[31]
Panda et al.	2017	Experimental	Conference Proceedings	Extrusion	FA (Class F), Slag, SF	Mortar	Concrete	[32]
Nematollahi et al.	2018	Experimental	Journal	Extrusion	FA (Class F), PP fibers (PP),	Mortar	NA	[33]
Nematollahi et al.et al.	2018	Experimental	Journal	Extrusion	FA (Class F), PVA fibers, PP fibers, PBO fibers	Concrete	Concrete	[34]
Panda and Tan	2018	Experimental	Journal	Extrusion	FA (Class F), GGBFS,	Paste, Mortar	Concrete	[35]
Lim et al.	2018	Experimental	Journal	Extrusion	FA (Class F), GGBFS, PVA fibers	Mortar, Concrete	Concrete	[36]
Panda et al.	2018	Experimental	Journal	Extrusion	FA (Class F), GGBFS, SF,	Paste, Mortar	Construction	[37]
Al-Qutaifi et al.	2018	Experimental	Journal	Extrusion	FA (Class F), Hooked-end steel fibers, PP fibers	Paste, Concrete	Concrete	[38]
Panda et al.	2018	Experimental	Journal	Extrusion	FA (Class F), GGBFS, SF,	Mortar	Concrete	[39]
Panda and Tan	2018	Experimental	Conference Proceedings	Extrusion	FA (Class F), GGBFS, SF,	Mortar	NA	[40]
Annapareddy et al.	2018	Experimental	Conference Proceedings	Extrusion	FA (Class F), GGBFS, SF,	Concrete	NA	[41]
Xia et al.	2018	Experimental	Journal	Powder Bed	Slag powder,	Concrete	Construction	[42]
Christos et al.	2018	Review	Conference Proceedings	Extrusion	MK	Paste	Smart Material, Structural Health monitoring & repair	[43]
Kashani and Ngo	2018	Experimental	Conference Proceedings	Extrusion	FA (Class F), GGBFS, SF,	Paste	Construction	[44]
Panda et al.	2018	Review	Journal	Extrusion	NA	NA	Construction	[45]

Table 6 (continued)

Authors	Year	Document type	Publication type	3D printing type	Binder materials	Composite matrix	Applications	References
Zhang et al.	2018	Experimental	Journal	NA	Slag	Paste	Construction	[46]
Singh	2018	Review	Journal	NA	FA	NA	Construction	[47]
Xia and Sanjayan	2018	Experimental	Journal	Powder Bed	FA (Class F)	Paste	Construction	[48]
Zhang et al.	2018	Experimental	Journal	Extrusion	GGBFS, Steel Slag	Paste	Construction	[49]
Korniejenko et al.	2019	Experimental	Conference Proceedings	Extrusion	FA, GTF fibers	Paste	Construction	[50]
Hirayama et al.	2019	Experimental	Conference Proceedings	Extrusion	FA, BFS, SF	Concrete	Construction	[51]
Agnoli et al.	2019	Experimental	Journal	Extrusion	MK, Microalgal Biomass	Paste	Construction, Inorganic foams, Water filtration, Thermal insulation	[52]
Toniolo et al.	2019	Experimental	Journal	Extrusion	FA, Waste glass	Paste	Ceramics, Construction	[53]
Panda et al.	2019	Experimental	Journal	Extrusion	FA (Class F), GGBFS, Nanoclay	Paste, Mortar	Construction	[54]
Bong et al.	2019	Experimental	Journal	Extrusion	FA (Class F), GGBFS	Concrete	Construction	[55]
Ma et al.	2019	Experimental	Journal	Extrusion	FA (Class F), Slag, SF, PP fibers	Concrete	Construction	[56]
Fu et al.	2019	Experimental	Journal	NA	MK	Paste	Ceramics	[57]
Marczyk et al.	2019	Review	Conference Proceedings	Extrusion	NA	Paste, Mortar, Concrete	Construction	[58]
Nematollahi et al.	2019	Experimental	Journal	Powder Bed	Slag	NA	Construction	[59]
Xia et al.	2019	Experimental	Journal	Powder Bed	FA (Class F), Slag	Concrete	Construction	[60]
Alghamdi and Neithalath	2019	Experimental	Journal	Extrusion	FA (Class F), OPC, SF, Limestone	Foam	Thermal Insulation	[61]
Panda et al.	2019	Experimental	Journal	Extrusion	FA (Class F), GGBFS	Concrete	Construction	[62]
Nematollahi et al.	2019	Experimental	Book Chapter	Extrusion	FA (Class F), GGBFS	Concrete	Construction	[63]
Panda et al.	2019	Experimental	Book Chapter	Extrusion	FA (Class F), GGBFS, SF	Mortar	Construction	[64]
Bong et al.	2019	Experimental	Book Chapter	Extrusion	FA (Class F), GGBFS	Concrete	Construction	[65]
Singh et al.	2019	Review	Conference Proceedings	NA	MK, FA, GGBFS	NA	NA	[66]
Wu et al.	2019	Review	Journal	Extrusion	FA (Class F), GGBFS	NA	Construction	[67]
Chenchen et al.	2020	Experimental	Journal	Extrusion	GGBFS	Paste, Mortar	NA	[68]
Yin et al.	2020	Experimental	Conference Proceedings	Extrusion	FA, Slag	Paste	NA	[69]
Vlachakis et al.	2020	Experimental	Journal	Extrusion	MK, SF, PVA fibers	Paste, Concrete	Temperature sensing concrete repair	[70]
Zhou et al.	2020	Experimental	Journal	Extrusion	MK, GO	Paste	NA	[71]

Table 6 (continued)

Authors	Year	Document type	Publication type	3D printing type	Binder materials	Composite matrix	Applications	References
Rehman et al.	2020	Experimental	Journal	Powder Bed	MK	Concrete	Construction	[72]
Imtiaz et al.	2020	Review	Journal	NA	NA	NA	NA	[73]
Luhar and Luhar	2020	Review	Journal	Extrusion & Powder Bed-	NA	NA	Construction	[74]
Luukkonen et al.	2020	Report	Journal	Extrusion	MK	Paste	Water treatment	[75]
Muthukrishnan et al.	2020	Experimental	Journal	Extrusion	FA (Class F), GGBFS, PVA fibers	Concrete	NA	[76]
Nematollahi et al.	2020	Experimental	Book chapter	Extrusion	FA (Class F), GGBFS	Concrete	Construction	[77]
Bong et al.	2020	Experimental	Book chapter	Extrusion	FA, Slag, Wollastonite	Concrete	Construction	[78]
Albar et al.	2020	Experimental	Journal	Extrusion	FA, GGBFS	Paste	NA	[79]
Nematollahi et al.	2020	Experimental	Book chapter	Powder Bed	Slag	NA	Construction	[80]
Voney et al.	2020	Experimental	Book chapter	Powder Bed	MK	NA	Construction	[81]
Korniejenko and Łach	2020	Review	Journal	Extrusion & Powder Bed-	FA, Fibers	NA	Construction	[82]
Guo et al.	2020	Experimental	Journal	Extrusion	FA, Slag, SF	Mortar	NA	[83]
Li et al.	2020	Experimental	Journal	Extrusion	FA (Class F), Slag, SF	Mortar	Construction	[84]
Korniejenko et al.	2020	Experimental	Journal	Extrusion	FA (Class F), GTF fiber, Carbon fiber	Paste, Concrete	Construction	[85]
Voney et al.	2020	Experimental	Conference Proceedings	Powder Bed	MK, Quarry waste	NA	Quarry waste recycling	[86]
Franchin et al.	2020	Experimental	Journal	Extrusion	MK	Paste	Wastewater treatment	[87]
Panda et al.	2020	Experimental	Book chapter	Extrusion	FA (Class F), GGBFS	Mortar	Construction	[88]
Xia et al.	2020	Experimental	Book chapter	Powder Bed	Slag	Concrete	Construction	[89]
Li et al.	2020	Experimental	Journal	Extrusion	FA (Class F), GGBFS, SF	Paste, Mortar	Construction	[90]
Sun et al.	2020	Experimental	Journal	Extrusion	MK	NA	Construction, Electronics	[91]
Chougan et al.	2020	Experimental	Journal	Extrusion	FA (Class F), GGBFS, SF, Nano-graphite platelets	Paste	Smart construction material	[92]
Bong et al.	2020	Experimental	Book chapter	Extrusion	FA (Class F), GGBFS, PVA fibers	NA	Construction	[93]
Odaglia et al.	2020	Experimental	Book chapter	Powder Bed	MK	NA	Construction	[94]
Khan et al.	2020	Review	Conference Proceedings	Extrusion	NA	Concrete	NA	[95]
Jia et al.	2020	Review	Book chapter	NA	NA	NA	NA	[96]
Bagheri and Cremona	2020	Experimental	Journal	Extrusion	NA	NA	Construction	[97]
Perumal et al.	2020	Review	Book Chapter	Extrusion & Powder Bed-	NA	NA	NA	[98]
Korniejenko et al.	2020	Experimental	Conference Proceedings	Extrusion	FA, MK	Concrete	Construction	[99]

Table 6 (continued)

Authors	Year	Document type	Publication type	3D printing type	Binder materials	Composite matrix	Applications	References
Pilehvar et al.	2020	Experimental	Journal	Extrusion	Lunar regolith simulant (ESA), FA (Class F)	NA	Lunar Construction	[100]
Emelyanov et al.	2020	Experimental	Conference Proceedings	Extrusion	NA	Concrete	NA	[101]
Lazarev et al.	2020	Experimental	Conference Proceedings	Extrusion	NA	Concrete	Construction	[102]
Yin et al.	2020	Experimental	Conference Proceedings	Extrusion	FA, Slag, MK	Mortar	NA	[103]
Santos et al.	2021	Experimental	Journal	Extrusion	MK	Paste	Biocatalyst	[104]
Santana et al.	2021	Experimental	Journal	NA	MK, SF	Concrete	Construction	[105]
Ma et al.	2021	Experimental	Journal	Extrusion	MK, carbon fibers	Paste	NA	[106]
Youssef et al.	2021	Experimental	Journal	Extrusion	Clay	Mortar	Construction	[107]
Botti et al.	2021	Experimental	Journal	Extrusion	MK	Paste	Catalyst	[108]
G¨okçe et al.	2021	Review	Journal	Extrusion	NA	NA	Construction	[109]
Bong et al.	2021	Experimental	Journal	Extrusion	FA (Class F), GGBFS	Mortar	Construction	[110]
S¸ahin et al.	2021	Experimental	Journal	Extrusion	Construction Demolition Waste	Paste	NA	[111]
Munir and Kärki	2021	NA	Journal	Extrusion	NA	NA	Construction	[112]
Cepollaro et al.	2021	Experimental	Journal	Extrusion	MK	Paste	Catalyst	[113]
Ma et al.	2021	Experimental	Journal	Extrusion	MK	Paste	NA	[114]
Zhao et al.	2021	Review	Journal	Extrusion	NA	NA	Construction	[115]
Muthukrishnan et al.	2021	Experimental	Journal	Extrusion	FA (Class F), GGBFS	Paste, Concrete	NA	[116]
Voney et al.	2021	Experimental	Journal	Powder Bed	MK	Paste	NA	[117]
Nmiri	2021	Review	Book chapter	Extrusion	NA	NA	Construction	[118]
Ly et al.	2021	Experimental	Journal	Extrusion	FA	Mortar	Artificial reefs	[119]
Munir et al.	2021	Experimental	Journal	Extrusion	Industrial side stream waste, CDW, bark boiler ash, mine tailings, MK	Concrete	Construction, Insulation, backfill	[120]
Sambucci et al.	2021	Review	Journal	Extrusion	NA	NA	Construction	[121]
Wang et al.	2021	Experimental	Journal	Extrusion	MK	Paste	Construction, Nuclear waste coating, Insolation, Insulation	[122]
Souza et al.	2021	Experimental	Journal	Extrusion	MK	Paste	Construction	[123]
Archez et al.	2021	Experimental	Journal	Extrusion	MK, Glass fibers, Wollastonite	Concrete	NA	[124]
Bhattacherjee et al.	2021	Review	Journal	Extrusion	NA	NA	NA	[125]
Scanferla et al.	2021	Experimental	Journal	Extrusion	MK	Paste	Filters, Catalysts	[126]

Table 6 (continued)

Authors	Year	Document type	Publication type	3D printing type	Binder materials	Composite matrix	Applications	References
Pilehvar et al.	2021	Experimental	Journal	Extrusion	DNA-1 lunar regolith simulant	Paste, Concrete	Lunar construction	[127]
Kocherla et al.	2021	Experimental	Conference Proceedings	Extrusion	FA, Slag, SF	Paste, Concrete	PZT Sensor	[128]
Kleshchevnikova et al.	2021	Experimental	Book Chapter	Extrusion	Geopolymer Cement, Slag, PP fibers	Concrete	NA	[129]
Singh	2021	Review	Book Chapter	NA	FA	NA	Construction	[130]
Archez et al.	2021	Experimental	Journal	Extrusion	MK, Glass fibers	Paste	Industrial	[131]
Perry et al.	2021	Experimental	Conference Proceedings	Extrusion	FA, MK	Paste	Self-Sensing	[132]
Ranjbar et al.	2021	Experimental	Journal	Extrusion	FA	Mortar	NA	[133]
Muthukrishnan et al.	2021	Review	Journal	Extrusion	NA	NA	Smart material, Construction	[134]
Lv et al.	2021	Experimental	Journal	Extrusion	GGBFS	Paste	NA	[135]
Tang et al.	2021	Experimental	Journal	Extrusion	MK	Paste	Thermal Insulation	[136]
Marczyk et al.	2021	Experimental	Journal	Extrusion	FA, MK	Paste, Mortar, Concrete	Construction	[137]
Paiva et al.	2021	Experimental	Journal	Extrusion	MK	Paste, Mortar	Construction	[138]
Jin et al.	2022	Experimental	Journal	Extrusion	MK	Paste	Adsorption	[139]
Ziejewska et al.	2022	Experimental	Journal	Extrusion	OPC, FA, MK	Concrete	Fire Resistance	[140]
G¨okçe et al.	2022	Experimental	Journal	Extrusion	NA	NA	Construction	[141]
Elsayed et al.	2022	Experimental	Journal	Powder Bed	MK	NA	Construction	[142]
Yuan et al.	2022	Experimental	Journal	Extrusion	FA, GGBFS	Mortar	NA	[143]
Lazorenko and Kasprzhitskii	2022	Review	Journal	Extrusion & Powder Bed-	NA	NA	NA	[144]
Oliveira et al.	2022	Experimental	Journal	Extrusion	MK, Activated carbon, Hydrotalcite	Paste	Adsorption, Water treatment	[145]
Chen et al.	2022	Experimental	Journal	Extrusion	FA, GGBFS	Mortar, Concrete	NA	[146]
Marczyk et al.	2022	Experimental	Journal	Extrusion	FA, MK	Paste, Concrete	Construction	[147]
Liu and Lv	2022	Review	Journal	Extrusion	NA	Mortar	NA	[148]
Bong et al.	2022	Experimental	Journal	Extrusion	FA (Class F), GGBFS, Wollastonite fiber	Concrete	Construction	[149]
Raza et al.	2022	Review	Journal	Extrusion & Powder Bed-	NA	NA	NA	[150]
Ilcan et al.	2022	Experimental	Journal	Extrusion	CDW	Mortar	NA	[151]
Tang and Tang	2022	Experimental	Journal	Extrusion	Geopolymer powder	NA	Energy storage, Refractory	[152]
Muthukrishnan et al.	2022	Experimental	Journal	Extrusion	FA (Class F), GGBFS	Paste, Concrete	Construction	[153]
Guo et al.	2022	Experimental	Journal	NA	FA, Slag	Mortar	NA	[154]
Shakor et al.	2022	Review	Journal	Powder Bed	NA	Mortar	Construction	[155]
Na et al.	2022	Experimental	Journal	Extrusion	FA, GGBFS, Steel slag	Concrete	NA	[156]

Table 6 (continued)

Authors	Year	Document type	Publication type	3D printing type	Binder materials	Composite matrix	Applications	References
Kong et al.	2022	Experimental	Journal	Extrusion	FA, GGBFS, Sekanf straw core, Kenaf fiber	NA	Construction	[157]
Korniejenko et al.	2022	Experimental	Journal	Extrusion	FA, GTF, Carbon fiber	NA	Construction	[158]
Li et al.	2022	Experimental	Journal	Extrusion	Graphene	NA	Microwave absorption	[159]
Zhong and Zhang	2022	Review	Journal	Extrusion	NA	NA	NA	[160]
Ma et al.	2022	Experimental	Journal	Extrusion	MK, SiC whiskers	Paste	NA	[161]
Liu et al.	2022	Experimental	Journal	Extrusion	NA	Concrete	Construction	[162]
Kondepudi et al.	2022	Experimental	Journal	Extrusion	FA, Slag	Paste	Construction	[163]
Ma et al.	2023	Experimental	Journal	Extrusion	MK	Paste	Waste water treatment	[164]
Salazar et al.	2023	Review	Journal	Extrusion	NA	NA	Construction	[165]
Rahemipoor et al.	2023	Experimental	Journal	Extrusion	FA, PCM	Paste	Thermal Energy Storage	[166]
Pasupathy et al.	2023	Experimental	Journal	Extrusion	FA, Slag, BW	Concrete	Construction	[167]
Ramezani et al.	2023	Review	Journal	Extrusion	Fibers	Concrete, Mortar	Construction	[168]
Chen et al.	2023	Experimental	Journal	Extrusion	FA, Slag, Steel Fiber	Mortar	Construction	[169]
Jaji et al.	2023	Experimental	Conference	Extrusion	Slag, MK, PP	Mortar	NA	[170]
Tran et al.	2023	Experimental	Journal	Extrusion	Slag, FA	Mortar	NA	[171]
Basha et al.	2023	Review	Journal	Extrusion, Powder Bed	Carbon Nanomaterials	Mortar, Concrete	NA	[172]
Masi et al.	2023	Experimental	Conference	Extrusion	MK	Paste	Recycling	[173]
Ilcan et al.	2023	Experimental	Journal	Extrusion	CDW	Mortar	Construction	[174]
Muthukrishnan et al.	2023	Experimental	Journal	Extrusion	FA, Slag, Lime	Concrete	NA	[175]
Khan et al.	2023	Experimental	Journal	Extrusion	CDW, Slag	Concrete	Numerical Modeling	[176]
Chaiyotha et al.	2023	Experimental	Journal	Extrusion	FA	Mortar	Construction	[177]
Ranjbar et al.	2023	Experimental	Journal	Extrusion	FA, HA	Mortar	NA	[178]
Gonçalves et al.	2023	Experimental	Journal	Extrusion	MK, RM	Paste	Adsorption	[179]

Table 7 Review for extrusion-based AM geopolymer technologies

Raw material(s)	Activator(s)	Admixture(s)	Key finding(s)	References
CDW	Na_2SiO_3 + NaOH + $Ca(OH)_2$	N/A	CDW-based geopolymers could be used for AM without any additional chemical admixtures Na_2SiO_3 decreased the viscosity of the mixtures (increases flowability, reduces buildability, and vane shear stress) Using $Ca(OH)_2$ increases the matrix viscosity, buildability, and vane shear stress and decreases flowability	[111]
FA (Class F) + GGBFS + Silica sand	Na_2SiO_3 Powder + Anhydrous Na_2SiO_3 Powder	Sucrose powder (retarder)	Handling dangerous alkaline liquids and the need for heat curing are eliminated by the 'just-add-water' formulation (composed of FA, slag, and solid activators), which could be cured at ambient temperature. It improves the feasibility of large-scale and commercial applications The printed specimens had a 28-day FS of 3.5–8.4 MPa, depending on the direction of testing	[110]
FA (Class F), SF, Slag, Silica sand	Na_2SiO_3 Pentahydrate Powder	PP fibers (anti-shrinkage agent), VMA, Hydroxyethyl cellulose (increasing water retention), Steel micro-cable (reinforcement)	Optimization micro-cable reinforcement – three different printing path configurations are compared The results show significant improvement in the mechanical strength of the reinforced composites	[56]
MK	Na_2SiO_3 solution	Hexagonal boron nitride h-BN powder, Urea (shape retention)	3D structures of 300–400 µm thick features were fabricated using the synthesized geopolymer/hexagonal boron nitride suspension The extruded elements exhibited high regularity and shape retention	[91]
MK	Na_2SiO_3, Sodium hydroxide	GO (properties modification)	Large GO sheets do not improve the mechanical properties of the geopolymer Large GO sheets improve the rheological behavior and structure failure mode of geopolymers	[26, 71]
MK	Na_2SiO_3, NaOH	Polyethylene glycol – PEG 1000 (rheological agent), Surface coated with NH_2 groups by adding a 3% solution of 3-aminopropyltriethoxysilane in hexane (ion-exchange)	AM successfully prepared lattice-shaped geopolymers for enzyme immobilization (Candida rugosa lipase) The mesoporous structure favors chemical functionalization	[104]

Table 7 (continued)

Raw material(s)	Activator(s)	Admixture(s)	Key finding(s)	References
MK	Na_2SiO_3, NaOH	Polyethylene glycol – PEG 1000 (rheological agent) – 5% wt	The printed geopolymer sorbents (for removing ions from wastewater) show a high cation exchange capacity The printed geopolymer sorbents provide a valid alternative to synthetic zeolites and conventional ceramics	[87]
FA, GGBFS, SF	Na_2SiO_3, NaOH	Nano-graphite platelets (properties modification)	Nano-additives improved AM composites' mechanical performance, shape retention, and buildability Nano-additives reduce micro-crack propagation Rheology measurements play an essential role in the selection of printable feedstock	[210]
FA, GGBFS, SF, Quartz sand	Na_2SiO_3 solution	Glass fiber ARG (formability), AE Master Air 785 (water-reducing fluidity)	Geopolymers are for use in AM robots, being able to be used for building large structures	[51]
FA, GGBFS, Sand (coarse and fine)	Anhydrous Na_2SiO_3 (solid activator)	Magnesium aluminosilicate (thixotropic enhancer), Sucrose powder (retarder)	The mixing regime plays a vital role in obtaining a consistent mix Sucrose influences the growth of static yield strength with time	[116]
MK, Calcined callovo-oxfordian argillites, Powdered fillers (callovo-cxfordian argillites – not-calcinated, kaolin, sand)	K_2SiO_3 solution	AR glass fibers (length: 6 mm), wollastonite (length 5–170 µm) – reinforcement	The decreasing printing speed and the inorganic elements, such as MK, wollastonite, glass fibers, or nonreactive aluminosilicate, reduce the slump observed during the AM	[124]
FA (Class F), GGBFS, Sand (coarse and fine)	Anhydrous Na_2SiO_3 (solid activator)	PVA fibers (length 6 mm) – against crack propagation	The buildability of geopolymer concrete improved with microwave heating The best properties are achieved at 10 s exposure to microwave heating, including decreasing lateral deformation	[76]
FA, GGBFS, Silica sand	Anhydrous Na_2SiO_3 (solid activator)	N/A	The microwave heating of geopolymer concrete before extrusion increases the interlayer adhesion of the printed elements Microwave heating enhances the viscosity recovery of geopolymer concrete Microwave heating can also be applied to OPC	[211]

Table 7 (continued)

Raw material(s)	Activator(s)	Admixture(s)	Key finding(s)	References
F (Class F), GGBFS, SF, Sand	Na_2SiO_3 pentahydrate powder	Steel micro-cable (type SUS304)	The failure mode of the reinforced structures changed from brittle to ductile The micro-cable reinforcement altered the strain evolution patterns The specific configurations of the AM structures play a crucial role in resisting deformation and damage	[90]
MK, Ground geopolymer (filler)	Na_2SiO_3, NaOH, K_2SiO_3, KOH, Sodium & Potassium solution	Polyethylene glycol – PEG 1000 (rheological agent)	Printed geopolymers were successfully applied to manufacture cylindrical lattices to act as heterogeneous catalysts for biodiesel processing The lattices possessed a porosity of up to 64.2 vol%	[108]
MK	Na_2SiO_3, NaOH	N/A	The preheating process can be helpful in AM for rheology improvement	[123]
MK, Sand, Ground geopolymer (filler)	Na_2SiO_3, NaOH	Polyethylene glycol – PEG 1000 (rheological agent) – 5 wt.%	Adding a filler to a pure geopolymer ink enhanced its rheological properties Ground geopolymer filler was the most effective due to its smaller dimension and higher affinity with the matrix Printed geopolymer lattices could be used as water or gas purification filters or catalyst supports	[212]
FA, Sands (limestone sand, glass sand, shell sand)	NaOH	Superplasticizer	The artificial reefs were prepared using printed geopolymer and cement Biofouling and mechanical properties in the medium-term are better with cement than geopolymer as activators	[119]
FA, GGBFS, SF	Na_2SiO_3, NaOH	N/A	The cost-effective extrusion-based AM system confirms the possibility of using this technology for geopolymeric materials (without using expensive equipment such as robotic arms)	[79]
FA (Class F), GGBFS, SF, sand	Na_2SiO_3 pentahydrate powder	Steel, Nylon, Carbon, Aramid, Polyethylene micro-cables	The reinforcing cables increase the compressive strength (CS), strain at peak strength, and toughness of the material The design of the printing path is essential in achieving the required strength The shear strength is mainly governed by the matrix rather than the reinforcement	[84]

Table 7 (continued)

Raw material(s)	Activator(s)	Admixture(s)	Key finding(s)	References
FA, Slag	Na_2SiO_3 solution	N/A	Reasonable extrudability and shape retainability can be achieved by adjusting the water-to-activator ratio The buildability can be improved by adjusting the gap time	[69]
MK, SF	Na_2SiO_3, NaOH	0.5 wt.% PVA fibers (3 mm length) – reducing shrinkage	The AM temperature sensing repair for concrete was produced using the multifunctional material, which can be electrically interrogated to act as a sensor	[70]
FA, Slag, SF, Quartz sand	Anhydrous Na_2SiO_3	ATTAGEL-50 (thixotropic thickener)	According to rheological properties, the optimum content for slag powder is 10% The optimum content for SF is also 10% in mass SEM analysis showed that the printing layers are connected through bridges	[83]
MK	Na_2SiO_3, NaOH	Polyethylene glycol – PEG 1000 (rheological agent), Ag or Cu (impregnate, disinfecting, or catalytic properties)	AM is an appropriate method for producing highly porous geopolymer components for water treatment applications. The components have mesoporosity, suitable mechanical strength, and water permeability	[75]
MK	NaOH	Ba $(NO_3)_2$, Sr $(NO_3)_2$ (ion-exchanged)	The synthetic procedure to prepare monoclinic celsian ceramics through thermal treatment of ion-exchanged AM geopolymer precursors was successfully applied During the ion exchange process, AM geopolymer precursors kept fine integrity and stable 3D structure AM is a versatile and robust way to yield monoclinic celsian ceramics and related components of complex shapes	[57]
FA (Class F), GGBFS, MS fume, River sand	Na_2SiO_3 solution	N/A	SF has a significant influence on fresh properties (e.g., recovery of viscosity) Slag led to higher early strength development of geopolymer materials	[37]

Table 7 (continued)

Raw material(s)	Activator(s)	Admixture(s)	Key finding(s)	References
FA (Class F), OPC, SF, Fine limestone powder	Na_2SiO_3, NaOH, Sodium sulfate	Lightcrete 02™ (foaming agent and foam stabilizer)	AM is relevant to creating geopolymeric foams for thermal insulation applications, for example, in sandwich wall panels The thermal conductivity of the foamed matrices was between 0.15 and 0.25 W/m–K, and porosity was between 55 and 75% 3Dprinted geopolymeric allows the creation of products with dual-porosity systems – smaller pores in the foam and larger pores in the printed paths	[61]
FA (Class F), GGBFS, River sand	Anhydrous Na_2SiO_3 (solid activator)	N/A	The possibility of improving thixotropy property geopolymer mixes for AM-printed sections with a height of up to 300 mm by depositing consistent filaments without any noticeable deformation of the bottom layers	[62]
GGBFS, calcium carbonate powder-fine aggregate	Na_2SiO_3, NaOH	Sodium carboxymethyl starch (viscosity)	Sodium carboxymethyl starch admixture increases water retention and the setting time of geopolymer composite paste Sodium carboxymethyl starch decreases slurry fluidity and can yield the printing effect with little or no deformation after extrusion Suitable sodium carboxymethyl starch content in geopolymer paste brought AM products low drying shrinkage and high mechanical strength	[68]
FA (Class F), Blast furnace slag	K_2SiO_3, KOH	Attapulgite Nano-clay (thixotropy)	Nano-clay improves the rheological properties and fresh properties of geopolymer activators The AM small-scale bathroom unit was produced	[54]
FA (Class F), GGBFS, Silica sands	Na_2SiO_3, NaOH, K_2SiO_3, KOH	Anhydrous borax, Sodium carboxymethyl cellulose (retarder and viscosity-modifying agents)	The sodium-based geopolymers had higher workability and CS properties than the potassium-based ones (lower yield stress of the sodium-based geopolymers)	[55]

Table 7 (continued)

Raw material(s)	Activator(s)	Admixture(s)	Key finding(s)	References
MK, Bentonite (absorbent aluminum phyllosilicate clay)	Na_2SiO_3, NaOH	Two microalgal biomass species (*Spirulina platensis* and *Tetraselmis suecica*) and lignin (reference biomass)	The microalgae reduce the rheology and porosity of geopolymer concrete Microalgal biomass can be used as a biofiller in these construction materials because it does not affect the mechanical properties; the composite is hardened without noticeable shrinkage and cracking problems Using microalgal biomass wastes in geopolymer cement paste for AM applications is possible	[52]
Soda-lime waste glass, FA (Class F)	NaOH	N/A	AM technology can obtain porous grid-like components from a geopolymer based on FA and waste glass	[53]
FA (Class F), GGBFS	Anhydrous Na_2SiO_3 (solid activator)	Oil-coated PVA (length – 8 mm)	The AM samples exhibited CS of 25.1–49.8 Mpa, modulus of rupture of 8.6–10.2 Mpa, and deflection capacity of 2.9–5.3 mm	[93]
FA (Class F), GGBFS, Fine river sand	K2SiO3, KOH	N/A	The extruded one-part geopolymer exhibits high-yield stress and shear-thinning behavior	[88]
FA (Class F), GGBFS, Silica sand	Anhydrous Na_2SiO_3 powder, Na_2SiO_3 powder	Wollastonite powder	Wollastonite increases the shape retention ability and yield stress evolution of the fresh geopolymer mixture and the FS (up to 29%) Wollastonite does not affect the CS The AM specimens exhibited anisotropic behavior in compression and flexure	[78]
FA (Class F), GGBFS, Silica sand	Anhydrous Na_2SiO_3 (solid activator)	N/A	Depending on the curing temperature, curing time, and delay time, specimens exhibited the following properties: CS of 17.7–43.2 Mpa, FS of 2.8–6.2 Mpa, and interlayer strength of 0.7–2.0 Mpa	[77]
FA/MK, silica sand	Na_2SiO_3 solution	Concrete	Geopolymers and hybrids based on a geopolymer matrix with the addition of 5% cement resulted in the final materials behaving similarly to a non-Newtonian fluid The hybrid materials based on cement with a 5% addition of geopolymer, based on both FA and MK, enabled precise detail printing	[213, 214]

Table 8 Review for powder-based AM geopolymer technologies

Raw material(s)	Activator(s)	Admixture(s)	Key finding(s)	References
MK, Silica sand	Na_2SiO_3, NaOH	N/A	The thickness of the printed specimen increases with the exceeding amount of alkaline liquid solution The AM process is relevant for large-scale construction applications	[72]
FA (Class F), Slag, Silica sand	Anhydrous Na_2SiO_3 powder	N/A	Slag increases fresh and post-processed CSs The CS of the printed samples shows orthotropic properties FA increases the activator droplet penetration time	[60]
Slag, Fine silica sand	Anhydrous Na_2SiO_3 (solid activator)	Zb® 63 (viscosity)	2D images made by flatbed scanners are an efficient method for shape accuracy evaluation for AM small elements for the construction industry	[89]
MK, Fine quartz sand	Na_2SiO_3, NaOH	N/A	The printing parameters can control the macro-porosity in the printed part	[81, 224]
MK, Quarry different types of stone waste, Silica sand	K_2SiO_3 solution	N/A	The silica sand can be successfully replaced by waste granulated from a gneiss quarry AM has a high potential to be scaled up and used in construction	[86]
Slag, Fine silica sand	Anhydrous Na_2SiO_3 (solid activator)	N/A	The immersion in alkaline solutions is an effective method for post-processing powder bed technologies The strength of the printed geopolymer samples cured in the potassium-based activators was lower than that of the sodium-based ones The 28-day CS of the ambient temperature-cured sample is comparable to the 7-day CS of heat-cured samples The CS shows orthotropic properties	[59]
Slag, Fine silica sand	Na_2SiO_3, NaOH, K_2SiO_3, KOH, Sodium and potassium solution	Zb® 63 (viscosity)	The advanced post-processing method for ambient temperature curing promotes broader applications of the developed powder bed AM geopolymers in the construction industry The CS of the samples cured in the sodium-based alkaline solution was about 14%–31% higher than that of the potassium-based samples The CS shows orthotropic properties	[80]

Table 9 Review of AM Geopolymer composite properties from past publications

AM type	Geopolymer precursors and activators	Additives/reinforcements	Curing conditions	Properties				Key findings	References
				CS	FS	YM, BD, AD, TD, AP	TP, EC, ILBS		
Fused Deposition Modeling	MK, FA (Class F) + KOH (15 M), (NaOH, Na_2SiO_3)		48–72 h (Ambient Temperature)	8.5 MPa	–	– 1.30 ± 0.001 g/cm^3 BD, 2.23 ± 0.001 g/cm^3 AD, 2.436 ± 0.0002 g/cm^3 TD –	71% TP	PLA sacrificial templates with different pattern combinations were printed in 3D with great precision, and a geopolymer slurry mixture was employed to generate similar inverse replicas with densely interconnected macroscopic networks and micro- and mesoporosity in the struts, making them highly desirable for filtration or catalyst support applications	[23]
Powder Bed-based	Slag-based geopolymer powder + Na_2SiO_3 + Sand + Zb® 63		2 h (Ambient Temperature) + 7 days (60˚C, Na_2SiO_3)	16.5 MPa	–	– 1.20 ± 0.04 g/cm^3 BD, – 2.81 g/cm^3 TD 57.1 ± 1.4% AP	– – –	Geopolymer end products were developed by a powder bed 3D printer, obtaining adequate deposit ability, wettability, and reduced anisotropy while gaining strength through a Na_2SiO_3-based post-processing method	[25]
Melted Extrusion Modeling	ASOPs + ALSPs	GO (5 wt.%)	17 °C (5 Days) + 1000 °C (0.5 h)	36 MPa	-	700 MPa YM, – – – –	10^2 S/m EC	The inclusion of GO greatly influences the rheology of geopolymer precursors, thereby facilitating the AM of geopolymer and indicating a strong GO-HGPP engagement	[26]

Table 9 (continued)

AM type	Geopolymer precursors and activators	Additives/reinforcements	Curing conditions	Properties				Key findings	References
				CS	FS	YM, BD, AD, TD, AP	TP, EC, ILBS		
Extrusion-based	FA (Class F), GGBFS, SF + Sand + Thixotropic filler (Actigel & Cellulose) + NaOH (8 M), Na_2SiO_3		28 Days (Ambient Temperature)	36.25 MPa	9.5 MPa	– 2250 kg/m^3 BD, – – –		Mechanical properties of the AM geopolymer are greatly influenced by the loading/printing directions and bring about higher mechanical strength as compared to casted geopolymer in specific directions	[27]
Extrusion-based	FA (Class F), GGBFS + MS + Na_2SiO_3 + Hydroxypropyl methylcellulose (HPMC)	Glass Fiber (1 wt. %)	28 Days (Ambient Temperature)	26.5 MPa	7 MPa	– – – – –	– – –	Glass fiber reinforcement certainly enhances the mechanical properties of the printed composite, whereas the printing direction and technique play a vital role	[28]
Extrusion-based	FA (Class F) + MS sand + NaOH (8 M), Na_2SiO_3 + Sodium carboxymethyl cellulose	Polypropylene Fibers (0.25 vol. %)	60 °C (24 h)	36 MPa	7.8 MPa	– – – – 10.1% AP	3.1 MPa ILBS	Polypropylene fibers positively affect the properties of AM geopolymer mortar while demonstrating deflection-softening behavior with lower quantities (0.25–0.5 vol %) and deflection-hardening behavior with higher quantities (0.75–1.0 vol %)	[33]
Extrusion-based	FA (Class F) + MS sand + NaOH (8 M), Na_2SiO_3 + Sodium carboxymethyl cellulose	Polyphenylene Benzobisoxazole (PBO)	60 °C (24 h) + 2 Day (Ambient Temperature)	–	10.3 MPa	– – – – –	2.33 MPa ILBS	The incorporation of polymeric fibers enhances the FS of the 3D geopolymer but gradually reduces the interlayer bond strength	[34]

Table 9 (continued)

AM type	Geopolymer precursors and activators	Additives/reinforcements	Curing conditions	Properties				Key findings	References
				CS	FS	YM, BD, AD, TD, AP	TP, EC, ILBS		
Extrusion-based	FA (Class F), GGBFS + Sand + Anhydrous Na_2SiO_3 + Water		60 °C (24 h)	25.2 MPa	6.1 MPa	– – – – –	1.3 MPa ILBS	The printing direction (i.e., Perpendicular, Longitudinal, and lateral) of the AM geopolymer is relevant while considering the end resultant composite properties	[63]
Extrusion-based	FA (Class F), GGBFS + Micro Silica + K_2SiO_3 + Sand + Magnesium Aluminum–silicate Nano-clay	Polyvinyl Alcohol (PVA) (0.5 wt. %) + Stainless Steel Cable (SUS304–2 mm)	7 days (Ambient Temperature)	–	290% (Increase)	– – – – –	– – –	Hybrid reinforcement in AM geopolymer effectively elevates the flexural properties along with fracture toughness and alleviates the challenge of cable slippage	[36]
Powder Bed-based	Slag-based geopolymer powder + Na_2SiO_3 + Sand + Zb® 63		6 h (Ambient Conditions) + 60 °C (7 days)	19.3 MPa	–	– – – – –	– – –	The activator saturation level of the geopolymer inherently influences the strength of the 3D-printed composite	[42]
Powder Bed-based	FA (Class F + NaOH (8 M), Na_2SiO_3		6 h (Ambient Conditions) + 60 °C (7 days)	29.6 MPa	–	– – – – –	– – –	The AM composite could be significantly improved by implementing post-processing methods as both alkaline solutions and FA-based geopolymer slurries prove to be effective curing agents	[48]
NA	FA (Class F) + Sand + NaOH (10 M), Na_2SiO_3	Flax Fiber (1 wt. %)	75 °C (24 h) + 28 Days (Ambient Temperature)	48.7 MPa	9.4 MPa	– – – – –	– – – –	Adding green tow flax fibers provided better mechanical properties in geopolymer AM as compared to carbon fibers	[158]

Table 9 (continued)

AM type	Geopolymer precursors and activators	Additives/reinforcements	Curing conditions	Properties				Key findings	References
				CS	FS	YM, BD, AD, TD, AP	TP, EC, ILBS		
Extrusion-based	FA (Class F), GGBFS + SF + Sand + NaOH (10 M), Na_2SiO_3	NGPs (0.1 wt. %)	60 °C (24 h) + 7 Days (Ambient Temperature)	59 MPa	10.74 MPa	3.05 g/cm^3 BD		The incorporation of NGPs in geopolymer mixture has increased the mechanical hardened properties of the printed blocks while affecting the fresh properties	[210]
Extrusion-based	CDW + NaOH (10 M) + RCA	Ca $(OH)_2$ (4 wt. %)	23 °C (24 h) + 28 Days (Ambient Temperature)	16.35	5.48 MPa		1.23 MPa ILBS	Appropriate utilization of CDW with Ca $(OH)_2$ can enhance geopolymerization reactivity for necessary mechanical properties because geopolymer mortar illustrates anisotropic behavior	[225]
Extrusion-based	FA (Class F), GGBFS + Sand + Sodium Gluconate + Barium Chloride + Na_2SiO_3	Steel Fiber (8 mm, 0.01 wt. %)	20 °C (24 h) + 56 Days (Ambient Temperature)	104.05 MPa	26.1 MPa			Utilization of appropriate steel fibers could significantly enhance the tensile and bending properties of 3D-printed one-part geopolymer composites	[169]
Extrusion-based	FA + GGBS + Gypsum + Sand + Na_2SiO_3	Steel Slag (10 wt. %)	20 °C (24 h) + 28 Days (Ambient Temperature)	39.87 MPa	5.08 MPa		0.87% TP	Steel slag aided in the strength development of quaternary blend 3D printed geopolymer mortar through the support in the generation of N©–A–S–H gel, C–S–H, Aft and CH reaction products	[156]

Table 9 (continued)

AM type	Geopolymer precursors and activators	Additives/reinforcements	Curing conditions	Properties				Key findings	References
				CS	FS	YM, BD, AD, TD, AP	TP, EC, ILBS		
Extrusion-based	FA + GGBS + Sand + Na_2SiO_3 + Sucrose + Water	Wollastonite Microfiber (10 wt. %)	23 °C (24 h) + 28 Days (Ambient Temperature)	52.4 MPa	8.7 MPa			The addition of Wollastonite Microfibers assisted in enhancing the thixotropy properties as well as the mechanical properties of the 3D-printed geopolymer mortars	[149]
Extrusion-based	FA + GGBS + NaOH + Na_2SiO_3 + Water + Sand + Naphthalene		20 °C (24 h) + 28 Days (Ambient Temperature)	38.37 MPa	12.47 MPa		8.05% TP	The incorporation of high amounts of FA worsens the mechanical anisotropy due to the weak activation reactivity and high thixotropy	[146]

CS, Compressive Strength; FS, Flexural Strength; YM, Young's Modulus; BD, Bulk Density; AD, Apparent Density; TD, True Density; AP, Apparent Porosity; TP, Total Porosity; EC, Electrical Conductivity; ILBS, Inter-Layer Bond Strength

Acknowledgements The authors are grateful for R.S Krishna's Student Project Grant Award from ASTM (USA). The authors are also grateful for the academic support from their affiliate organizations and universities, Western Sydney University (Australia), Veer Surendra Sai University of Technology (India), ERMAKSAN Innovative Technologies (Turkey), Gazi University (Turkey), National Institute of Technology Calicut (India), Cracow University of Technology (Poland), Nanjing Tech University (China), University of Trento (Italy), Curtin University (Australia) and University of the West of England (UK). The authors are also grateful for Tanvir Qureshi's Vice-Chancellor's Early Career Researcher Development Award (VC ECR), and the New Investigator award from the University of the West of England.

Author contributions R.S Krishna: Conceptualization, Methodology, Investigation, Visualization, Writing—Original Draft, Project administration, Asif Ur Rehman: Investigation, Writing—Original Draft, Jyotirmoy Mishra: Writing—Original Draft, Suman Saha: Investigation, Writing—Original Draft, Kinga Korniejenko: Investigation, Writing—Original Draft, Rashid Ur Rehman: Supervision, Kashif Ur Rehman: Supervision, Metin Uymaz Salamci: Supervision, Vincenzo M. Sglavo: Supervision, Writing—review and editing, Faiz Uddin Ahmed Shaikh: Writing—original draft, Writing—review and editing, Tanvir S. Qureshi: Supervision, Writing—review and editing.

Data availability This literature review uses only publicly available data from peer-reviewed journals, books, product websites, and other academic publications. These sources are properly cited in the manuscript.

Declarations

Conflict of interest The authors declare that they have no known competing financial interests or personal relationships that could have appeared to influence the work reported in this paper.

References

1. European Commission Eurostat Waste Statistics-Statistics Explained (2021). https://ec.europa.eu/eurostat/statistics-explained/index.php?title=Waste_statistics. Accessed Feb 4, 2022
2. The World Bank Group, Trends in Solid Waste Management (2023). https://datatopics.worldbank.org/what-a-waste/trends_in_solid_waste_management.html. Accessed July 22, 2023
3. Olivier JGJ, Peters JAHW (2020) Trends in global CO2 and total greenhouse gas emissions report, The Hague. https://www.pbl.nl/sites/default/files/downloads/pbl-2020-trends-in-global-
4. Ghazali N, Muthusamy K, Wan Ahmad S (2019) Utilization of fly ash in construction. IOP Conf Ser Mater Sci Eng 601:012023. https://doi.org/10.1088/1757-899X/601/1/012023

5. Maghool F, Arulrajah A, Horpibulsuk S, Mohajerani A (2020) Engineering and leachate characteristics of granulated blast-furnace slag as a construction material. J Mater Civ Eng. https://doi.org/10.1061/(ASCE)MT.1943-5533.0003212
6. Kiventerä J, Perumal P, Yliniemi J, Illikainen M (2020) Mine tailings as a raw material in alkali activation: a review. Int J Miner Metall Mater 27:1009–1020. https://doi.org/10.1007/s12613-020-2129-6
7. Türköz M, Umu SU, Öztürk O (2021) Effect of silica fume as a waste material for sustainable environment on the stabilization and dynamic behavior of dispersive soil. Sustainability 13:4321. https://doi.org/10.3390/su13084321
8. Amran M, Fediuk R, Murali G, Vatin N, Karelina M, Ozbakkaloglu T, Krishna RS, Kumar AS, Kumar DS, Mishra J (2021) Rice husk ash-based concrete composites: a critical review of their properties and applications. Crystals (Basel) 11:1–33. https://doi.org/10.3390/cryst11020168
9. Zhang J, Yao Z, Wang K, Wang F, Jiang H, Liang M, Wei J, Airey G (2021) Sustainable utilization of bauxite residue (Red Mud) as a road material in pavements: a critical review. Constr Build Mater 270:121419. https://doi.org/10.1016/j.conbuildmat.2020.121419
10. Zhang R, Qureshi TS, Panesar DK (2022) Management of industrial waste and cost analysis. In: Handbook of sustainable concrete and industrial waste management. Elsevier, London, pp 595–614. https://doi.org/10.1016/B978-0-12-821730-6.00027-9
11. Zhang R, Qureshi TS, Panesar DK (2022) Use of industrial waste in construction and a cost analysis. In: Handbook of sustainable concrete and industrial waste management. Elsevier, London, pp 615–635. https://doi.org/10.1016/B978-0-12-821730-6.00019-X
12. Bertoldo N, Qureshi T, Simpkins D, Arrigoni A, Dotelli G (2023) Concrete with organic waste materials as aggregate replacement. Appl Sci 14:108. https://doi.org/10.3390/app14010108
13. Bos F, Wolfs R, Ahmed Z, Salet T (2016) Additive manufacturing of concrete in construction: potentials and challenges of 3D concrete printing. Virtual Phys Prototyp 11:209–225. https://doi.org/10.1080/17452759.2016.1209867
14. Lipson H, Kurman M (2013) Fabricated: the new world of 3D printing, Wiley. https://www.wiley.com/en-us/Fabricated%3A+The+New+World+of+3D+Printing-p-9781118416945. Accessed Feb 4, 2022
15. Vaezi M, Chua CK (2011) Effects of layer thickness and binder saturation level parameters on 3D printing process. Int J Adv Manuf Technol 53:275–284. https://doi.org/10.1007/s00170-010-2821-1
16. Lloret E, Shahab AR, Linus M, Flatt RJ, Gramazio F, Kohler M, Langenberg S (2015) Complex concrete structures: merging existing casting techniques with digital fabrication. CAD Comput Aided Des 60:40–49. https://doi.org/10.1016/j.cad.2014.02.011
17. Ma GW, Wang L, Ju Y (2018) State-of-the-art of 3D printing technology of cementitious material—an emerging technique for construction. Sci China Technol Sci 61:475–495. https://doi.org/10.1007/s11431-016-9077-7
18. Elhag H, Glass J, Gibb AGF, Clarke M, Budge C, Bailey G (2008) Implementing environmental improvements in a manufacturing context: a structured approach for the precast concrete industry. Int J Environ Technol Manag 8:369–384. https://doi.org/10.1504/IJETM.2008.017508
19. Colee RJ (1998) Energy and greenhouse gas emissions associated with the construction of alternative structural systems. Build Environ 34:335–348. https://doi.org/10.1016/S0360-1323(98)00020-1
20. Tam VWY, Tam CM, Chan JKW, Ng WCY (2014) Cutting construction wastes by prefabrication. Int J Constr Manag 6:15–25. https://doi.org/10.1080/15623599.2006.10773079
21. Holt C, Edwards L, Keyte L, Moghaddam F, Townsend B (2019) Construction 3D printing. In: 3D concrete printing technology. Elsevier, London, pp 349–370. https://doi.org/10.1016/b978-0-12-815481-6.00017-8
22. Rehman AU, Sglavo VM (2022) 3D printing of Portland cement-containing bodies. Rapid Prototyp J 28:197–203. https://doi.org/10.1108/RPJ-08-2020-0195
23. Franchin G, Colombo P (2015) Porous geopolymer components through inverse replica of 3D printed sacrificial templates. J Ceram Sci Technol 6:105–112. https://doi.org/10.4416/JCST2014-00057
24. Montes C, Broussard K, Gongre M, Simicevic N, Mejia J, Tham J, Allouche E, Davis G (2015) Evaluation of lunar regolith geopolymer binder as a radioactive shielding material for space exploration applications. Adv Space Res 56:1212–1221. https://doi.org/10.1016/j.asr.2015.05.044
25. Xia M, Sanjayan J (2016) Method of formulating geopolymer for 3D printing for construction applications. Mater Des 110:382–390. https://doi.org/10.1016/j.matdes.2016.07.136
26. Zhong J, Zhou GX, He PG, Yang ZH, Jia DC (2017) 3D printing strong and conductive geo-polymer nanocomposite structures modified by graphene oxide. Carbon N Y 117:421–426. https://doi.org/10.1016/j.carbon.2017.02.102
27. Panda B, Paul SC, Hui LJ, Tay YWD, Tan MJ (2017) Additive manufacturing of geopolymer for sustainable built environment. J Clean Prod 167:281–288. https://doi.org/10.1016/j.jclepro.2017.08.165
28. Panda B, Chandra Paul S, Jen Tan M (2017) Anisotropic mechanical performance of 3D printed fiber reinforced sustainable construction material. Mater Lett 209:146–149. https://doi.org/10.1016/j.matlet.2017.07.123
29. Nematollahi B, Xia M, Sanjayan J (2017) Current progress of 3D concrete printing technologies. In: Proceedings of the international symposium on automation and robotics in construction. IAARC Publications. https://doi.org/10.22260/ISARC2017/0035
30. Davis G, Montes C, Eklund S (2017) Preparation of lunar regolith based geopolymer cement under heat and vacuum. Adv Space Res 59:1872–1885. https://doi.org/10.1016/j.asr.2017.01.024
31. Dechang J, Peigang H, Jingkun Y, Ruifei W (2017) Research progress of aluminosilicate polymers and their composites. Acta Silicate. https://doi.org/10.14062/j.issn.0454-5648.2017.12.02.html. Accessed June 26, 2022
32. Panda B, Lim JH, Ahamed N, Mohamed N, Chandra S, Yi P, Tay WD, Tan MJ (2017) Automation of robotic concrete printing using feedback control system
33. Nematollahi B, Vijay P, Sanjayan J, Nazari A, Xia M, Nerella VN, Mechtcherine V (2018) Effect of polypropylene fibre addition on properties of geopolymers made by 3D printing for digital construction. Materials. https://doi.org/10.3390/ma11122352
34. Nematollahi B, Xia M, Sanjayan J, Vijay P (2018) Effect of type of fiber on inter-layer bond and flexural strengths of extrusion-based 3D printed geopolymer. In: Materials science forum. Trans Tech Publications Ltd, pp 155–162. https://doi.org/10.4028/www.scientific.net/MSF.939.155
35. Panda B, Tan MJ (2018) Experimental study on mix proportion and fresh properties of fly ash based geopolymer for 3D concrete printing. Ceram Int 44:10258–10265. https://doi.org/10.1016/j.ceramint.2018.03.031
36. Lim JH, Panda B, Pham QC (2018) Improving flexural characteristics of 3D printed geopolymer composites with in-process steel cable reinforcement. Constr Build Mater 178:32–41. https://doi.org/10.1016/j.conbuildmat.2018.05.010
37. Panda B, Unluer C, Tan MJ (2018) Investigation of the rheology and strength of geopolymer mixtures for extrusion-based

3D printing. Cem Concr Compos 94:307–314. https://doi.org/10.1016/j.cemconcomp.2018.10.002
38. Al-Qutaifi S, Nazari A, Bagheri A (2018) Mechanical properties of layered geopolymer structures applicable in concrete 3D-printing. Constr Build Mater 176:690–699. https://doi.org/10.1016/j.conbuildmat.2018.04.195
39. Panda B, Paul SC, Mohamed NAN, Tay YWD, Tan MJ (2018) Measurement of tensile bond strength of 3D printed geopolymer mortar. Measurement (Lond) 113:108–116. https://doi.org/10.1016/j.measurement.2017.08.051
40. Panda B, Noor Mohamed NA, Tay YWD, He L, Tan MJ (2018) Effects of slag addition on bond strength of 3D printed geopolymer mortar: An experimental investigation. In: Proceedings of the international conference on progress in additive manufacturing, Pro-AM, pp 62–67. https://doi.org/10.25341/D4QG6D
41. Annapareddy A, Panda B, Ting GHA, Li M, Tan MJ (2018) Flow and mechanical properties of 3D printed cementitious material with recycled glass aggregates. In: Proceedings of the international conference on progress in additive manufacturing, Pro-AM, pp 68–73. https://doi.org/10.25341/D41P4H
42. Xia M, Nematollahi B, Sanjayan J (2018) Influence of binder saturation level on compressive strength and dimensional accuracy of powder-based 3D printed geopolymer. In: Materials science forum. Trans Tech Publications Ltd, pp 177–183. https://doi.org/10.4028/www.scientific.net/MSF.939.177
43. Vlachakis C, Biondi L, Perry M (2018) 3D printed smart repairs for civil infrastructure. In: 9th European workshop on structural health monitoring (EWSHM 2018), Manchester. https://www.ndt.net/search/docs.php3?id=23442&file=article/ewshm2018/papers/0338-Vlachakis.pdf. Accessed June 26, 2022
44. Kashani A, Ngo TD, Optimisation of mixture properties for 3D printing of geopolymer concrete, n.d.
45. Panda B, Tay YWD, Paul SC, Tan MJ (2018) Current challenges and future potential of 3D concrete printing. Materwiss Werkstech 49:666–673. https://doi.org/10.1002/mawe.201700279
46. Zhang D, Wang D, Piao C, Lin X, Zhang T, Xia J (2018) Effect of steel slag content on rheological properties of 3D printing geopolymer materials. J Basic Sci Eng 26:596–604. https://doi.org/10.16058/j.issn.1005-0930.2018.03.013
47. Singh NB (2018) Fly ash-based geopolymer binder: a future construction material. Minerals. https://doi.org/10.3390/min8070299
48. Xia M, Sanjayan JG (2018) Methods of enhancing strength of geopolymer produced from powder-based 3D printing process. Mater Lett 227:281–283. https://doi.org/10.1016/j.matlet.2018.05.100
49. Zhang DW, Min Wang D, Lin XQ, Zhang T (2018) The study of the structure rebuilding and yield stress of 3D printing geopolymer pastes. Constr Build Mater 184:575–580. https://doi.org/10.1016/j.conbuildmat.2018.06.233
50. Korniejenko K, Łach M, Chou SY, Lin WT, Mikuła J, Mierzwiński D, Cheng A, Hebda M (2019) A comparative study of mechanical properties of fly ash-based geopolymer made by casted and 3D printing methods. In: IOP Conf Ser Mater Sci Eng. IOP Publishing Ltd, https://doi.org/10.1088/1757-899X/660/1/012005
51. Hirayama Y, Zhang J, Kawahara Y (2019) A method to evaluate the formability and fluidity of concrete based materials for 3D printing. In: Proceedings of the ACM symposium on computational fabrication. ACM, New York, NY, USA, pp 1–10. https://doi.org/10.1145/3328939.3329002
52. Agnoli E, Ciapponi R, Levi M, Turri S (2019) Additive manufacturing of geopolymers modified with microalgal biomass biofiller fromwastewater treatment plants. Materials. https://doi.org/10.3390/ma12071004
53. Toniolo N, Bednarzig V, Roether JA, Rost H, Boccaccini AR (2019) Advancing processing technologies for designed geopolymers: 3D printing and mechanical machining. Interceram Int Ceram Rev 68:18–21. https://doi.org/10.1007/s42411-018-0059-3
54. Panda B, Unluer C, Tan MJ (2019) Extrusion and rheology characterization of geopolymer nanocomposites used in 3D printing. Compos B Eng. https://doi.org/10.1016/j.compositesb.2019.107290
55. Bong SH, Nematollahi B, Nazari A, Xia M, Sanjayan J (2019) Method of optimisation for ambient temperature cured sustainable geopolymers for 3D printing construction applications. Materials. https://doi.org/10.3390/ma12060902
56. Ma G, Li Z, Wang L, Bai G (2019) Micro-cable reinforced geopolymer composite for extrusion-based 3D printing. Mater Lett 235:144–147. https://doi.org/10.1016/j.matlet.2018.09.159
57. Fu S, He P, Wang M, Wang M, Wang R, Yuan J, Jia D, Cui J (2019) Monoclinic-celsian ceramics formation: through thermal treatment of ion-exchanged 3D printing geopolymer precursor. J Eur Ceram Soc 39:563–573. https://doi.org/10.1016/j.jeurceramsoc.2018.08.036
58. Marczyk J, Ziejewska C, Łach M, Korniejenko K, Lin WT, Hebda M (2019) Possibilities of using the 3D printing process in the concrete and geopolymers application. IOP Conf Ser Mater Sci Eng. https://doi.org/10.1088/1757-899X/706/1/012019
59. Nematollahi B, Xia M, Sanjayan J (2019) Post-processing methods to improve strength of particle-bed 3D printed geopolymer for digital construction applications. Front Mater. https://doi.org/10.3389/fmats.2019.00160
60. Xia M, Nematollahi B, Sanjayan J (2019) Printability, accuracy and strength of geopolymer made using powder-based 3D printing for construction applications. Autom Constr 101:179–189. https://doi.org/10.1016/j.autcon.2019.01.013
61. Alghamdi H, Neithalath N (2019) Synthesis and characterization of 3D-printable geopolymeric foams for thermally efficient building envelope materials. Cem Concr Compos. https://doi.org/10.1016/j.cemconcomp.2019.103377
62. Panda B, Singh GB, Unluer C, Tan MJ (2019) Synthesis and characterization of one-part geopolymers for extrusion based 3D concrete printing. J Clean Prod 220:610–619. https://doi.org/10.1016/j.jclepro.2019.02.185
63. Nematollahi B, Xia M, Bong SH, Sanjayan J (2019) Hardened properties of 3D printable 'One-Part' geopolymer for construction applications. In: RILEM bookseries. Springer, London, pp 190–199. https://doi.org/10.1007/978-3-319-99519-9_17
64. Panda B, Noor Mohamed NA, Tay YWD, Tan MJ (2019) Bond strength in 3D printed geopolymer mortar. In: RILEM bookseries. Springer, London, pp 200–206. https://doi.org/10.1007/978-3-319-99519-9_18
65. Bong SH, Nematollahi B, Nazari A, Xia M, Sanjayan JG (2019) Fresh and hardened properties of 3D printable geopolymer cured in ambient temperature. In: RILEM bookseries. Springer, London, pp 3–11. https://doi.org/10.1007/978-3-319-99519-9_1
66. Singh NB, Saxena SK, Kumar M, Rai S (2019) Geopolymer cement: synthesis, characterization, properties and applications. www.sciencedirect.comwww.materialstoday.com/proceedings2214-7853
67. Wu Y, Lu B, Bai T, Wang H, Du F, Zhang Y, Cai L, Jiang C, Wang W (2019) Geopolymer, green alkali activated cementitious material: synthesis, applications and challenges. Constr Build Mater 224:930–949. https://doi.org/10.1016/j.conbuildmat.2019.07.112
68. Sun C, Xiang J, Xu M, He Y, Tong Z, Cui X (2020) 3D extrusion free forming of geopolymer composites: materials modification and processing optimization. J Clean Prod. https://doi.org/10.1016/j.jclepro.2020.120986

69. Yin X, Liu K, Zheng S, Zhuang K, Wang X, Fang Y, Ding Z (2020) 3D printable "just-add-water glass and water" geopolymer—an experimental research based on extrusion-based 3D printing practices. In: IOP Conf Ser Mater Sci Eng. Institute of Physics Publishing. https://doi.org/10.1088/1757-899X/780/4/042044
70. Vlachakis C, Perry M, Biondi L, McAlorum J (2020) 3D printed temperature-sensing repairs for concrete structures. Addit Manuf. https://doi.org/10.1016/j.addma.2020.101238
71. Zhou GX, Li C, Zhao Z, Qi YZ, Yang ZH, Jia DC, Zhong J, Zhou Y (2020) 3D printing geopolymer nanocomposites structure: graphene oxide size effects on a reactive matrix. Carbon N Y 164:215–223. https://doi.org/10.1016/j.carbon.2020.02.021
72. Rehman AU, Sglavo VM (2020) 3D printing of geopolymer-based concrete for building applications. Rapid Prototyp J 26:1783–1788. https://doi.org/10.1108/RPJ-09-2019-0244
73. Imtiaz L, Rehman SKU, Memon SA, Khan MK, Javed MF (2020) A review of recent developments and advances in eco-friendly geopolymer concrete. Appl Sci (Switzerland) 10:1–56. https://doi.org/10.3390/app10217838
74. Luhar S, Luhar I (2020) Additive manufacturing in the geopolymer construction technology: a review. Open Constr Build Technol J 14:150–161. https://doi.org/10.2174/1874836802014010150
75. Luukkonen T, Yliniemi J, Sreenivasan H, Ohenoja K, Finnilä M, Franchin G, Colombo P (2020) Ag- or Cu-modified geopolymer filters for water treatment manufactured by 3D printing, direct foaming, or granulation. Sci Rep. https://doi.org/10.1038/s41598-020-64228-5
76. Muthukrishnan S, Ramakrishnan S, Sanjayan J (2020) Effect of microwave heating on interlayer bonding and buildability of geopolymer 3D concrete printing. Constr Build Mater. https://doi.org/10.1016/j.conbuildmat.2020.120786
77. Nematollahi B, Bong SH, Xia M, Sanjayan J (2020) Digital fabrication of 'just-add-water' geopolymers: effects of curing condition and print-time interval. In: RILEM bookseries. Springer, London, pp 93–102. https://doi.org/10.1007/978-3-030-49916-7_10
78. Bong SH, Nematollahi B, Arunothayan AR, Xia M, Sanjayan J (2020) Effect of wollastonite micro-fiber addition on properties of 3D-printable 'just-add-water' geopolymers. In: RILEM bookseries. Springer, London, pp 23–31. https://doi.org/10.1007/978-3-030-49916-7_3
79. Albar A, Chougan M, Al-Kheetan MJ, Swash MR, Ghaffar SH (2020) Effective extrusion-based 3D printing system design for cementitious-based materials. Results Eng. https://doi.org/10.1016/j.rineng.2020.100135
80. Nematollahi B, Xia M, Sanjayan J (2020) Enhancing strength of powder-based 3D printed geopolymers for digital construction applications. In: RILEM bookseries. Springer, London, pp 417–425. https://doi.org/10.1007/978-3-030-22566-7_48
81. Voney V, Odaglia P, Brumaud C, Dillenburger B, Habert G (2020) Geopolymer formulation for binder jet 3D printing. In: RILEM bookseries. Springer, London, pp 153–161. https://doi.org/10.1007/978-3-030-49916-7_16
82. Korniejenko K, Łach M (2020) Geopolymers reinforced by short and long fibres—innovative materials for additive manufacturing. Curr Opin Chem Eng 28:167–172. https://doi.org/10.1016/j.coche.2020.06.005
83. Guo X, Yang J, Xiong G (2020) Influence of supplementary cementitious materials on rheological properties of 3D printed fly ash based geopolymer. Cem Concr Compos. https://doi.org/10.1016/j.cemconcomp.2020.103820
84. Li Z, Wang L, Ma G (2020) Mechanical improvement of continuous steel microcable reinforced geopolymer composites for 3D printing subjected to different loading conditions. Compos B Eng. https://doi.org/10.1016/j.compositesb.2020.107796
85. Korniejenko K, Łach M, Chou SY, Lin WT, Cheng A, Hebdowska-Krupa M, Gadek S, Mikuła J (2020) Mechanical properties of short fiber-reinforced geopolymers made by casted and 3D printing methods: a comparative study. Materials. https://doi.org/10.3390/ma13030579
86. Voney V, Odaglia P, Schenker F, Brumaud C, Dillenburger B, Habert G (2020) Powder bed 3D printing with quarry waste. In: IOP Conf Ser Earth Environ Sci. IOP Publishing Ltd. https://doi.org/10.1088/1755-1315/588/4/042056
87. Franchin G, Pesonen J, Luukkonen T, Bai C, Scanferla P, Botti R, Carturan S, Innocentini M, Colombo P (2020) Removal of ammonium from wastewater with geopolymer sorbents fabricated via additive manufacturing. Mater Des. https://doi.org/10.1016/j.matdes.2020.109006
88. Panda B, Noor Mohamed NA, Tan MJ (2020) Rheology and structural rebuilding of one-part geopolymer mortar in the context of 3D concrete printing. In: RILEM bookseries. Springer, London, pp 426–431. https://doi.org/10.1007/978-3-030-22566-7_49
89. Xia M, Nematollahi B, Sanjayan J (2020) Shape accuracy evaluation of geopolymer specimens made using particle-bed 3D printing. In: RILEM bookseries. Springer, London, pp 1011–1019. https://doi.org/10.1007/978-3-030-49916-7_98
90. Li Z, Wang L, Ma G, Sanjayan J, Feng D (2020) Strength and ductility enhancement of 3D printing structure reinforced by embedding continuous micro-cables. Constr Build Mater. https://doi.org/10.1016/j.conbuildmat.2020.120196
91. Sun Q, Peng Y, Georgolamprou X, Li D, Kiebach R (2020) Synthesis and characterization of a geopolymer/hexagonal-boron nitride composite for free forming 3D extrusion-based printing. Appl Clay Sci. https://doi.org/10.1016/j.clay.2020.105870
92. Chougan M, Hamidreza Ghaffar S, Jahanzat M, Albar A, Mujaddedi N, Swash R (2020) The influence of nano-additives in strengthening mechanical performance of 3D printed multi-binder geopolymer composites. Constr Build Mater. https://doi.org/10.1016/j.conbuildmat.2020.118928
93. Bong SH, Nematollahi B, Xia M, Nazari A, Sanjayan J, Pan J (2020) Properties of 3D-printable ductile fibre-reinforced geopolymer composite for digital construction applications. In: RILEM bookseries. Springer, London, pp 363–372 https://doi.org/10.1007/978-3-030-22566-7_42
94. Odaglia P, Voney V, Dillenburger B, Habert G (2020) Advances in binder-jet 3D printing of non-cementitious materials, pp 103–112. https://doi.org/10.1007/978-3-030-49916-7_11
95. Khan MA (2020) Mix suitable for concrete 3D printing: a review. In: Mater Today Proc. Elsevier, London, pp 831–837. https://doi.org/10.1016/j.matpr.2020.03.825
96. Jia D, He P, Wang M, Yan S (2020) Geopolymers and their matrix composites: a state-of-the-art review, pp 7–34. https://doi.org/10.1007/978-981-15-9536-3_2
97. Bagheri A, Cremona C (2020) Formulation of mix design for 3D printing of geopolymers: a machine learning approach. Mater Adv 1:720–727. https://doi.org/10.1039/d0ma00036a
98. Perumal P, Luukkonen T, Sreenivasan H, Kinnunen P, Illikainen M (2020) Porous alkali-activated materials. In: New materials in civil engineering. Elsevier, London, pp 529–563. https://doi.org/10.1016/B978-0-12-818961-0.00015-6
99. Korniejenko K, Łach M, Mikuła J, Hebdowska-Krupa M, Mierzwiński D, Gądek S, Hebda M, Development of 3D printing technology for geopolymers, n.d.
100. Pilehvar S, Arnhof M, Pamies R, Valentini L, Kjøniksen AL (2020) Utilization of urea as an accessible superplasticizer on

the moon for lunar geopolymer mixtures. J Clean Prod. https://doi.org/10.1016/j.jclepro.2019.119177
101. Emelyanov RT, Turysheva ES, Yakshina AA, Makeich VV, Berseneva ML (2020) Assessment method for fresh concrete spreadability. In: J Phys Conf Ser. Institute of Physics Publishing. https://doi.org/10.1088/1742-6596/1515/3/032048
102. Lazarev Y, Krotov O, Belyaeva S, Petrochenko M (2020) 3D environmentally friendly concrete printing model preparation. In: E3S web of conferences. EDP Sciences. https://doi.org/10.1051/e3sconf/202017511024
103. Yin X, Wang X, Fang Y, Ding Z (2020) Influence of curing age on high-temperature properties of additive manufactured geopolymer mortar. In: E3S web of conferences, EDP sciences. https://doi.org/10.1051/e3sconf/202021803019
104. dos Santos LK, Botti RF, de Innocentini MDM, Marques RFC, Colombo P, de Paula AV, Flumignan DL (2021) 3D printed geopolymer: an efficient support for immobilization of Candida rugosa lipase. Chem Eng J. https://doi.org/10.1016/j.cej.2021.128843
105. Santana HA, Amorim Júnior NS, Ribeiro DV, Cilla MS, Dias CMR (2021) 3D printed mesh reinforced geopolymer: notched prism bending. Cem Concr Compos. https://doi.org/10.1016/j.cemconcomp.2020.103892
106. Ma S, Yang H, Zhao S, He P, Zhang Z, Duan X, Yang Z, Jia D, Zhou Y (2021) 3D-printing of architectured short carbon fiber-geopolymer composite. Compos B Eng. https://doi.org/10.1016/j.compositesb.2021.109348
107. Youssef N, Rabenantoandro AZ, Lafhaj Z, Dakhli Z, Hage Chehade F, Ducoulombier L (2021) A novel approach of geopolymer formulation based on clay for additive manufacturing. Constr Robot 5:175–190. https://doi.org/10.1007/s41693-021-00060-1
108. Botti RF, Innocentini MDM, Faleiros TA, Mello MF, Flumignan DL, Santos LK, Franchin G, Colombo P (2021) Additively manufactured geopolymer structured heterogeneous catalysts for biodiesel production. Appl Mater Today. https://doi.org/10.1016/j.apmt.2021.101022
109. Gökçe HS, Tuyan M, Nehdi ML (2021) Alkali-activated and geopolymer materials developed using innovative manufacturing techniques: a critical review. Constr Build Mater. https://doi.org/10.1016/j.conbuildmat.2021.124483
110. Bong SH, Xia M, Nematollahi B, Shi C (2021) Ambient temperature cured 'just-add-water' geopolymer for 3D concrete printing applications. Cem Concr Compos. https://doi.org/10.1016/j.cemconcomp.2021.104060
111. Şahin O, İlcan H, Ateşli AT, Kul A, Yıldırım G, Şahmaran M (2021) Construction and demolition waste-based geopolymers suited for use in 3-dimensional additive manufacturing. Cem Concr Compos. https://doi.org/10.1016/j.cemconcomp.2021.104088
112. Munir Q, Kärki T (2021) Cost analysis of various factors for geopolymer 3D printing of construction products in factories and on construction sites. Recycling. https://doi.org/10.3390/recycling6030060
113. Cepollaro EM, Botti R, Franchin G, Lisi L, Colombo P, Cimino S (2021) Cu/ZSM5-geopolymer 3D-printed monoliths for the NH3-SCR of NO*x*. Catalysts 11:1212. https://doi.org/10.3390/catal11101212
114. Ma S, Fu S, Zhao S, He P, Ma G, Wang M, Jia D, Zhou Y (2021) Direct ink writing of geopolymer with high spatial resolution and tunable mechanical properties. Addit Manuf. https://doi.org/10.1016/j.addma.2021.102202
115. Zhao J, Tong L, Li B, Chen T, Wang C, Yang G, Zheng Y (2021) Eco-friendly geopolymer materials: a review of performance improvement, potential application and sustainability assessment. J Clean Prod. https://doi.org/10.1016/j.jclepro.2021.127085
116. Muthukrishnan S, Ramakrishnan S, Sanjayan J (2021) Effect of alkali reactions on the rheology of one-part 3D printable geopolymer concrete. Cem Concr Compos. https://doi.org/10.1016/j.cemconcomp.2020.103899
117. Voney V, Odaglia P, Brumaud C, Dillenburger B, Habert G (2021) From casting to 3D printing geopolymers: a proof of concept. Cem Concr Res. https://doi.org/10.1016/j.cemconres.2021.106374
118. Nmiri A (2021) Incorporation of phase change materials and application of 3D printing technology in the geopolymer development. In: Advances in geopolymer-zeolite composites-synthesis and characterization. IntechOpen. https://doi.org/10.5772/intechopen.96886
119. Ly O, Yoris-Nobile AI, Sebaibi N, Blanco-Fernandez E, Boutouil M, Castro-Fresno D, Hall AE, Herbert RJH, Deboucha W, Reis B, Franco JN, Teresa Borges M, Sousa-Pinto I, van der Linden P, Stafford R (2021) Optimisation of 3D printed concrete for artificial reefs: biofouling and mechanical analysis. Constr Build Mater. https://doi.org/10.1016/j.conbuildmat.2020.121649
120. Munir Q, Peltonen R, Kärki T (2021) Printing parameter requirements for 3D printable geopolymer materials prepared from industrial side streams. Materials. https://doi.org/10.3390/ma14164758
121. Sambucci M, Sibai A, Valente M (2021) Recent advances in geopolymer technology. A potential eco-friendly solution in the construction materials industry: a review. J Compos Sci. https://doi.org/10.3390/jcs5040109
122. Wang Y, Xiong W, Tang D, Hao L, Li Z, Li Y, Cheng K (2021) Rheology effect and enhanced thermal conductivity of diamond/metakaolin geopolymer fabricated by direct ink writing. Rapid Prototyp J 27:837–850. https://doi.org/10.1108/RPJ-06-2020-0124
123. Tramontin-Souza M, Simão L, Guzi de Moraes E, Senff L, de Castro-Pessôa JR, Ribeiro MJ, Novaes de Oliveira AP (2021) Role of temperature in 3D printed geopolymers: evaluating rheology and buildability. Mater Lett. https://doi.org/10.1016/j.matlet.2021.129680
124. Archez J, Texier-Mandoki N, Bourbon X, Caron JF, Rossignol S (2021) Shaping of geopolymer composites by 3D printing. J Build Eng. https://doi.org/10.1016/j.jobe.2020.101894
125. Bhattacherjee S, Basavaraj AS, Rahul AV, Santhanam M, Gettu R, Panda B, Schlangen E, Chen Y, Copuroglu O, Ma G, Wang L, Basit Beigh MA, Mechtcherine V (2021) Sustainable materials for 3D concrete printing. Cem Concr Compos. https://doi.org/10.1016/j.cemconcomp.2021.104156
126. Scanferla P, Conte A, Sin A, Franchin G, Colombo P (2021) The effect of fillers on the fresh and hardened properties of 3D printed geopolymer lattices. Open Ceramics. https://doi.org/10.1016/j.oceram.2021.100134
127. Pilehvar S, Arnhof M, Erichsen A, Valentini L, Kjoniksen AL (2021) Investigation of severe lunar environmental conditions on the physical and mechanical properties of lunar regolith geopolymers. J Market Res 11:1506–1516. https://doi.org/10.1016/j.jmrt.2021.01.124
128. Kocherla A, Kamakshi TA, Subramaniam KVL (2021) In situ embedded PZT sensor for monitoring 3D concrete printing: application in alkali-activated fly ash-slag geopolymers. Smart Mater Struct 30:125024. https://doi.org/10.1088/1361-665X/ac3438
129. Kleshchevnikova V, Belyaeva S, Baranov A (2021) Optimization of mix designs and experimental study of the properties of concrete mix for 3D printing, pp 151–160. https://doi.org/10.1007/978-3-030-72404-7_16
130. Singh NB (2022) Fly ash in the construction industry. In: Handbook of fly ash. Elsevier, London, pp 565–610. https://doi.org/10.1016/B978-0-12-817686-3.00025-6

131. Archez J, Maitenaz S, Demont L, Charrier M, Mesnil R, Texier-Mandoki N, Bourbon X, Rossignol S, Caron JF (2021) Strategy to shape, on a half-meter scale, a geopolymer composite structure by additive manufacturing. Open Ceramics. https://doi.org/10.1016/j.oceram.2021.100071
132. Perry M, Biondi L, McAlorum J, Vlachakis C (2021) Self-sensing concrete repairs based on alkali-activated materials: recent progress. In: Conference record—IEEE instrumentation and measurement technology conference. Institute of Electrical and Electronics Engineers Inc. https://doi.org/10.1109/I2MTC50364.2021.9459969
133. Ranjbar N, Mehrali M, Kuenzel C, Gundlach C, Pedersen DB, Dolatshahi-Pirouz A, Spangenberg J (2021) Rheological characterization of 3D printable geopolymers. Cem Concr Res. https://doi.org/10.1016/j.cemconres.2021.106498
134. Muthukrishnan S, Ramakrishnan S, Sanjayan J (2021) Technologies for improving buildability in 3D concrete printing. Cem Concr Compos. https://doi.org/10.1016/j.cemconcomp.2021.104144
135. Lv X, Qin Y, Liang H, Cui X (2021) Effects of modifying agent on rheology and workability of alkali-activated slag paste for 3D extrusion forming. Constr Build Mater. https://doi.org/10.1016/j.conbuildmat.2021.124062
136. Tang D, Wang Y, Cheng K (2021) Simulation and optimization of lightweight insulating geopolymer composites via dual gradient slurry deposition. J Manuf Process 71:249–259. https://doi.org/10.1016/j.jmapro.2021.09.034
137. Marczyk J, Ziejewska C, Gadek S, Korniejenko K, Łach M, Góra M, Kurek I, Dogan-Saglamtimur N, Hebda M, Szechynska-Hebda M (2021) Hybrid materials based on fly ash, metakaolin, and cement for 3D printing. Materials. https://doi.org/10.3390/ma14226874
138. Paiva MDM, Rocha LDF, Fernandez LIC, Filho RDT, Silva ECCM, Neumann R, Reales OAM (2021) Rheological properties of metakaolin-based geopolymers for three-dimensional printing of structures. ACI Mater J. https://doi.org/10.14359/51733122
139. Jin H, Zhang Y, Zhang X, Chang M, Li C, Lu X, Wang Q (2022) 3D printed geopolymer adsorption sieve for removal of methylene blue and adsorption mechanism. Colloids Surf A Physicochem Eng Asp. https://doi.org/10.1016/j.colsurfa.2022.129235
140. Ziejewska C, Marczyk J, Korniejenko K, Bednarz S, Sroczyk P, Łach M, Mikuła J, Figiela B, Szechyńska-Hebda M, Hebda M (2022) 3D printing of concrete-geopolymer hybrids. Materials. https://doi.org/10.3390/ma15082819
141. Gökçe HS, Güngör O, Öksüzer N (2022) A novel internal curing method for 3D-printed geopolymer structures reinforced with a steel cable: electro-heating. Mater Lett. https://doi.org/10.1016/j.matlet.2021.131364
142. Elsayed H, Gobbin F, Picicco M, Italiano A, Colombo P (2022) Additive manufacturing of inorganic components using a geopolymer and binder jetting. Addit Manuf 56:102909. https://doi.org/10.1016/j.addma.2022.102909
143. Yuan Q, Gao C, Huang T, Zuo S, Yao H, Zhang K, Huang Y, Liu J (2022) Factors influencing the properties of extrusion-based 3D-printed alkali-activated fly ash-slag mortar. Materials. https://doi.org/10.3390/ma15051969
144. Lazorenko G, Kasprzhitskii A (2022) Geopolymer additive manufacturing: a review. Addit Manuf. https://doi.org/10.1016/j.addma.2022.102782
145. Oliveira KG, Botti R, Kavun V, Gafiullina A, Franchin G, Repo E, Colombo P (2022) Geopolymer beads and 3D printed lattices containing activated carbon and hydrotalcite for anionic dye removal. Catal Today 390–391:57–68. https://doi.org/10.1016/j.cattod.2021.12.002
146. Chen Y, Jia L, Liu C, Zhang Z, Ma L, Chen C, Banthia N, Zhang Y (2022) Mechanical anisotropy evolution of 3D-printed alkali-activated materials with different GGBFS/FA combinations. J Build Eng. https://doi.org/10.1016/j.jobe.2022.104126
147. Marczyk J, Ziejewska C, Pławecka K, Bąk A, Łach M, Korniejenko K, Hager I, Mikuła J, Lin W-T, Hebda M (2022) Optimizing the L/S ratio in geopolymers for the production of large-size elements with 3D printing technology. Materials 15:3362. https://doi.org/10.3390/ma15093362
148. Liu J, Lv C (2022) Properties of 3D-printed polymer fiber-reinforced mortars: a review. Polymers (Basel). https://doi.org/10.3390/polym14071315
149. Bong SH, Nematollahi B, Xia M, Ghaffar SH, Pan J, Dai JG (2022) Properties of additively manufactured geopolymer incorporating mineral wollastonite microfibers. Constr Build Mater. https://doi.org/10.1016/j.conbuildmat.2022.127282
150. Raza MH, Zhong RY, Khan M (2022) Recent advances and productivity analysis of 3D printed geopolymers. Addit Manuf. https://doi.org/10.1016/j.addma.2022.102685
151. Ilcan H, Sahin O, Kul A, Yildirim G, Sahmaran M (2022) Rheological properties and compressive strength of construction and demolition waste-based geopolymer mortars for 3D-printing. Constr Build Mater. https://doi.org/10.1016/j.conbuildmat.2022.127114
152. Tang D, Tang H (2022) Self-healing diamond/geopolymer composites fabricated by extrusion-based additive manufacturing. Addit Manuf 56:102898. https://doi.org/10.1016/j.addma.2022.102898
153. Muthukrishnan S, Ramakrishnan S, Sanjayan J (2022) Set on demand geopolymer using print head mixing for 3D concrete printing. Cem Concr Compos. https://doi.org/10.1016/j.cemconcomp.2022.104451
154. Guo X, Yang J, Xiong G (2022) Effect of magnesium aluminum silicate and rest time on rheological property of 3D printing geopolymer mortar. J Build Mater 25:89–96
155. Shakor P, Chu SH, Puzatova A, Dini E (2022) Review of binder jetting 3D printing in the construction industry. Prog Add Manuf. https://doi.org/10.1007/s40964-021-00252-9
156. Ma G, Yan Y, Zhang M, Sanjayan J (2022) Effect of steel slag on 3D concrete printing of geopolymer with quaternary binders. Ceram Int. https://doi.org/10.1016/j.ceramint.2022.05.305
157. Kong X, Dai L, Wang Y, Qiao D, Hou S, Wang S (2022) Influence of kenaf stalk on printability and performance of 3D printed industrial tailings based geopolymer. Constr Build Mater. https://doi.org/10.1016/j.conbuildmat.2021.125787
158. Korniejenko K, Kejzlar P, Louda P (2022) The influence of the material structure on the mechanical properties of geopolymer composites reinforced with short fibers obtained with additive technologies. Int J Mol Sci. https://doi.org/10.3390/ijms23042023
159. Li Z, Li Y, Shi B, Tang D, Wang Y, Hao L (2022) Dual gradient direct ink writing of functional geopolymer-based carbonyl-iron/graphene composites for adjustable broadband microwave absorption. Ceram Int 48:9277–9285. https://doi.org/10.1016/j.ceramint.2021.12.114
160. Zhong H, Zhang M (2022) 3D printing geopolymers: a review. Cem Concr Compos. https://doi.org/10.1016/j.cemconcomp.2022.104455
161. Ma S, Zhao S, Zheng Y, Wang Q, Yang H, Liu X, He P, Duan X (2022) Preparation and mechanical performance of SiC_w/geopolymer composites through direct ink writing. J Am Ceram Soc 105:3555–3567. https://doi.org/10.1111/jace.18308
162. Liu S, Lu B, Li H, Pan Z, Jiang J, Qian S (2022) A comparative study on environmental performance of 3D printing and conventional casting of concrete products with industrial wastes. Chemosphere 298:134310. https://doi.org/10.1016/j.chemosphere.2022.134310

163. Kondepudi K, Subramaniam KVL, Nematollahi B, Bong SH, Sanjayan J (2022) Study of particle packing and paste rheology in alkali activated mixtures to meet the rheology demands of 3D concrete printing. Cem Concr Compos 131:104581. https://doi.org/10.1016/j.cemconcomp.2022.104581
164. Ma S, Yang H, Fu S, He P, Duan X, Yang Z, Jia D, Colombo P, Zhou Y (2023) Additive manufacturing of geopolymers with hierarchical porosity for highly efficient removal of Cs+. J Hazard Mater 443:130161. https://doi.org/10.1016/j.jhazmat.2022.130161
165. Robayo-Salazar R, Mejía de Gutiérrez R, Villaquirán-Caicedo MA, Delvasto Arjona S (2023) 3D printing with cementitious materials: challenges and opportunities for the construction sector. Autom Constr 146:10463. https://doi.org/10.1016/j.autcon.2022.104693
166. Rahemipoor S, Hasany M, Mehrali M, Almdal K, Ranjbar N, Mehrali M (2023) Phase change materials incorporation into 3D printed geopolymer cement: a sustainable approach to enhance the comfort and energy efficiency of buildings. J Clean Prod 417:138005. https://doi.org/10.1016/j.jclepro.2023.138005
167. Pasupathy K, Ramakrishnan S, Sanjayan J (2023) 3D concrete printing of eco-friendly geopolymer containing brick waste. Cem Concr Compos 138:104943. https://doi.org/10.1016/j.cemconcomp.2023.104943
168. Ramezani A, Modaresi S, Dashti P, GivKashi MR, Moodi F, Ramezanianpour AA (2023) Effects of different types of fibers on fresh and hardened properties of cement and geopolymer-based 3D printed mixtures: a review. Buildings 13:945. https://doi.org/10.3390/buildings13040945
169. Chen W, Pan J, Zhu B, Ma X, Zhang Y, Chen Y, Li X, Meng L, Cai J (2023) Improving mechanical properties of 3D printable 'one-part' geopolymer concrete with steel fiber reinforcement. J Build Eng 75:107077. https://doi.org/10.1016/j.jobe.2023.107077
170. Jaji MB, Ibrahim KA, van Zijl GPAG, Babafemi AJ (2023) Effect of anisotropy on permeability index and water absorption of 3D printed metakaolin-based geopolymer concrete. Mater Today Proc. https://doi.org/10.1016/j.matpr.2023.06.394
171. Tran MV, Vu TH, Nguyen THY (2023) Simplified assessment for one-part 3D-printable geopolymer concrete based on slump and slump flow measurements. Case Stud Constr Mater 18:e01889. https://doi.org/10.1016/j.cscm.2023.e01889
172. Inayath Basha S, Rehman AU, Khalid HR, Aziz MA, Kim J (2023) 3D printable geopolymer composites reinforced with carbon-based nanomaterials—a review. Chem Rec. https://doi.org/10.1002/tcr.202300054
173. Masi G, Saccani A, Chiara-Bignozzi M (2023) Influence of different waste-derived fillers in extruded geopolymeric matrix for 3D printing. Mater Today Proc. https://doi.org/10.1016/j.matpr.2023.06.184
174. Ilcan H, Sahin O, Kul A, Ozcelikci E, Sahmaran M (2023) Rheological property and extrudability performance assessment of construction and demolition waste-based geopolymer mortars with varied testing protocols. Cem Concr Compos 136:104891. https://doi.org/10.1016/j.cemconcomp.2022.104891
175. Muthukrishnan S, Ramakrishnan S, Sanjayan J (2023) Early age strength of in-line activated geopolymer for concrete 3D printing, SSRN. https://papers.ssrn.com/sol3/papers.cfm?abstract_id=4385678. Accessed July 22, 2023
176. Khan SA, İlcan H, Aminipour E, Şahin O, Al Rashid A, Şahmaran M, Koç M (2023) Buildability analysis on effect of structural design in 3D concrete printing (3DCP): an experimental and numerical study. Case Stud Constr Mater 19:e02295. https://doi.org/10.1016/j.cscm.2023.e02295
177. Chaiyotha D, Kantawong W, Payakaniti P, Pinitsoontorn S, Chindaprasirt P (2023) Finding optimized conditions for 3D printed high calcium fly ash based alkali-activated mortar. Case Stud Constr Mater 18:e01976. https://doi.org/10.1016/j.cscm.2023.e01976
178. Ranjbar N, Kuenzel C, Gundlach C, Kempen P, Mehrali M (2023) Halloysite reinforced 3D-printable geopolymers. Cem Concr Compos 136:104894. https://doi.org/10.1016/j.cemconcomp.2022.104894
179. Gonçalves NPF, Olhero SM, Labrincha JA, Novais RM (2023) 3D-printed red mud/metakaolin-based geopolymers as water pollutant sorbents of methylene blue. J Clean Prod 383:135315. https://doi.org/10.1016/j.jclepro.2022.135315
180. Albidah AS (2021) Effect of partial replacement of geopolymer binder materials on the fresh and mechanical properties: a review. Ceram Int 47:14923–14943. https://doi.org/10.1016/j.ceramint.2021.02.127
181. Krishna RS, Mishra J, Nanda B, Patro SK, Adetayo A, Qureshi TS (2021) The role of graphene and its derivatives in modifying different phases of geopolymer composites: a review. Constr Build Mater. https://doi.org/10.1016/j.conbuildmat.2021.124774
182. Wu S, Qureshi T, Wang G (2021) Application of graphene in fiber-reinforced cementitious composites: a review. Energies (Basel) 14:4614. https://doi.org/10.3390/en14154614
183. Qureshi T, Wang G, Mukherjee S, Akibul-Islam M, Filleter T, Singh CV, Panesar DK (2022) Graphene-based anti-corrosive coating on steel for reinforced concrete infrastructure applications: Challenges and potential. Constr Build Mater 351:128947. https://doi.org/10.1016/j.conbuildmat.2022.128947
184. Krishna RS, Saha S, Korniejenko K, Qureshi TS, Mustakim SM (2023) Investigation of the electrical properties of graphene-reinforced geopolymer composites. In: 10th MATBUD'2023 scientific-technical conference, MDPI, Basel Switzerland, 2023, p 34. https://doi.org/10.3390/materproc2023013034
185. Islam MA, Serles P, Kumral B, Demingos PG, Qureshi T, Meiyazhagan A, Puthirath AB, Bin Abdullah MS, Faysal SR, Ajayan PM, Panesar D, Singh CV, Filleter T (2022) Exfoliation mechanisms of 2D materials and their applications. Appl Phys Rev. https://doi.org/10.1063/5.0090717
186. Sadiq MM, Soroushian P, Bakker MG, Balachandra AM (2021) Ultra-high-performance cementitious composites with enhanced mechanical and durability characteristics. SN Appl Sci 3:676. https://doi.org/10.1007/s42452-021-04628-y
187. Łach M (2021) Geopolymer foams—will they ever become a viable alternative to popular insulation materials? A critical opinion. Materials. https://doi.org/10.3390/ma14133568
188. Qureshi TS, Panesar DK (2020) Nano reinforced cement paste composite with functionalized graphene and pristine graphene nanoplatelets. Compos B Eng 197:108063. https://doi.org/10.1016/j.compositesb.2020.108063
189. Qureshi T, Ootim S (2023) Multifunctional concrete with graphene-based nanomaterials and superabsorbent polymer. J Mater Civ Eng. https://doi.org/10.1061/(ASCE)MT.1943-5533.0004699
190. Imtiaz L, Rehman SKU, Ali-Memon S, Khizar-Khan M, Faisal-Javed M (2020) A review of recent developments and advances in eco-friendly geopolymer concrete. Appl Sci 10:7838. https://doi.org/10.3390/app10217838
191. Rahul AV, Santhanam M, Meena H, Ghani Z (2019) 3D printable concrete: mixture design and test methods. Cem Concr Compos 97:13–23. https://doi.org/10.1016/j.cemconcomp.2018.12.014
192. Panda B, Tan MJ (2019) Rheological behavior of high volume fly ash mixtures containing micro silica for digital construction application. Mater Lett 237:348–351. https://doi.org/10.1016/j.matlet.2018.11.131

193. Soltan DG, Li VC (2018) A self-reinforced cementitious composite for building-scale 3D printing. Cem Concr Compos 90:1–13. https://doi.org/10.1016/j.cemconcomp.2018.03.017
194. BetAbram P1 Overview, Aniwaa (2022). https://www.aniwaa.com/product/3d-printers/betabram-p1/. Accessed October 30, 2022
195. THE BOD2, COBOD (2022). https://cobod.com/products/bod2/. Accessed October 30, 2022
196. MaxiPrinter, Constructions-3D (2022). https://en.constructions-3d.com/la-maxi-printer. Accessed October 30, 2022
197. CyBe RC (Robot Crawler), CyBe Construction (2022). https://cybe.eu/3d-concrete-printing/printers/. Accessed October 30, 2022
198. ICON Vulcan II, Aniwaa (2022). https://www.aniwaa.com/product/3d-printers/icon-vulcan-ii/. Accessed October 30, 2022
199. 3D Concrete Printers, MUDBOTS 3D CONCRETE PRINTING (2022). https://www.mudbots.com/concrete-3d-printers.php. Accessed October 30, 2022
200. StroyBot 6.2, Total Kustom (2022). http://www.totalkustom.com/3d-concrete-printers.html. Accessed October 30, 2022
201. Crane WASP, WASP Srl (2022). https://www.3dwasp.com/stampante-3d-per-case-crane-wasp/. Accessed October 30, 2022
202. Technology, Apis Cor Inc. (2022). https://apis-cor.com/technologies/. Accessed October 30, 2022
203. Shaping Tomorrow, BATIPRINT 3D (2022). https://www.batiprint3d.com/en. Accessed October 30, 2022
204. 3D printed houses, commercial buidings, infrastructure, SQ4D (2022). https://www.sq4d.com/. Accessed October 30, 2022
205. The large-scale 3D, XtreeE (2022). https://xtreee.com/en/solutions/. Accessed October 30, 2022
206. CONCR3DE YOUR 3D POWERHOUSE, Large-scale 3D printing (2023). https://www.concr3de.com/product_large-scale-printing.php. Accessed July 22, 2023
207. ExOne, Sand 3D Printers (2023). https://www.exone.com/en-US/3D-printing-systems/sand-3d-printers. Accessed July 22, 2023
208. voxeljet, VX4000: The world's largest 3D printer for sand (2020). https://www.voxeljet.com/industrial-3d-printer/serial-production/vx4000/#anchor-4. Accessed July 22, 2023
209. Markin V, Sahmenko G, Nerella VN, Näther M, Mechtcherine V (2019) Investigations on the foam concrete production techniques suitable for 3D-printing with foam concrete. IOP Conf Ser Mater Sci Eng 660:012039. https://doi.org/10.1088/1757-899X/660/1/012039
210. Chougan M, Hamidreza Ghaffar S, Jahanzat M, Albar A, Mujaddedi N, Swash R (2020) The influence of nano-additives in strengthening mechanical performance of 3D printed multi-binder geopolymer composites. Constr Build Mater 250:118928. https://doi.org/10.1016/j.conbuildmat.2020.118928
211. Muthukrishnan S, Ramakrishnan S, Sanjayan J (2020) Buildability of geopolymer concrete for 3D printing with microwave heating. In: RILEM bookseries. Springer, London, pp 926–935. https://doi.org/10.1007/978-3-030-49916-7_90
212. Scanferla P, Conte A, Sin A, Franchin G, Colombo P (2021) The effect of fillers on the fresh and hardened properties of 3D printed geopolymer lattices. Open Ceramics 6:100134. https://doi.org/10.1016/j.oceram.2021.100134
213. Ziejewska C, Marczyk J, Korniejenko K, Bednarz S, Sroczyk P, Łach M, Mikuła J, Figiela B, Szechyńska-Hebda M, Hebda M (2022) 3D printing of concrete-geopolymer hybrids. Materials 15:2819. https://doi.org/10.3390/ma15082819
214. Marczyk J, Ziejewska C, Gądek S, Korniejenko K, Łach M, Góra M, Kurek I, Doğan-Sağlamtimur N, Hebda M, Szechyńska-Hebda M (2021) Hybrid materials based on fly ash, metakaolin, and cement for 3D printing. Materials 14:6874. https://doi.org/10.3390/ma14226874
215. Buswell RA, Leal de Silva WR, Jones SZ, Dirrenberger J (2018) 3D printing using concrete extrusion: a roadmap for research. Cem Concr Res 112:37–49. https://doi.org/10.1016/j.cemconres.2018.05.006
216. Mohan MK, Rahul AV, De Schutter G, Van Tittelboom K (2021) Extrusion-based concrete 3D printing from a material perspective: a state-of-the-art review. Cem Concr Compos. https://doi.org/10.1016/j.cemconcomp.2020.103855
217. Ambrosi A, Pumera M (2016) 3D-printing technologies for electrochemical applications. Chem Soc Rev 45:2740–2755. https://doi.org/10.1039/c5cs00714c
218. Lowke D, Dini E, Perrot A, Weger D, Gehlen C, Dillenburger B (2018) Particle-bed 3D printing in concrete construction—possibilities and challenges. Cem Concr Res 112:50–65. https://doi.org/10.1016/j.cemconres.2018.05.018
219. Chen L, Wang Z, Wang Y, Feng J (2016) Preparation and properties of alkali activated metakaolin-based geopolymer. Materials. https://doi.org/10.3390/ma9090767
220. Matalkah F, Soroushian P (2018) Freeze thaw and deicer salt scaling resistance of concrete prepared with alkali aluminosilicate cement. Constr Build Mater 163:200–213. https://doi.org/10.1016/j.conbuildmat.2017.12.119
221. Dini E (2012) Printing architecture. In: Yuan P, Leach N (eds) Fabricating the future. Tongji University Press, Shanghai, p 114
222. Leach N, Carlson A, Khoshnevis B, Thangavelu M (2012) Robotic construction by contour crafting: the case of lunar construction. Int J Archit Comput 10:423–438. https://doi.org/10.1260/1478-0771.10.3.423
223. Meurisse A, Makaya A, Willsch C, Sperl M (2018) Solar 3D printing of lunar regolith. Acta Astronaut 152:800–810. https://doi.org/10.1016/j.actaastro.2018.06.063
224. Voney V, Odaglia P, Brumaud C, Dillenburger B, Habert G (2021) From casting to 3D printing geopolymers: a proof of concept. Cem Concr Res 143:106374. https://doi.org/10.1016/j.cemconres.2021.106374
225. Demiral NC, Ozkan Ekinci M, Sahin O, Ilcan H, Kul A, Yildirim G, Sahmaran M (2022) Mechanical anisotropy evaluation and bonding properties of 3D-printable construction and demolition waste-based geopolymer mortars. Cem Concr Compos 134:104814. https://doi.org/10.1016/j.cemconcomp.2022.104814
226. Ordoñez E, Gallego JM, Colorado HA (2019) 3D printing via the direct ink writing technique of ceramic pastes from typical formulations used in traditional ceramics industry. Appl Clay Sci 182:105285. https://doi.org/10.1016/j.clay.2019.105285
227. Qaidi S, Yahia A, Tayeh BA, Unis H, Faraj R, Mohammed A (2022) 3D printed geopolymer composites: a review. Mater Today Sustain. https://doi.org/10.1016/j.mtsust.2022.100240
228. Long W-J, Tao J-L, Lin C, Gu Y, Mei L, Duan H-B, Xing F (2019) Rheology and buildability of sustainable cement-based composites containing micro-crystalline cellulose for 3D-printing. J Clean Prod 239:118054. https://doi.org/10.1016/j.jclepro.2019.118054
229. Chougan M, Ghaffar SH, Sikora P, Chung S-Y, Rucinska T, Stephan D, Albar A, Swash MR (2021) Investigation of additive incorporation on rheological, microstructural and mechanical properties of 3D printable alkali-activated materials. Mater Des 202:109574. https://doi.org/10.1016/j.matdes.2021.109574
230. Archez J, Texier-Mandoki N, Bourbon X, Caron JF, Rossignol S (2020) Adaptation of the geopolymer composite formulation binder to the shaping process. Mater Today Commun 25:101501. https://doi.org/10.1016/j.mtcomm.2020.101501
231. Kashani A, Ngo TD (2018) Optimisation of mixture properties for 3D printing of geopolymer concrete. In: ISARC 2018-35th international symposium on automation and robotics in construction and international AEC/FM hackathon: the future of building

things. International Association for Automation and Robotics in Construction I.A.A.R.C. https://doi.org/10.22260/isarc2018/0037
232. Chandra-Paul S, Basit MA, Hasan NMS, Dey D, Panda B (2023) 3D printing of geopolymer mortar: Overview of the effect of mix design and printing parameters on the strength. Mater Today Proc. https://doi.org/10.1016/j.matpr.2023.04.292
233. Tan J (2023) ROBOT ARM-GEOPOLYMER 3D PRINT, Adobe Portfolio (2023). https://junrentan.com/robot-arm-geopolymer-3d-print. Accessed Sept 21, 2023
234. Le TT, Austin SA, Lim S, Buswell RA, Gibb AGF, Thorpe T (2012) Mix design and fresh properties for high-performance printing concrete. Mater Struct/Mater Constr 45:1221–1232. https://doi.org/10.1617/s11527-012-9828-z
235. Zhang C, Nerella VN, Krishna A, Wang S, Zhang Y, Mechtcherine V, Banthia N (2021) Mix design concepts for 3D printable concrete: a review. Cem Concr Compos 122:104155. https://doi.org/10.1016/j.cemconcomp.2021.104155
236. Jaji MB, Ibrahim KA, van Zijl GPAG, Babafemi AJ (2023) Thixotropic characterisation of slag modified 3D printable metakaolin based geopolymer composite. Mater Today Proc. https://doi.org/10.1016/j.matpr.2023.03.530
237. Deb PS, Nath P, Sarker PK (2015) Drying shrinkage of slag blended fly ash geopolymer concrete cured at room temperature. Proc Eng 125:594–600. https://doi.org/10.1016/j.proeng.2015.11.066
238. Zhang B, Zhu H, Feng P, Zhang P (2022) A review on shrinkage-reducing methods and mechanisms of alkali-activated/geopolymer systems: effects of chemical additives. J Build Eng 49:104056. https://doi.org/10.1016/j.jobe.2022.104056
239. Frasson BJ, Rocha JC (2023) Drying shrinkage behavior of geopolymer mortar based on kaolinitic coal gangue. Case Stud Constr Mater 18:e01957. https://doi.org/10.1016/j.cscm.2023.e01957
240. Duan P, Yan C, Luo W, Zhou W (2016) Effects of adding nano-TiO_2 on compressive strength, drying shrinkage, carbonation and microstructure of fluidized bed fly ash based geopolymer paste. Constr Build Mater 106:115–125. https://doi.org/10.1016/j.conbuildmat.2015.12.095
241. Hanjitsuwan S, Injorhor B, Phoo-ngernkham T, Damrongwiriyanupap N, Li LY, Sukontasukkul P, Chindaprasirt P (2020) Drying shrinkage, strength and microstructure of alkali-activated high-calcium fly ash using FGD-gypsum and dolomite as expansive additive. Cem Concr Compos 114:103760. https://doi.org/10.1016/j.cemconcomp.2020.103760
242. Panda B, Mohamed NAN, Tan MJ (2018) Effect of 3D printing on mechanical properties of fly ash-based inorganic geopolymer. In: International congress on polymers in concrete (ICPIC 2018). Springer, London, pp 509–515. https://doi.org/10.1007/978-3-319-78175-4_65
243. Innocentini MDM, Botti RF, Bassi PM, Paschoalato CFPR, Flumignan DL, Franchin G, Colombo P (2019) Lattice-shaped geopolymer catalyst for biodiesel synthesis fabricated by additive manufacturing. Ceram Int 45:1443–1446. https://doi.org/10.1016/j.ceramint.2018.09.239
244. Ma S, Jiang Y, Fu S, He P, Sun C, Duan X, Jia D, Colombo P, Zhou Y (2023) 3D-printed Lunar regolith simulant-based geopolymer composites with bio-inspired sandwich architectures. J Adv Ceram 12:510–525. https://doi.org/10.26599/JAC.2023.9220700
245. He Z, Hu C-P, Chen H, Chen X, Lim SKJ, Hu J, Hu X (2023) Direct ink writing of geopolymer-based membranes with anisotropic structures for water treatment. J Memb Sci. https://doi.org/10.1016/j.memsci.2023.121953
246. Chen Y, Kuva J, Mohite A, Li Z, Rahier H, Al-Neshawy F, Shu J (2023) Investigation of the internal structure of hardened 3D-printed concrete by X-CT scanning and its influence on the mechanical performance. Materials 16:2534. https://doi.org/10.3390/ma16062534
247. Wangler T, Roussel N, Bos FP, Salet TAM, Flatt RJ (2019) Digital concrete: a review. Cem Concr Res 123:105780. https://doi.org/10.1016/j.cemconres.2019.105780
248. Le CH, Louda P, Buczkowska KE, Dufkova I (2021) Investigation on flexural behavior of geopolymer-based carbon textile/basalt fiber hybrid composite. Polymers (Basel) 13:1–18. https://doi.org/10.3390/polym13050751
249. Zhu B, Pan J, Nematollahi B, Zhou Z, Zhang Y, Sanjayan J (2019) Development of 3D printable engineered cementitious composites with ultra-high tensile ductility for digital construction. Mater Des. https://doi.org/10.1016/j.matdes.2019.108088
250. Korniejenko K, Łach M, Chou S, Lin W, Mikuła J, Mierzwiński D, Cheng A, Hebda M (2019) A comparative study of mechanical properties of fly ash-based geopolymer made by casted and 3D printing methods. IOP Conf Ser Mater Sci Eng 660:012005. https://doi.org/10.1088/1757-899X/660/1/012005
251. Qureshi TS, Panesar DK, Sidhureddy B, Chen A, Wood PC (2019) Nano-cement composite with graphene oxide produced from epigenetic graphite deposit. Compos B Eng 159:248–258. https://doi.org/10.1016/j.compositesb.2018.09.095
252. Qureshi TS, Panesar DK (2019) Impact of graphene oxide and highly reduced graphene oxide on cement based composites. Constr Build Mater 206:71–83. https://doi.org/10.1016/j.conbuildmat.2019.01.176
253. Perrot A, Rangeard D, Pierre A (2016) Structural built-up of cement-based materials used for 3D-printing extrusion techniques. Mater Struct/Mater Constr 49:1213–1220. https://doi.org/10.1617/s11527-015-0571-0
254. Hambach M, Volkmer D (2017) Properties of 3D-printed fiber-reinforced Portland cement paste. Cem Concr Compos 79:62–70. https://doi.org/10.1016/j.cemconcomp.2017.02.001
255. Nematollahi B, Xia M, Vijay P, Sanjayan JG (2019) Properties of extrusion-based 3D printable geopolymers for digital construction applications. In: 3D concrete printing technology. Elsevier, London, pp 371–388. https://doi.org/10.1016/b978-0-12-815481-6.00018-x
256. Weng Y, Li M, Ruan S, Wong TN, Tan MJ, Ow Yeong KL, Qian S (2020) Comparative economic, environmental and productivity assessment of a concrete bathroom unit fabricated through 3D printing and a precast approach. J Clean Prod. https://doi.org/10.1016/j.jclepro.2020.121245
257. Cherdo L (2024) The 13 best construction 3D printers in 2023, Aniwaa (n.d.). https://www.aniwaa.com/buyers-guide/3d-printers/%20house-3d-printer-construction/. Accessed March 3, 2024
258. Weger D, Lowke D, Gehlen C (2016) 3D printing of concrete structures with calcium silicate based cements using the selective binding method-effects of concrete technology on penetration depth of cement paste. In: Ultra-high performance concrete and high performance construction materials, Kassel. https://www.researchgate.net/publication/321491219